

The copyright of this thesis vests in the author. No quotation from it or information derived from it is to be published without full acknowledgement of the source. The thesis is to be used for private study or non-commercial research purposes only.

Published by the University of Cape Town (UCT) in terms of the non-exclusive license granted to UCT by the author.

University of Cape Town

Abstract

In this thesis we analyse the coaxial multivortices of the Ginzburg-Landau, the Euclidean complex sine-Gordon-1 and -2 theories on the plane. More specifically, we determine the number of continuous free parameters describing the largest family of solutions, with these vortices as members. This is accomplished by obtaining the zero modes of the vortices. For the Ginzburg-Landau model we show that the multivortices do not belong to a larger family of solutions and only depend on parameters describing their global $U(1)$ symmetry and translations in the plane. Thus it is not possible to continuously deform these coaxial multivortices into a system of multiple, separated vortices. In contrast, the multivortices of complex sine-Gordon-1 model are shown to have an infinite number of zero modes and can be continuously deformed into a configuration of multiple, separated vortices. We also show that the largest family of solutions, with these coaxial multivortices as members, is a recently discovered family describing non-coaxial multivortices. For the complex sine-Gordon-2, we show the coaxial multivortices belong to a larger family of solutions which depend on a finite number of continuous free parameters. We also speculate as to the form of solutions that this larger family can describe.

Acknowledgements

First and foremost, I would like to thank my family for their continued and unwavering support during this dark and deranged time. Thank-you!! Thanks also go to my supervisor, Professor I.V. Barashenkov, for all his guidance and patience during this thesis. He has definitely helped improve my research skills.

I would also like to thank my friends who helped in all their weird and wonderful ways. Special thanks go to Jeff Murugan and Mark Horner for all their help and most importantly their friendship. Jeff has been my guiding light in field theory. Also his pro placement is bomb, with out it I am sure I would have many a broken bone. To Mark Horner, thanks boet! It is always good to know that no matter where we are we will always be best mates. Life would be very dull without Horner.

To Megan Butler and Tarin Brown, thanks for introducing me to some of the more beautiful sides of life. And without Megs, this thesis would be even more difficult to read than it is, with my language skills being what they are:)

To the rest of my friends who endured my pestering for help with editing: Sarah Blyth, Spencer Wheaton, Bruce Becker and Sam Haliday, thanks guys, its now over and you have some time to relax before the PhD swings by. I apologise to anyone I have left off this list.

Then there are the special people in room 319 in the mathematics department, without whom the department would come to a standstill. Thanks ladies for all your help and smiles.

This research was supported by the NRF of South Africa, a UCT research associateship grant and the Manuel & Luby Washkansky scholarship.

Finally I would like to thank my best friend, my sister Megan Adams. Thanks for being my little sis.

Contents

Abstract	i
Acknowledgements	ii
Introduction	1
1 Zero Modes	10
1.1 What are Zero Modes?	10
1.2 Some Real Scalar Fields	12
1.2.1 φ^4 Theory	12
1.2.2 The sine-Gordon kink	13
1.2.3 Massless cubic-quintic Klein-Gordon equation	14
1.2.4 Rosen's equation	17
1.3 Complex Scalar Fields	20
1.3.1 Klein-Gordon	20
1.3.2 Nonlinear Schrödinger	21
1.3.3 Logarithmic Gausson equation	22
1.4 The Nonlinear $O(3)$ σ -model	25
1.4.1 Single BP soliton	27
1.4.2 Double BP soliton	29
1.5 Summary	32
2 The Ginzburg-Landau Model	34
2.1 Linearisation	35
2.2 Asymptotic Behaviour of Zero Modes	39
2.2.1 Asymptotics for small r	39
2.2.2 Asymptotics for large r	41
2.3 Numerical Calculation of the Zero Modes	46
2.3.1 Single vortex ($n = 1$)	46
2.3.2 Double vortex ($n = 2$)	50
2.3.3 Triple vortex ($n = 3$)	54
2.4 Summary	58

3	Complex Sine-Gordon-1	59
3.1	Linearisation	60
3.2	Asymptotic Behaviour of Zero Modes	65
3.2.1	Asymptotics for small r	65
3.2.2	Asymptotics for large r	66
3.3	The Numerical Solutions	71
3.3.1	Azimuthal quantum number $m = 0$	73
3.3.2	Azimuthal quantum number $m = 1$	75
3.3.3	Excitations of the single vortex with $m \geq 2$	79
3.3.4	Excitations of the coaxial double-vortex with $m \geq 2$	85
3.3.5	Excitations of the coaxial triple-vortex with $m \geq 2$	92
3.4	Summary	98
4	Complex Sine-Gordon-2	99
4.1	Linearisation	100
4.2	Asymptotic Behaviour of Zero Modes	102
4.2.1	Asymptotics for small r	102
4.2.2	Asymptotics for large r	104
4.3	Numerical Calculations	108
4.3.1	Azimuthal quantum number $m = 0$	110
4.3.2	Azimuthal quantum number $m = 1$	111
4.3.3	Excitations of the single vortex with $m \geq 2$	112
4.3.4	Excitations of the coaxial double-vortex with $m \geq 2$	116
4.3.5	Excitations of the coaxial triple-vortex with $m \geq 2$	118
4.4	Summary	121
	Conclusion	122
	A Finite Difference Scheme for the Eigenvalue Problem	124
	Bibliography	125

Introduction

One of our fundamental roles as scientists is to model our world and try to understand it better, whether it be from a physical, chemical or biological viewpoint. Generally the best language available to us is that of mathematics and, most often, this modelling is achieved by means of differential equations. It would be wonderful if these differential equations were linear as linear differential equations are well understood and there are many means available to us for solving them. However, the real world is not that simple and most processes are described by nonlinear differential equations which are far more complex to solve and to understand. It is these nonlinear differential equations that prompted the study of "soliton methods". And in turn the soliton methods have facilitated many breakthroughs in the description of physical processes in various fields. By "soliton methods" we refer to the various methods and techniques which have been developed for finding solitons of differential equations.

At this stage it is appropriate for us to define the term soliton. There is, actually, a fair measure of variation in the definition of a soliton amongst various disciplines. The most restrictive of these is the original definition used by mathematicians. Heuristically, a soliton is a solution to a nonlinear evolution equation which satisfies the following two conditions:

- A localised structure which propagates with velocity and shape retention
- Asymptotic shape and velocity retained after collisions

For a more formal definition the reader may consult the review paper [1]. The importance of these "linear" characteristics only becomes apparent when one considers that they are required of solutions to a *nonlinear equation*. These two conditions greatly restrict the number of nonlinear evolution equations that exhibit the "mathematicians" solitons. (Naturally, one might wonder just what is meant by the term "localised structure" in the above definition. For this text, we will adopt the treatment in [2] and define localised structures in terms of energy densities. This, obviously, restricts us to theories for which an energy density is defined but this will suffice for our purposes. A localised structure is a solution whose energy density $\epsilon(\vec{x})$ is localised in space, in other words $\epsilon(\vec{x}) \rightarrow 0$ sufficiently fast as $|\vec{x}| \rightarrow \infty$.)

For particle physicists, however, the important characteristics are just the stability and localisation of the solution. If the shape of the localised solution is altered after collision then on the quantum level, the quantum numbers have changed. This case can actually be more interesting from a particle physicist's point of view than the alternative where they remain the same. For this reason, particle physicists have a broader definition of a soliton. They define a soliton as a solution which obeys only the first point mentioned above, namely that it be localised and propagate with velocity and shape retention. A nonlinear scientist refers to such a solution as a solitary wave. For this text we will follow the latter and define a *soliton* as a particle-like solution whose energy density is localised

and stable.

It was actually a while before soliton methods made their way into particle physics, as the perturbative methods which were in use were well established and understood. In the perturbative formalism, free “particles” are described by quantised modes of the classical system linearised about trivial vacua. The term ‘perturbative’ is derived from the manner in which nonlinear interactions are considered via perturbative expansions. The fact that the particles emerge from the interactions is guaranteed by their being quanta of some classical field. However, perturbative expansions are deficient in certain regimes as for example the strong interactions of QCD. It was the problems with the perturbative formalism, such as the one just mentioned, which led particle physicists to seek non-perturbative techniques. Thus, the non-perturbative, soliton methods were rediscovered by particle physicists in the early and mid seventies.

Within the non-perturbative formalisms, the solitons are also considered as particles. Now that nontrivial classical vacua were obtained, methods of quantising them were needed. These quantisation methods were not long to follow. For a review of soliton quantisation methods, we refer the reader to [5, 6, 2]. With the quantisation methods at hand, it quickly emerged that certain properties of solitons, for example the nontrivial topologies of the target spaces, led to interesting quantum phenomena, not observed in the perturbative formalism. At present the literature on solitons in particle physics is extensive*.

As the particle physicists were rediscovering most of solitonic methods for themselves they naturally started off with simple models. The first to come under the spot light were the (1+1)-dimensional scalar field theories that exhibit solitonic solutions. Amongst these were the well known Klein-Gordon and the sine-Gordon equations on $\mathbb{R}(1, 1)$. One might think that the easiest extension to more realistic systems would be to increase the number of spatial dimensions in the scalar field theories. However, a simple scaling argument by Derrick [7, 8] furnishes a powerful no-go theorem that disallows the naive extension of relativistic, pure scalar field theories of the Klein-Gordon type to more than (1+1)-dimensions. Fortunately, although Derrick’s theorem is heavily constrained it is easily circumvented by the introduction of gauge fields. Generally the addition of gauge fields introduces topological charges to the field theories. These topological charges then ensure the existence of nontrivial stable solutions, in the higher dimensions.

Solitons in Physics

Soliton methods have been applied to many fields with great success, for example condensed matter physics. Among some of the successes in condensed matter physics are the description of vortices in superfluids and superconductors, line and edge defects in crystals, Bloch wall motion in ferromagnets and monopoles and interacting strings in liquid crystals (fig 1). Ordered systems, such as crystals, allow for the definition of an “order parameter” ψ . This parameter characterises the extent to which the system

*It is fitting to note that soliton methods are not the only non-perturbative methods in use today. Lattice gauge theory [3, 4] is another non-perturbative method which makes use of powerful numerical methods, in particular Monte Carlo procedures, to solve gauge field theories.

is “ordered” in a region of the system. An example of this is the rotation angle in a continuous model of coupled pendula. When dislocations are modelled in crystals, the motion of the atoms from their equilibrium positions is used as an order parameter. Applying a shearing force to a crystal causes the planes of atoms to slide over each other. This can result in edge dislocations, if the deformation is continuous. The propagation of these dislocations is effectively modelled by a soliton bearing theory, the sine-Gordon equation [10].

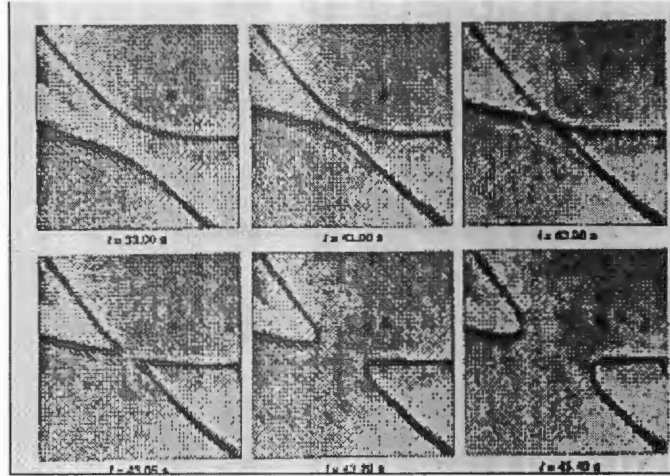


Figure 1: Photographs of intercommuting strings in a nematic liquid crystal [9]

The sine-Gordon equation has also been used to describe the motion of Bloch walls in ferromagnets. Ferromagnets are characterised by the fact that they have large regions where the magnetic dipoles in the crystal lattice are parallel. To reduce the total magnetic energy of the ferromagnet, normally, more than one of these regions, called ferromagnet domains, exist. It is the boundaries between these domains that are known as Bloch walls. The order parameter here, is the magnetic moment field $\vec{m}(\vec{x})$ since the different regions will have different magnetic moments. In this scheme the Bloch walls are characterised by the transitions of the order parameter between the domains. The order parameter and an “effective magnetic field” can then be used to reduce the equation of motion to the sine-Gordon equation in certain circumstances [10]. In two spatial dimensions, the isotropic Heisenberg ferromagnet exhibits pseudoparticle (instanton) solutions. This model is in fact identical, from an effective field theory perspective, to the nonlinear $O(3)$ σ -model or the so-called CP^1 model. The CP^1 model is remarkable in the richness of its solution space, with the first topologically stable solitons discovered by Belavin and Polyakov [11] and general classical solutions discovered by Din and Zakrzewski [12].

Of the solitons found in condensed matter physics, the vortices of superfluids and superconductors are the most relevant to our work. In a latter part of this text we shall consider the static vortex solutions to the Ginzburg-Landau model and the equations known as the complex sine-Gordon 1 and complex sine-Gordon 2 equations. The Ginzburg-Landau equation describes static vortex solutions in both superfluids and su-

perconductors. One form for the Ginzburg-Landau equation is:

$$-(\nabla - i\mathbf{A})^2\psi + \frac{\lambda}{4}(|\psi|^2 - 1)\psi = 0, \quad (1)$$

where the complex field ψ is the continuous order parameter. *Vortices* are characterised by the way they realise a $S^1 \rightarrow S^1$ map of a circle with infinitely large radius on the (x, y) -plane to a unit circle in the internal space $(\text{Re}\psi, \text{Im}\psi)$. The vortices are classified according to the Brouwer degree of the map,

$$Q = \lim_{R \rightarrow \infty} \frac{1}{2\pi} \oint_{C_R} d(\arg \psi) = \frac{1}{2\pi} \int_{\mathbb{R}^2} \epsilon_{ij} \partial_i \partial_j (\arg \psi) d^2x. \quad (2)$$

frequently called the topological charge. This topological charge is also known as the winding number, or vorticity of the vortex.

Superfluids are described by the Ginzburg-Landau equation with no gauge field, i.e. equation (1) with $\mathbf{A} = 0$, also known in condensed matter physics as the Ginzburg-Pitaevskii [14] equation. This equation is the static form of the Gross-Pitaevskii equation: A Schrödinger equation with a nonlinear self-interaction term, used to describe condensates of an interacting Bose system. The most commonly studied superfluid is HeII, which is He^4 that has been cooled to temperatures below 2.17 K at vapour pressure. Since the He^4 atoms have integer spin, they are able to form a Bose condensate, allowing superfluidity to occur. The field ψ , the order parameter, can be written as $\psi = |\psi|e^{iS}$, where $|\psi|^2$ is proportional to the density of superfluid and S is a real valued phase such that ∇S is proportional to the velocity of the superfluid. The vortices which are observed in HeII appear as vortex lines; structures whose spatial cross sections are 2D vortices. Basically, the cores of these 2D vortices trace out a line in the third spatial dimension. The vortex lines are observed by cooling a bucket of HeII while rotating it about the z -axis with constant angular velocity. Vinen [13] was the first to obtain experimental evidence of a single quantum of circulation, while the theory of quantised circulation was initiated by the work of Onsager [15] and Feynman [16].

In superconductors, vortices are observed when a magnetic field is applied to a so-called type-II superconductor. Superconductors may exist as the electrons (which are fermions) in the superconductor form bound pairs known as Cooper pairs, or superconducting electrons [17]. These pairs of bound electrons have twice the mass and twice the charge of an electron but have no spin. Thus the Cooper pairs are bosons and may form a Bose-Einstein condensate; in an aggregate all the pairs may occupy the same state. For superconductors, the complex order parameter, ψ can be written as $|\psi|e^{i\chi}$, where $|\psi|^2$ is proportional to the density of superconducting electrons and the real valued phase χ is such that $\nabla\chi$ is proportional to the supercurrents. The Ginzburg-Landau parameter $\frac{\lambda}{4}$ in equation (1) is related to the ratio of two physical constants, both of which are dependent on temperature. These are the penetration depth κ of the magnetic field and the coherence length ξ (or core radius) of the vortices. For a detailed descriptions of vortices in superconductors and superfluids we refer the reader to [18, 19].

Vortices are, however, not restricted to condensed matter physics but also occur in other fields. In particle physics there is a well known field-theoretic model, the Abelian

Higgs model, which admits vortex solutions. It consists of a pure gauge field term, of the Maxwell type, and a self-interacting charged scalar field minimally coupled to the gauge field. The action is of the form

$$S_{AH} = \frac{1}{2} \int \left\{ |D_\mu \psi|^2 + \frac{1}{2} F_{\mu\nu} F^{\mu\nu} + \frac{\lambda}{4} (|\psi|^2 - 1)^2 \right\} d^n x, \quad (3)$$

where $D_\mu = \partial_\mu - iA_\mu$ is the gauge covariant derivative and $F_{\mu\nu} = \partial_\mu A_\nu - \partial_\nu A_\mu$ the curvature of the connection A_μ . Physically, the gauge field may be interpreted as an electromagnetic 4-vector potential and $F_{\mu\nu}$ as the electromagnetic strength tensor. The complex scalar field ψ is the (charged) Higgs field. Note that the static version of the Abelian Higgs model is mathematically equivalent to the Ginzburg-Landau theory [20]. This equivalence was exploited by Nielsen and Olesen [20] to construct vortex line solutions to the Abelian Higgs model. It was also shown that the dynamics of the Nielsen-Olesen vortices is governed by a Nambu type action [21, 22]. This supports the thesis that they may be identified with dual strings, in some “super-quantum” mechanical limit. At present the Nielsen-Olesen vortices are usually identified with cosmic strings. For a while, it was thought that these cosmic strings might have been seeds for structure formation [23] in the early universe. However, calculations of Durrer [24] indicate that cosmic string loops are, most probably, unimportant in structure formation. An interesting “digression” is the Falaco soliton [25], which is analogous to cosmic strings but can be produced in a swimming pool.

Another set of field theoretic models which display vortex solutions, are the Chern-Simons models in (2+1)-dimensions. It has long been known that, with the introduction of a term proportional to $\epsilon^{\mu\nu\rho} A_\mu F_{\nu\rho}$ in the action, odd-dimensional spacetimes allow for the possibility of topologically massive gauge dynamics. This term is known as the Chern-Simons term. Vortices of the Nielsen-Olesen type, have been found for certain Chern-Simons-Higgs theories [27, 28], however, the Chern-Simons vortices are charged while the Nielsen-Olesen vortices are not. Vortex solutions have also been constructed for Maxwell-Chern-Simons theories coupled to nonrelativistic bosonic [29, 30] and fermionic [31, 32, 33, 34] fields. The action in [29, 30] is a modified version of the one found in [35], such that the usual integrals for the number of particles and the momentum yield the regularised integrals. In [34] the charge conservation laws allow for a stable configuration of multiple vortices (with binding energy).

Solving nonlinear evolution equations

Obviously, once a field theory is formulated a means for solving the nonlinear equations of motion is needed. Since this is a relatively complex procedure, the development of methods and techniques for finding soliton solutions, to nonlinear evolution equations, and studying their properties has become one of the fastest growing fields in mathematical physics and nonlinear science. Fortunately, many equations which exhibit solitons have various special properties which have facilitated the development of methods for solving them. Some of these special properties are; an infinite number of conserved charges, Lie-Bäcklund symmetries [36], Bäcklund transformations and reduction to ordinary differential equations of the Painlevé type (Painlevé property)[37]. It is also possible that the nonlinear evolution equations may be recast in Lax’s form [38], implying they

are completely integrable. Amongst the various methods developed for solving completely integrable nonlinear evolution equations, are the inverse scattering transform, the Estabrook-Wahlquist prolongation method and the symmetry approach. There are also methods like the bilinear approach of Hirota [39] and the dressing method of Zakharov and Shabat [40], which are probably the most convenient for finding particular solutions.

The first application of the inverse scattering transform, a method for solving an initial value problem, occurred while finding a solution to the Korteweg-de Vries (KdV) equation for shallow water waves [41]. This formalism was then generalised by Lax [38]. For a simple review of the inverse scattering transform we refer the reader to [1]. Lax's technique was then adapted to solve the nonlinear Schrödinger equation [42], then generalised allowing us to solve the initial value problem for a broad class of physically relevant problems [43], such as the sine-Gordon, Benney-Newell and modified KdV equations. The power of the inverse scattering transform lies in its reduction of the nonlinear equation in question to a sequence of *linear* equations, which are then solved. Closely linked to the inverse scattering transform are the Bäcklund transformations and symmetries. An interesting discussion on the link between Bäcklund transformation laws and the inverse scattering transform may be found in [44]. Bäcklund transformations are very useful as they are transformations in the solution space of the nonlinear equations. Thus once one has a solution to a nonlinear evolution equation, the Bäcklund transformations generates new solutions. For an introduction to the Estabrook-Wahlquist prolongation method and the symmetry approach mentioned above we refer the reader to the introductory chapters in [45] and references therein.

There are, however, some simpler methods for proving the existence of and for finding new solutions to nonlinear field theories. For example, by counting the number of zero modes we are able to determine if a given soliton φ , to a nonlinear evolution equation, belongs to a larger family of solutions. In fact, it is this method of calculating zero modes which we will implement in this thesis. For a more detailed description of why zero modes count the number of continuous transformations that generate new solitons, we refer the reader to section 1.1. For now, we will present a brief overview of zero modes and their history in field theory.

Zero Modes

Firstly, what are zero modes? *We will call a zero mode an eigenfunction of the operator obtained by linearising the nonlinear evolution equation about the soliton φ , corresponding to a zero eigenvalue.* Generally, the zero mode is a solution which has the same time dependence as the soliton itself. We immediately notice a powerful property of counting zero modes; we need only find solutions to *linear* differential equations. The most important feature of zero modes, for us, is that the number of zero modes counts the number of *continuous degrees of freedom* of the soliton. By this we mean that they count the number of independent parameters of continuous transformations that take the soliton φ to another solitonic solution. For *static* solitons the number of zero modes is exactly the *dimension* of the moduli space of the soliton plus the number of gauge transformations of the theory. The moduli space of a soliton is the parameter space of

such solitonic solutions which are gauge equivalent [46, 47].

Another interpretation of zero modes is as follows: Suppose that φ , a soliton of an equation of motion, belongs to a larger class of solitonic solutions Ψ :

$$\varphi = \Psi(\alpha_1, \dots, \alpha_n)|_{\alpha_1 = \dots = \alpha_n = 0}, \quad (4)$$

and that the real parameters, α_i , are continuous. Then φ has n zero modes with each zero mode corresponding to one of the parameters, α_i . Thus the zero modes count the continuous parameters of the largest class of solitonic solutions to which the soliton in question, φ , belongs.

Originally studies of the modes of the linearised equations of motion were motivated by stability considerations. Depending on the form of the assumed solution to the linearised equation of motion and the eigenvalue problem obtained, certain eigenvalue regimes could correspond to unstable solutions. To illustrate this consider the following example: Suppose we assume a solution of the form $f(\vec{x})e^{i\omega t}$ to a linearised equation of motion, reducing it to an eigenvalue problem of the form $L[f] = \omega^2 f$, where L is a differential operator independent of t . If this eigenvalue problem has negative eigenvalues ($\omega^2 < 0$) then ω is pure imaginary, i.e. $\omega = i\alpha$ for $\alpha \in \mathbb{R}$. Thus the solution to the linearised equation of motion grows exponentially with time. Hence the soliton of the nonlinear equation of motion is unstable.

The method of counting zero modes, has been fairly popular for finding the number of free parameters of multi-solitons [51, 57, 59, 64, 65]. Why is it useful to know the number of free parameters? One reason is that the number of free parameters gives an indication as to whether the multi-soliton can be separated into a configuration of multiple solitons with finite separation. In fact, this analysis may be extended to determining possible bound states of the solitonic configurations. This application was realised by Rebbi and Jackiw while studying small fluctuations about instantons in the $SU(2)$ Euclidean Yang-Mills model. At the time, they were addressing the question of how to extract information of the quantum theory from the classical fields [48].

Applications of counting zero modes

The existence of an n -instanton solution to an $SU(2)$ Yang-Mills theory on \mathbb{R}^4 , was proved by Belavin *et al.* [50]. They found that, when the field is self- or anti-self dual ($F_{\mu\nu} = \pm \frac{1}{2}\epsilon_{\mu\nu\rho\gamma}F^{\rho\gamma}$), the Yang-Mills action obtains a local minimum. These authors also constructed the *unit charge* solution ($n = 1$), depending on 5 parameters; 4 parameters specifying the position and a scale parameter. If the pseudoparticles were non-interacting, one would expect exactly $5n$ parameters necessary to describe an n -instanton configuration. Such a solution was discovered by 't Hooft. However, Jackiw *et al.* [51] were able to show that 't Hooft's solution must be generalised to ensure that it is covariant under conformal transformations. The new solution required five parameters for the single pseudoparticle, thirteen for two pseudoparticles at a finite separation and $5n + 4$ for $n \geq 3$ pseudoparticles. In fact, it was realised that these solutions are not the most general solutions [49]. By counting the number of zero modes of the linearised equation of motion, Jackiw and Rebbi were able to show that, on \mathbb{R}^4 , at least $8n - 3$

parameters are required to describe an n -instanton configuration of the $SU(2)$ Yang Mills. Thus this simple method was able to predict the existence of a larger class of solutions to the self-dual Yang Mills equations than known at that time. It is in the spirit of such discoveries that we claim that zero modes are able to shed light on the “size” of the moduli space of solutions. At the same time, Schwarz [52] also calculated the number of parameters describing a self-dual n -instanton configuration to be $8n - 3$, using the Atiyah-Singer index theorem [53]. Later on solutions with $8n - 3$ parameters were discovered [54, 55, 56]. The papers by Jackiw and Rebbi and by Schwarz appeared back to back in *Physics Letters* in 1977. This is just one of the cases in history where physics and mathematics have progressed, unbeknown to each other, along parallel paths.

Jackiw also used the method of calculating zero modes [57] to show that the kink of the sine-Gordon and that of the φ^4 theory only have one zero mode each, the zero mode corresponding to translational invariance. Therefore translational invariance is the only continuous invariance exhibited by these kinks. A

For a specific value of the self interaction parameter λ , of the scalar field in the Abelian Higgs model (and Ginzburg-Landau model), Bogomol’nyi [58] showed that a lower bound on the energy of a n -vortex configuration can be saturated. Recall that the Abelian Higgs model is a relativistic generalisation of the Ginzburg-Landau model. Weinberg [59] was then able to show, using a special case of the Atiyah-Singer index theorem and also by calculating zero modes, that for this specific value of λ , $2n$ parameters are needed for describing an n -vortex configuration in the Ginzburg-Landau model. These $2n$ parameters are the position parameters of the individual vortices. Thus one is able to split the coaxial n -vortex into n single vortices with finite separations. This agrees with the numerical work by Jacobs and Rebbi [60] which shows that for this critical value of λ the energy of the system is independent of the vortex separation. Following the formalism of Weinberg, Burzlaff and Tchrakian [61] were able to show that the rotationally symmetric self-dual n -vortex of a generalised Abelian Higgs model has also $2n$ zero modes.

In the late 1980’s high- T_c superconductors were discovered and it was thought that they were characterised by their 2-D structure and a P- and T-violating statistical interaction. It was for this reason that Hong *et al.* [62] considered the Ginzburg-Landau model with an additional Chern-Simons term. To solve the system they neglected the Maxwell term in the action as the Chern-Simons term is dominant:

$$S = \int \left\{ \frac{1}{4} \mu \epsilon^{\mu\nu\rho} A_\mu F_{\nu\rho} + \frac{1}{2} |(\partial_\mu - ieA_\mu) \varphi|^2 - V(|\varphi|^2) \right\} d^3x. \quad (5)$$

Also, it had been previously pointed out that the Higgs mechanism could transform a non-dynamical gauge field into a massive one. With the above assumption Hong *et al.* then solved the equations of motion in the Bogomol’nyi limit and found that $2n$ -moduli (position parameters) are needed to describe an n -vortex configuration. Essentially the same system was studied by Jackiw and Weinberg [63] with the same conclusions. The two papers appeared back to back in *Physical Review Letters* in May 1990. (Note that

Jackiw and Weinberg found the numerical solution to the field theory, while Hong *et al.* only considered the asymptotic behaviours.)

Another Chern-Simons field-theoretic model where zero modes have been used is the one considered in [64]. Here Kim *et al.* considered a nonlinear, planar Schrödinger equation of motion coupled to an $SU(2)$ Chern-Simons field. By counting the number of zero modes they were able to show that a $U(1)$ invariant n -soliton solution depends on $4n + 2$ parameters. Of these $2n$ are position parameters, n are phase and n are scale parameters. The last 2 are for the global $SU(2)$ phase. Another paper [65] demonstrated that non-relativistic Chern-Simons solitons with a flux number of $2n$ require $4n$ -parameters. This result was accomplished using both an index theorem and by counting zero modes.

The main aim of this thesis is to analyse the zero modes exhibited by the coaxial vortices of the Ginzburg-Landau (in the absence of a magnetic field), Euclidean complex sine-Gordon-1 and sine-Gordon-2 models. The Ginzburg-Landau model is a well known and widely studied theory. A motivation for studying the Euclidean complex sine-Gordon models is that they are remarkably similar to the Heisenberg ferromagnet model [66] with easy-plane anisotropy and the Ginzburg-Landau model. The complex sine-Gordon models also, as mentioned, display topological solitonic solutions; vortices [67]. However, unlike the Ginzburg-Landau and Heisenberg ferromagnet models, the vortices for the complex sine-Gordon models are known exactly and in closed analytic form. Therefore they provide a means for studying properties and phenomenology of vortices. These three models (Ginzburg-Landau and the two complex sine-Gordons) are discussed in more detail at the beginning of the relevant chapters.

A brief outline of this thesis

In Chapter 1 we present a short description of zero modes and what they correspond to. We then further explore zero modes and how their number corresponds to the number of continuous degrees of freedom of the solitons, by studying various “toy” models. At the end of the chapter there is a short discussion of our conclusions from the analysis of these models.

In Chapter 2 we make use of the ideas formulated in Chapter 1 and calculate the zero modes of the coaxial multivortices of the Ginzburg-Landau equation in $(2+1)$ dimensions. This system is solved numerically, as no analytical form is known for the vortices of the Ginzburg-Landau model. Chapter 3 concerns the analysis of the zero modes of one of the Euclidean complex sine-Gordon equations (complex sine-Gordon-1). Again the system is solved numerically, this time due to the complexity of the eigenvalue problem. We also compare the zero modes obtained numerically to the zero modes resulting from the free parameters describing a recently discovered non-coaxial, multivortex solution. In Chapter 4 we analyse the zero modes of the coaxial vortices of the complex sine-Gordon-2. Finally, the conclusions drawn from the results of this work are presented.

Chapter 1

Zero Modes

As mentioned in the introduction the number of zero modes counts the *continuous degrees of freedom* of the soliton: The number of continuous transformations which transform the soliton to another solitonic solution. An equivalent way of stating this is; the number of zero modes counts the number of continuous parameters of the largest class of solitonic solutions, of which the soliton in question is a member. In this chapter we answer the questions of why this is and of how to obtain the zero modes? First, we present a general methods and techniques section. Then, we gain a better intuition and understanding by analysing various “toy” models.

1.1 What are Zero Modes?

Before we discuss how zero modes count the degrees of freedom, we should know what zero modes are. Assume that we have the nonlinear equation of motion of the form

$$f(x_i)\partial_t^n\psi + \mathcal{F}[x_i, \partial_{x_i}; \psi] = 0, \quad (1.1)$$

where $f(x_i)$ takes its values in \mathbb{C} , the x_i are the spatial coordinates, t is time and ∂_ξ is the partial derivative with respect to ξ . We have restricted ourselves to a subset of all possible equations of motion but this subset will suffice for our purposes. Where necessary one may extend the theory appropriately. Note, that the field ψ is a scalar function of the x_i and t . We also assume that this equation of motion has the solitonic solution ψ_s . We now linearise the equation of motion (1.1) by replacing ψ in the equation of motion with the soliton plus an infinitesimal perturbation,

$$\psi(\vec{x}, t) \rightarrow \psi_s(\vec{x}, t) + \epsilon\delta\psi(\vec{x}, t), \quad \epsilon \ll 1 \quad (1.2)$$

and expand in ϵ . From this we obtain:

$$\{f(\vec{x})\partial_t^n\psi_s + \mathcal{F}[x_i, \partial_{x_i}; \psi_s]\} + \epsilon\{f(\vec{x})\partial_t^n + \mathcal{G}[x_i, \partial_{x_i}; \psi_s]\}\delta\psi + \mathcal{O}(\epsilon^2) = 0, \quad (1.3)$$

where the term of $\mathcal{O}(\epsilon^1)$ is a linear differential operator acting on $\delta\psi$. If this perturbed solution remains a solution then equation (1.3) must be satisfied. More importantly each coefficient in the expansion in ϵ must be zero. It is obvious that the coefficient of the term

$\mathcal{O}(\epsilon^0)$ is zero since ψ_s is a soliton of the equation of motion (1.1). Setting the coefficient of the term $\mathcal{O}(\epsilon)$ to zero, we obtain

$$\{f(\vec{x})\partial_t^n + \mathcal{G}[x_i, \partial_{x_i}; \psi_s]\} \delta\psi = 0. \quad (1.4)$$

We will refer to this as the linearised equation of motion.

For the moment we are going to restrict ourselves to the case of static solitons. When necessary we will generalise this procedure to include certain time-dependent solitons.

We now assume a solution to equation (1.4) of the form $\delta\psi(\vec{x}, t) = \varphi(\vec{x})e^{\lambda t}$, such that the linear equation of motion (1.4) reduces to:

$$\mathcal{G}[x_i, \partial_{x_i}; \psi_s]\varphi(\vec{x}) = \lambda^n f(\vec{x})\varphi(\vec{x}), \quad (1.5)$$

a generalised eigenvalue problem, with eigenvalue λ^n . Note that the eigenfunctions corresponding to $\lambda^n = 0$, the zero eigenvalue, are static. In other words, they have the same time dependence as the soliton ψ_s , about which we linearised. This is very important as it means the perturbation $\delta\psi$ is stable; it neither 'blows up' nor alters the time dependence of the soliton ψ_s . Another term for a zero eigenfunction is a zero mode. It is now evident where the term *zero mode* originates and that the zero modes have the same time dependence as the soliton.

Thus the zero modes of a soliton are solutions to the linearised equation of motion, which have the same time dependence as the soliton itself

Now that we know what zero modes are, we would like to know why they correspond to continuous degrees of freedom. Suppose that the soliton ψ_s is a member of a larger class of solutions,

$$\psi_s(\vec{x}) = \Psi(\vec{x}, \alpha)|_{\alpha=0}, \quad (1.6)$$

where $\Psi(\vec{x}, \alpha)$ is also a soliton solution of the field theory. Taking a Taylor expansion of $\Psi(\vec{x}, \alpha)$ in α we obtain:

$$\begin{aligned} \Psi(\vec{x}, \alpha) &= \Psi(\vec{x}, 0) + \alpha \left[\frac{\partial}{\partial \alpha} \Psi(\vec{x}, \alpha) \right]_{\alpha=0} + \mathcal{O}(\alpha^2) \\ &= \psi_s(\vec{x}) + \alpha \left[\frac{\partial}{\partial \alpha} \Psi(\vec{x}, \alpha) \right]_{\alpha=0} + \mathcal{O}(\alpha^2). \end{aligned} \quad (1.7)$$

Now if α is infinitesimal, then by comparing this to (1.2) it follows that $\frac{\partial}{\partial \alpha} \Psi(\vec{x}, \alpha)|_{\alpha=0}$ must solve (1.4). Also $\frac{\partial}{\partial \alpha} \Psi(\vec{x}, \alpha)|_{\alpha=0}$ has the same time dependence as the soliton ψ_s and must solve the eigenvalue problem (1.5) with $\lambda = 0$. Therefore $\frac{\partial}{\partial \alpha} \Psi(\vec{x}, \alpha)|_{\alpha=0}$ is a zero mode of the soliton ψ_s . From this it is clear that each continuous degree of freedom will give rise to a zero mode. Thus each transformation, which takes the soliton ψ_s to another solitonic solution of the same model, will give rise to a zero mode. We also now have a means of determining which zero mode corresponds to which transformation (or parameter α). *The zero mode corresponding to the free parameter α is given by*

$$\frac{\partial}{\partial \alpha} \Psi(\vec{x}, \alpha)|_{\alpha=0}. \quad (1.8)$$

We now proceed with the study of zero modes and corresponding degrees of freedom by considering various "toy" models: scalar field theories, real and complex, in several different dimensions.

1.2 Some Real Scalar Fields

Of the multitude of real scalar theories in (1+1)-dimensions (one spatial and one temporal) we consider the φ^4 theory and the real sine-Gordon equation.

1.2.1 φ^4 Theory

Firstly we examine the φ^4 theory in (1+1)-dimensions with a positive mass squared term. The action for this field theory

$$S = \frac{1}{2} \int \{\varphi_x^2 - \varphi_t^2 + \varphi^2 - \varphi^4\} d^2x, \quad (1.9)$$

attains a minimum when φ solves the equation of motion

$$-\varphi_{xx} + \varphi_{tt} + \varphi - 2\varphi^3 = 0. \quad (1.10)$$

One of the solutions to (1.10) is a bell-shaped soliton of the form $\varphi^s(x) = \text{sech } x$. When we linearise (1.10) about the soliton φ^s by letting $\varphi = \varphi^s + \epsilon\delta\varphi$ in (1.10) and collecting terms $\mathcal{O}(\epsilon)$, we obtain

$$-\delta\varphi_{xx} + \delta\varphi_{tt} + \delta\varphi - 6(\varphi^s)^2\delta\varphi = 0. \quad (1.11)$$

Assuming a separable solution to (1.11), of the form $\delta\varphi(x, t) = u(x)e^{i\omega t}$, reduces the equation to an eigenvalue problem

$$\begin{aligned} \mathcal{L}u(x) &= \omega^2 u(x), \\ \mathcal{L} &:= -\partial_x^2 + 1 - 6\text{sech}^2 x, \end{aligned} \quad (1.12)$$

for $u(x)$. If we can find an eigenfunction corresponding to the eigenvalue $\omega^2 = 0$, then the perturbation, $\delta\varphi$, is independent of time. Since the soliton φ^s is also time independent, the solution will be stable. It is easily seen that $u_0(x) = \text{sech } x \tanh x$ is a solution to (1.12) with $\omega^2 = 0$, which tends to zero as $|x| \rightarrow \infty$. Thus u_0 is an eigenfunction, more importantly it is a zero mode. Furthermore (1.12) is a one-dimensional, Sturm-Liouville eigenvalue problem thus the discrete eigenvalues are simple and u_0 is the *only* eigenfunction corresponding to $\omega^2 = 0$.

Now that we have found a zero mode we would like to know what continuous degree of freedom it corresponds to. Since we know, from the form of (1.10), that all of its solutions have translations in x as a degree of freedom, it is a reasonable ansatz that this is the origin of the zero mode u_0 . To verify this, we take a Taylor expansion of $\varphi^s(x + \epsilon)$ for an infinitesimal translation ($\epsilon \ll 1$):

$$\begin{aligned} \varphi^s(x + \epsilon) &= \varphi^s(x) + \epsilon \frac{d\varphi^s(x)}{dx} + \mathcal{O}(\epsilon^2) \\ &= \varphi^s(x) + \epsilon \left. \frac{d\varphi^s(x + \epsilon)}{d\epsilon} \right|_{\epsilon=0} + \mathcal{O}(\epsilon^2). \end{aligned} \quad (1.13)$$

Comparing this with $\varphi \rightarrow \varphi^s + \epsilon\delta\varphi$, for the perturbation, it is clear that $\frac{d\varphi^s}{dx}$ is a solution to the linearised equation of motion as the translated soliton is still a solution of the

ϕ^4 theory. Also $\frac{d\varphi^s}{dx}$ is static like the soliton ψ^s and thus solves the eigenvalue problem (1.12) with $\omega = 0$. Hence it is a zero mode. Since

$$u_0 = \frac{d\varphi^s}{dx} = \operatorname{sech} x \tanh x,$$

the zero mode u_0 we calculated corresponds to the translational degree of freedom.

Next we consider the kink solution of the sine-Gordon equation.

1.2.2 The sine-Gordon kink

The sine-Gordon action

$$\mathcal{S} = \frac{1}{2} \int \{\varphi_x^2 - \varphi_t^2 + 2(1 - \cos \varphi)\} d^2x, \quad (1.14)$$

in (1+1)-dimensions, is minimised when φ satisfies the equation of motion

$$\varphi_{tt} - \varphi_{xx} + \sin \varphi = 0. \quad (1.15)$$

This is a prolific theory and has appeared in many fields, *inter alia* condensed matter physics with the description of propagation of crystal dislocations, Bloch wall motion in magnetic materials [10] [70] and the propagation of magnetic flux on Josephson lines [71, 72]. It also appears in elementary particle physics originally through [73, 74] and has played a role in the theory of surfaces of constant, negative curvature [75]. The origin of the name sine-Gordon is quite interesting, as it appeared originally as a private joke in a letter by David Finkelstein.

The sine-Gordon equation of motion is known to have the stationary kink $\varphi^k(x) = 4 \arctan(e^x)$ as a solitonic solution. This is a soliton as the energy density of the static kink φ^k ,

$$\begin{aligned} \varepsilon &= \frac{1}{2} (\partial_x \varphi^k)^2 + (1 - \cos \varphi^k) \\ &= 4 \operatorname{sech}^2 x, \end{aligned}$$

is localised. When we take $\varphi \rightarrow \varphi^k + \varepsilon \delta\varphi$ in (1.15) and collect terms $\mathcal{O}(\varepsilon)$, in other words linearise (1.15) about φ^k , we obtain:

$$\delta\varphi_{tt} - \delta\varphi_{xx} + \cos \varphi^k(x) \delta\varphi = 0. \quad (1.16)$$

Assuming a separable solution of the form $\delta\varphi(x, t) = u(x) \exp(i\omega t)$ reduces (1.16) to an eigenvalue problem

$$\mathcal{L}u(x) = \omega^2 u(x), \quad (1.17)$$

where

$$\begin{aligned} \mathcal{L} &:= -\partial_x^2 + \cos \varphi^k(x) \\ &= -\partial_x^2 + 1 - 2 \operatorname{sech}^2 x. \end{aligned}$$

As with the previous section the eigenvalue problem (1.17) is a Sturm-Liouville problem and thus has simple eigenvalues. Therefore $u_0 = \text{sech } x$ is the *only* eigenfunction corresponding to the eigenvalue $\omega^2 = 0$. This zero mode, as with the φ^4 theory, corresponds to the translational degree of freedom in x since

$$\frac{d\varphi^k}{dx} = 2 \text{sech } x = 2u_0.$$

Remember that u_0 is an eigenfunction of a linear eigenvalue problem and as such any scalar multiple of u_0 is also an eigenfunction with the same eigenvalue.

For both the φ^4 lump and the sine-Gordon kink solitons there is only one zero mode each. Therefore the *translational* degree of freedom of both solitons is the *only* degree of freedom they exhibit.

We will now consider a real scalar field theory in (2+1)-dimensions with a cubic and a quintic term in the equation of motion.

1.2.3 Massless cubic-quintic Klein-Gordon equation

An action for this scalar field theory in (2+1)-dimensions is given by

$$S = \frac{1}{2} \int \{(\nabla\varphi)^2 - \varphi_t^2 + \frac{1}{2}\varphi^4 - \varphi^6\} d^3x, \quad (1.18)$$

where $\nabla \equiv \hat{r}\partial_r + \hat{\chi}\frac{1}{r}\partial_\chi$ and r and χ are the polar coordinates. The Euler-Lagrange equation of motion obtained from (1.18) is

$$\varphi_{tt} - \nabla^2\varphi + \varphi^3 - 3\varphi^5 = 0, \quad (1.19)$$

where $\nabla^2 \equiv \frac{1}{r}\partial_r(r\partial_r) + \frac{1}{r^2}\partial_\theta^2$ is the Laplace operator in two dimensions. This equation of motion has a "lump" solution of the form

$$\varphi^l(r) = (1 + r^2)^{-1/2}. \quad (1.20)$$

Linearising the equation of motion (1.19) about this solution, gives the equation

$$\delta\varphi_{tt} - \nabla^2\delta\varphi + 3(\varphi^l)^2\delta\varphi - 15(\varphi^l)^4\delta\varphi = 0, \quad (1.21)$$

for the perturbation $\delta\varphi$. This, we can then reduce to an eigenvalue problem

$$-u_{rr} - \frac{u_r}{r} - \frac{u_{\theta\theta}}{r^2} + \frac{3r^2 - 12}{(1 + r^2)^2}u = \omega^2u, \quad (1.22)$$

by assuming a separable solution of the form $\delta\varphi(r, \theta, t) = u(r, \theta)e^{i\omega t}$. The boundary conditions for the eigenfunctions of (1.22) are: $|u(0, \theta)| < \infty$ and $u(r, \theta) \rightarrow 0$ as $r \rightarrow \infty$. To solve (1.22) we take a Fourier series expansion of u in θ :

$$u(r, \theta) = \sum_{m=-\infty}^{\infty} R_m(r)e^{im\theta}, \quad (1.23)$$

and substitute this into (1.22). This converts (1.22) into an ordinary differential eigenvalue problem

$$-R_{rr} - \frac{1}{r}R_r + \left[\frac{m^2}{r^2} + \frac{3r^2 - 12}{(1 + r^2)^2} \right] R = \omega^2 R, \quad (1.24)$$

for each value of m^2 . The eigenfunctions R_m satisfy the boundary conditions $|R_m(0)| < \infty$ and $R_m(r) \rightarrow 0$ as $r \rightarrow \infty$. For uniqueness of u at the origin however, we require $R_m(0) = 0$ for $m \neq 0$. In addition to this, the index theorem indicates that $R_m(r) \sim r^{|m|}$ for $r \sim 0$: Substituting $R = r^n$ into (1.24) and taking a Taylor expansion about $r = 0$, we find the terms $\mathcal{O}(r^{n-2})$ give the constraint $m^2 = n^2$. Therefore, requiring regularity of R at the origin gives $n = |m|$.

Applying the transformation $R_m(r) = f(r)/\sqrt{r}$ to equation (1.24) reduces it to the simpler form:

$$-\frac{d^2 f}{dr^2} + \left[\frac{m^2}{r^2} - \frac{1}{4r^2} + \frac{3r^2 - 12}{(1 + r^2)^2} \right] f \equiv -\frac{d^2 f}{dr^2} + V_{m^2}(r)f = \omega^2 f, \quad (1.25)$$

where V_{m^2} can be considered as an effective potential. From the boundary conditions of R we easily derive the boundary conditions for $f(r)$: $f(r) \sim r^{|m|+1/2}$ for $r \sim 0$ and $f \rightarrow 0$ as $r \rightarrow \infty$.

Since the effective potential decays to 0 as $|r| \rightarrow \infty$, we are guaranteed that all values $\omega^2 > 0$ are eigenvalues. However, we are not guaranteed that the eigenvalue $\omega^2 = 0$ exists; in other words, there may or may not exist a bounded solution (eigenfunction) for $\omega^2 = 0$. For bound solutions of (1.25) with $\omega^2 = 0$ to occur, the potential

$$V_{m^2}(r) = \frac{r^4(4m^2 + 11) + r^2(8m^2 - 50) + (4m^2 - 1)}{4r^2(1 + r^2)^2}, \quad (1.26)$$

must be negative, in at least some region. This becomes clear if we multiply equation (1.25) by f and integrate over the plane:

$$\int \int_{\mathbb{R}^2} \left\{ -\frac{d^2 f}{dr^2} f + V_{m^2}(r)f^2 \right\} = 0, \quad (\omega^2 = 0),$$

and then integrate the first term on the right by parts:

$$\int \int_{\mathbb{R}^2} \left\{ \left(\frac{df}{dr} \right)^2 + V_{m^2}(r)f^2 \right\} + \left[\frac{df}{dr} f \right]_{\partial \mathbb{R}^2} = 0.$$

Since the boundary term is zero, the integral must be zero and this can only occur if V_{m^2} is negative in at least some region. This, in turn, will only occur if the discriminant of the quadratic (in r^2) numerator of (1.26),

$$\begin{aligned} \mathcal{D} &= (8m^2 - 50)^2 - 4(4m^2 + 11)(4m^2 - 1) \\ &= -960 \left(m^2 - \frac{53}{20} \right) \end{aligned}$$

is greater than zero, thus only if $m^2 \leq 53/20 < 3$.

Since m is integer, the *only* values of m , for which bound states may occur are $m = 0$ and $m = \pm 1$. Therefore these are the only values of m , for which zero modes may exist.

For $m^2 = 1$ the eigenfunction* of (1.25) corresponding to the eigenvalue $\omega^2 = 0$, is $f_{1,1} = r^{3/2}(1+r^2)^{-3/2}$. This is the only solution since (1.25) is a Sturm-Liouville problem for each m^2 and thus has simple eigenvalues. Hence

$$u_1 = \frac{r}{(1+r^2)^{3/2}} e^{i\theta} \quad (1.27)$$

$$u_2 = \frac{r}{(1+r^2)^{3/2}} e^{-i\theta} \quad (1.28)$$

are two zero modes ($u = f_{n,m^2} \sqrt{r} e^{\pm im\theta}$), corresponding to two continuous degrees of freedom of the "lump" solution φ^l . We now show that these zero modes correspond to the translational degrees of freedom in x and y directions. As previously, we take the partial derivative of φ^l with respect to x and y ;

$$\partial_x \varphi^l = \partial_r \varphi^l \partial_x r = \partial_r \varphi^l \frac{x}{r} = \partial_r \varphi^l \cos \theta$$

$$\partial_y \varphi^l = \partial_r \varphi^l \partial_y r = \partial_r \varphi^l \frac{y}{r} = \partial_r \varphi^l \sin \theta,$$

to obtain the zero modes corresponding to the translational degrees of freedom. These, however are not the same as u_1 and u_2 , so how do we know the zero modes from translations and the zero modes u_1 and u_2 are equivalent? Using the fact that $\partial_r \varphi^l = -r(1+r^2)^{-3/2}$, we discover that the two linearly independent, *linear* combinations,

$$-(\partial_x \varphi^l + i \partial_y \varphi^l) = r(1+r^2)^{-3/2} e^{i\theta},$$

$$\partial_x \varphi^l - i \partial_y \varphi^l = r(1+r^2)^{-3/2} e^{-i\theta},$$

which are also zero modes, are none other than u_1 and u_2 . Any linear combination of eigenfunctions, corresponding to the same eigenvalue, of a linear eigenvalue problem, such as (1.25), is still an eigenfunction corresponding to that eigenvalue. Hence the zero modes u_1 and u_2 correspond to the translational degree of freedom of φ^l .

For $m = 0$, we have not been able to show that a bound solution for (1.25) with $\omega^2 = 0$ exists nor that it does not exist.

Thus for the "lump" solution of the massless cubic-quintic equation we have only been able to find two degrees of freedom; those for translation in the x and y directions. There is the possibility that there is a third zero mode (for $m = 0$), however we do not know for certain. What we do know though is that the "lump" solution belongs to a family of solutions with no more than *three* continuous parameters.

*The notation $f_{m^2,n}$ denotes the eigenfunction with $n - 1$ nodes.

1.2.4 Rosen's equation

The action

$$S = \frac{1}{2} \int \{(\nabla\varphi)^2 - \varphi_t^2 - \varphi^6\} d^4x, \quad (1.29)$$

in (3+1)-dimensions, produces the Euler-Lagrange equation of motion

$$\varphi_{tt} - \nabla^2\varphi - 3\varphi^5 = 0, \quad (1.30)$$

Rosen's equation [76], where ∇^2 is the Laplace operator in 3 dimensions. Rosen found a solution of the form $\varphi^p = (1 + r^2)^{-1/2}$ [76], a metastable[†] particle-like solution, to this equation of motion. When we linearise the equation of motion (1.30) about this metastable solution we obtain

$$\begin{aligned} & \delta\ddot{\varphi} - \nabla^2\delta\varphi - 15(\varphi^4)\delta\varphi \\ &= \delta\ddot{\varphi} - \nabla^2\delta\varphi - \frac{15}{(1+r^2)^2}\delta\varphi = 0. \end{aligned} \quad (1.31)$$

If we then assume a solution of the form $\delta\varphi = ue^{i\omega t}$ to (1.31), it reduces to

$$-\nabla^2u - \frac{15}{(1+r^2)^2}u = \omega^2u, \quad (1.32)$$

a Schrödinger operator with energy $E_{nl} = \omega^2$ and a spherically symmetric potential $V(r) = \frac{-15}{(1+r^2)^2}$. Thus (1.32) can be reduced to a radial eigenvalue problem by means of the substitution $u(r, \theta, \phi) = R(r)Y_{lm}(\theta, \phi)$, where the Y_{lm} are the spherical harmonics.

We remind the reader that Y_{lm} is an eigenfunction of the momentum operator \hat{L}^2 with eigenvalue $l(l+1)$ ($l = 0, 1, 2, \dots$);

$$\begin{aligned} -\nabla^2u &= -\frac{1}{r^2}\partial_r(r^2\partial_ru) - \frac{1}{r^2}\left(\frac{1}{\sin\theta}\partial_\theta[\sin\theta\partial_\theta u] + \frac{1}{\sin^2\theta}\partial_\phi^2u\right) \\ &\equiv -\nabla_r^2u + \frac{\hat{L}^2}{r^2}u \\ &= -\nabla_r^2u + \frac{l(l+1)}{r^2}u. \end{aligned} \quad (1.33)$$

Also remember that m takes $(2l+1)$ values for each value of l : $-l \leq m \leq l$, $m \in \mathbb{Z}$.

On performing the above substitution, (1.32) reduces to:

$$-\nabla_r^2R(r) - \left(\frac{15}{(1+r^2)^2} - \frac{l(l+1)}{r^2}\right)R(r) = \omega^2R(r),$$

with the boundary conditions: $|R_r(0)| < \infty$ and $R \rightarrow 0$ as $r \rightarrow \infty$. For uniqueness of $u(0, \theta, \phi)$ we also require that $R(0) = 0$ for $l \neq 0$. However, as with the previous field theory (Section 1.2.3), the index theorem gives the more precise boundary condition;

[†]Rosen describes metastable solutions as solutions where "the rate of dissolution is very small relative to their quantum-theoretic characteristic frequencies E_0/\hbar based on the rest mass energy (E_0) [76]".

$R(r) \sim r^8$ for $r \sim 0$. Replacing $R(r) = f(r)/r$ in the above equation removes the first derivative and transforms the equation to:

$$-\frac{d^2 f}{dr^2} + \left[\left(\frac{l(l+1)}{r^2} - \frac{15}{(1+r^2)^2} \right) \right] f(r) \equiv -\frac{d^2 f}{dr^2} + V_l(r)f = \omega^2 f. \quad (1.34)$$

Here, we have combined the potential $-\frac{15}{(1+r^2)^2}$ and the centrifugal term $\frac{l(l+1)}{r^2}$ into an effective potential V_l . The boundary conditions $f(r) \sim r^{l+1}$ for $r \sim 0$ and $f \rightarrow 0$ as $r \rightarrow \infty$ are derived from those of $R(r)$. Again, as in with the previous field theory, bound states for $\omega^2 = 0$ of (1.34) may only occur if the potential

$$\begin{aligned} V_l &= \frac{l(l+1)(1+r^2)^2 - 15r^2}{r^2(1+r^2)^2} \\ &= \frac{r^4 l(l+1) + r^2(2l^2 + 2l - 15) + l(l+1)}{r^2(1+r^2)^2} \end{aligned} \quad (1.35)$$

is negative in, at least, some region. This in turn will only occur when the discriminant of the biquadratic in the numerator of (1.35) is non-negative. Clearly the discriminant

$$\begin{aligned} \mathcal{D} &= (2l^2 + 2l - 15)^2 - 4(l^2 + l)^2 \\ &= -15(2l - 3)(2l + 5), \end{aligned}$$

is only non-negative for $-\frac{5}{2} \leq l \leq \frac{3}{2}$. Thus bound states of (1.34) can *only* occur for $l = 0$ and $l = 1$.

When $l = 0$, the function $f_{2,0} = \frac{r(r^2-1)}{(1+r^2)^{3/2}}$ is an eigenfunction[†] of the operator (1.34) associated with the eigenvalue $\omega^2 = 0$. Substituting this into the relation $u = \frac{f_m(r)}{r} Y_{lm}(\theta, \phi)$, we obtain one zero mode:

$$u_1 = \frac{r^2 - 1}{(1+r^2)^{3/2}} Y_{0,0} = \frac{r^2 - 1}{(1+r^2)^{3/2}}. \quad (1.36a)$$

For $l = 1$, the function $f_{1,1} = \frac{r^2}{(1+r^2)^{3/2}}$ is an eigenfunction associated with $\omega^2 = 0$. Substituting this back into $u = \frac{1}{r} f_{nl}(r) Y_{lm}(\theta, \phi)$ gives us three more zero modes:

$$u_2 = \frac{r}{(1+r^2)^{3/2}} Y_{1,1} = \frac{r}{(1+r^2)^{3/2}} \sin \theta e^{i\phi}, \quad (1.36b)$$

$$u_3 = \frac{r}{(1+r^2)^{3/2}} Y_{1,0} = \frac{r}{(1+r^2)^{3/2}} \cos \theta, \quad (1.36c)$$

$$u_4 = \frac{r}{(1+r^2)^{3/2}} Y_{1,-1} = \frac{r}{(1+r^2)^{3/2}} \sin \theta e^{-i\phi}, \quad (1.36d)$$

as $-l \leq m \leq l$.

[†]The notation $f_{n,l}$ denotes the eigenfunction with $n - 1$ nodes.

Since (1.34) is a Sturm-Liouville eigenvalue problem, for each value of l , its eigenvalues are simple. Hence $f_{2,0}$ and $f_{1,1}$ are the only eigenfunctions of (1.34) corresponding to $\omega^2 = 0$. And u_1, u_2, u_3 and u_4 are the *only* zero modes of the metastable particle.

The last three zero modes u_2, u_3 and u_4 result from the translational degrees of freedom of φ^p in the x, y and z directions. Indeed, taking the partial derivative of φ^p with respect to x, y and z ;

$$\partial_x \varphi^p = \partial_r \varphi^p \partial_x r = \partial_r \varphi^p \frac{x}{r} = \partial_r \varphi^p \sin \theta \cos \phi$$

$$\partial_y \varphi^p = \partial_r \varphi^p \partial_y r = \partial_r \varphi^p \frac{y}{r} = \partial_r \varphi^p \sin \theta \sin \phi$$

$$\partial_z \varphi^p = \partial_r \varphi^p \partial_z r = \partial_r \varphi^p \frac{z}{r} = \partial_r \varphi^p \cos \theta$$

and using $\partial_r \varphi^p = -\frac{r}{(1+r^2)^{3/2}}$, we can form the linear combinations:

$$-\partial_x \varphi^p - i \partial_y \varphi^p = \frac{r}{(1+r^2)^{3/2}} \sin \theta e^{i\phi}$$

$$-\partial_x \varphi^p + i \partial_y \varphi^p = \frac{r}{(1+r^2)^{3/2}} \sin \theta e^{-i\phi}$$

$$-\partial_z \varphi^p = \frac{r}{(1+r^2)^{3/2}} \cos \theta.$$

These three linearly independent combinations, are none other than the zero modes u_2, u_3 and u_4 (1.36).

Finally we would like to know what degree of freedom gives rise to the first zero mode u_1 . As it turns out, this zero mode corresponds to a scaling degree of freedom, where the scaled solution $\hat{\varphi}^p(r) = \frac{a}{\sqrt{a^4+r^2}}$ is a solution to (1.32) for all a [76]. This becomes evident when we take a Taylor series expansion for an infinitesimal change in a (the scaling factor):

$$\frac{a + \epsilon}{\sqrt{(a + \epsilon)^4 + r^2}} = \frac{a}{\sqrt{a^4 + r^2}} + \partial_a \left(\frac{a}{\sqrt{a^4 + r^2}} \right) \epsilon + \mathcal{O}(\epsilon^2).$$

The coefficient of the term linear in ϵ ,

$$\partial_a \left(\frac{a}{\sqrt{a^4 + r^2}} \right) = \frac{r^2 - a^4}{(a^4 + r^2)^{3/2}}$$

coincides with u_1 (1.36a) and $\hat{\varphi}^p$ with φ^p when $a = 1$.

From these results it is evident that the metastable particle like solution φ^p to Rosen's equation (1.30) has only *four* zero modes. Three of these zero modes correspond to translational degrees of freedom in the x, y and z directions, while the fourth corresponds to a scaling degree of freedom of the soliton.

Something interesting to note is that the eigenfunction f_0 has a node, implying that there exists an eigenfunction, say $g(r)$, of the eigenvalue problem (1.34) with no nodes. Also we know that this eigenfunction $g(r)$ corresponds to an eigenvalue (ω^2) which is

smaller than zero. Therefore ω is pure imaginary and the perturbation $\delta\varphi = \frac{1}{r}g(r)Y_{00}e^{i\omega t}$ grows exponentially with time and Rosen's solution is *unstable*. This agrees with Derrick's Theorem [7]. Rosen did, however, show that rate of dissolution of φ^p is small and hence φ^p is a *metastable* solution.

This concludes our analysis of real scalar fields. We now proceed to complex scalar fields in various dimensions. As with the real fields we will examine the (1+1)-dimensional fields first. Of the various field theories in (1+1)-dimensions available to us, we consider the Klein Gordon model with a positive mass term and the nonlinear Schrödinger equation.

1.3 Complex Scalar Fields

1.3.1 Klein-Gordon

The action for the Klein-Gordon model in (1+1)-dimensions, with a positive mass squared term, is

$$S = \int \{ |\psi_x|^2 - |\psi_t|^2 + |\psi|^2 - \frac{1}{2}|\psi|^4 \} d^2x. \quad (1.39)$$

The equation of motion

$$\psi_{tt} - \psi_{xx} + \psi - |\psi|^2\psi = 0, \quad (1.40)$$

for the complex field ψ is obtained by varying the action (1.39) with respect to $\bar{\psi}$. The soliton solution $\psi^s(x) = \sqrt{2} \operatorname{sech} x$ is the solution which we are going to examine. When we linearise (1.40) about this soliton ψ^s by replacing $\psi \rightarrow \psi^s + \epsilon\delta\psi$ and collecting terms linear in ϵ we obtain

$$\begin{aligned} & \delta\psi_{tt} - \delta\psi_{xx} + \delta\psi - 2|\psi^s(x)|^2\delta\psi - (\psi^s)^2(x)\overline{\delta\psi} \\ & = \delta\psi_{tt} - \delta\psi_{xx} + \delta\psi - 4 \operatorname{sech}^2 x \delta\psi - 2 \operatorname{sech}^2 x \overline{\delta\psi} = 0, \end{aligned} \quad (1.41)$$

for the perturbation $\delta\psi$. We then assume a solution of the form $\delta\psi = \{u(x) + iv(x)\} \cos \omega t$ and substitute it into (1.41). This yields the matrix eigenvalue problem

$$\begin{bmatrix} \mathcal{L}_0 & 0 \\ 0 & \mathcal{L}_1 \end{bmatrix} \begin{pmatrix} u \\ v \end{pmatrix} = \omega^2 \begin{pmatrix} u \\ v \end{pmatrix}, \quad (1.42)$$

for the vector $\varphi = (u, v)^T$, where

$$\mathcal{L}_0 := -\partial_x^2 + 1 - 6 \operatorname{sech}^2 x \quad (1.43)$$

$$\mathcal{L}_1 := -\partial_x^2 + 1 - 2 \operatorname{sech}^2 x. \quad (1.44)$$

This eigenvalue problem has

$$\varphi_1 = \begin{pmatrix} \operatorname{sech} x \tanh x \\ 0 \end{pmatrix}, \quad \varphi_2 = \begin{pmatrix} 0 \\ \operatorname{sech} x \end{pmatrix}. \quad (1.45)$$

as two linearly independent eigenfunctions corresponding to the eigenvalue $\omega^2 = 0$. There are only two linearly independent eigenfunctions since (1.42) consists of two uncoupled

eigenvalue problems, both of which are Sturm-Liouville problems and as such have simple eigenvalues.

The first zero mode $\delta\psi_1 = \text{sech } x \tanh x$ corresponds to the translational degree of freedom of the soliton (Section 1.2.1) while the second $\delta\psi_2 = i \text{sech } x$ corresponds to the global $U(1)$ degree of freedom. A global $U(1)$ degree of freedom means that if ψ^s is a solution then so is $\hat{\psi}^s = \psi^s e^{i\alpha}$ for any real constant α . Note that degrees of freedom in both the *coordinate* space (translational) and in the *target* space ($U(1)$) give rise to zero modes.

To confirm that φ_2 does indeed correspond to a $U(1)$ degree of freedom, we take the Taylor expansion for an infinitesimal change in α :

$$\psi^s e^{i(\alpha+\epsilon)} = \hat{\psi}^s + i \frac{\partial \hat{\psi}^s}{\partial \alpha} \epsilon + \mathcal{O}(\epsilon^2). \quad (1.46)$$

Note that in the above expansion the term linear in ϵ , $\partial_\alpha \hat{\psi}^s = i\sqrt{2} \text{sech } x e^{i\alpha}$, is the second zero mode, up to the factor $\sqrt{2}$ when $\alpha = 0$. Thus for the Klein-Gordon model there are two zero modes, one corresponding to a translational and the other to a $U(1)$ degree of freedom. We now continue with another well known field theoretic model in (1+1)-dimensions, the nonlinear Schrödinger.

1.3.2 Nonlinear Schrödinger

The nonlinear Schrödinger equation,

$$i\psi_t + \psi_{xx} + 2|\psi|^2\psi = 0, \quad (1.47)$$

in (1+1)-dimensions, is obtained from the action

$$\mathcal{S} = \int \left\{ \frac{i}{2}(\psi_t \bar{\psi} - \psi \bar{\psi}_t) - |\psi_x|^2 + |\psi|^4 \right\} d^2x \quad (1.48)$$

by taking the functional derivative of (1.48) with respect to $\bar{\psi}$. This is a very well known field theoretic model and has been used to describe, *inter alia* stationary 2-dimensional self focusing of plane waves, the self-trapping phenomena of nonlinear optics, 1-dimensional self modulation of monochromatic waves, propagation of heat pluses in solids as well as Langmuir waves in plasmas ([1] and references therein).

The nonlinear Schrödinger equation is known to have $\psi_s(x, t) = e^{iA^2 t} A \text{sech } Ax$, where $A \in \mathbb{R}$, as a solitonic solution. The linearisation of the nonlinear Schrödinger equation about this soliton gives

$$\begin{aligned} & i\delta\psi_t + \delta\psi_{xx} + 4|\psi_s|^2 \delta\psi + 2\psi_s^2 \overline{\delta\psi} \\ & = i\delta\psi_t + \delta\psi_{xx} + 4A^2 \text{sech}^2 Ax \delta\psi + 2A^2 \text{sech}^2 Ax e^{2iA^2 t} \overline{\delta\psi} = 0. \end{aligned} \quad (1.49)$$

Note that this soliton has a time dependence and we, therefore, have to expand our method to allow for this. In this case, we assume a separable solution of the form $\delta\psi(x, t) = \{u(x) + iv(x)\} e^{(iA^2 + \lambda)t}$. Substituting this ansatz for $\delta\psi$ into (1.49) reduces it to the matrix problem

$$\begin{bmatrix} \mathcal{L}_0 & 0 \\ 0 & \mathcal{L}_1 \end{bmatrix} \begin{pmatrix} u \\ v \end{pmatrix} = \lambda J \begin{pmatrix} u \\ v \end{pmatrix} \quad (1.50)$$

for the vector $\varphi = (u, v)^T$, where

$$\begin{aligned}\mathcal{L}_0 &:= -\partial_x^2 + A^2(1 - 6 \operatorname{sech}^2 Ax) \\ \mathcal{L}_1 &:= -\partial_x^2 + A^2(1 - 2 \operatorname{sech}^2 Ax) \\ J &:= \begin{bmatrix} 0 & 1 \\ -1 & 0 \end{bmatrix}.\end{aligned}$$

The reason we choose the above form for the perturbations is that the eigenfunctions corresponding to $\lambda = 0$, zero modes, will have the same time dependence as ψ^s . Therefore they will be “stable” perturbations: They transform the soliton φ^s into another soliton which has the same time dependence as φ^s . Thus it is obvious that the degree of freedom for translations in time will not be realised using this method.

When $\lambda = 0$ the matrix problem (1.50) becomes two uncoupled, second order differential equations for $u(x)$ and $v(x)$. Therefore there can be at most one solution for $u(x)$ and one for $v(x)$ which satisfy the required boundary conditions: $|u(x)| \rightarrow 0$ as $|x| \rightarrow \infty$ and $|u(0)| < \infty$; $|v(0)| < \infty$ as $|x| \rightarrow \infty$ and $|v(x)| \rightarrow 0$. This implies that there can be at most two linearly independent solutions to (1.50), for $\lambda = 0$. Two linearly independent eigenfunctions which do correspond to $\lambda = 0$ are

$$\varphi_1 = \begin{pmatrix} \operatorname{sech} Ax \tanh Ax \\ 0 \end{pmatrix}, \quad \varphi_2 = \begin{pmatrix} 0 \\ \operatorname{sech} Ax \end{pmatrix}. \quad (1.51)$$

As for the Klein-Gordon model, the first zero mode

$$\delta\psi_1 = e^{iA^2t} \operatorname{sech} Ax \tanh Ax$$

corresponds to the translational degree of freedom while the second

$$\delta\psi_2 = e^{iA^2t} \operatorname{sech} Ax$$

corresponds to the global U(1) degree of freedom of the soliton ψ^s .

We now proceed to a complex field theory in (3+1)-dimensions, the logarithmic gausson equation.

1.3.3 Logarithmic Gausson equation

The action [77]

$$\mathcal{S} = \int \{ |\psi_t|^2 - |\nabla\psi|^2 - (1 + \mu)|\psi|^2 + \mu|\psi|^2 \ln |\psi|^2 \} d^4x \quad (1.52)$$

gives rise to the equation of motion

$$-\psi_{tt} + \nabla^2\psi - \psi + \mu \ln(|\psi|^2) \psi = 0, \quad (1.53)$$

the logarithmic gausson equation, where ∇^2 is the Laplacian operator in three dimensions. This was first used by Rosen [77] while discussing the dilatation covariance of local relativistic field theories. In particular, he discussed the solution to (1.53) of the form

$$\begin{aligned}\psi^s &= Ae^{-i\Omega t - \mu r^2/2} \\ A &= \exp \left\{ \frac{3\mu + 1 - \Omega^2}{2\mu} \right\},\end{aligned} \quad (1.54)$$

where Ω and μ are real constants. This solution is obtained from Rosen's solution by choosing the four-vector constant of integration as $k_\mu = (-\Omega, 0, 0, 0)$. When we linearise (1.53) about the solution (1.54) we obtain

$$\begin{aligned} \delta\psi_{tt} - \nabla^2\delta\psi + \delta\psi - \mu \ln(|\psi^s|^2)\delta\psi - \mu\delta\psi - \mu\frac{\overline{\psi^s}}{\psi^s}\delta\overline{\psi} \\ = \delta\psi_{tt} - \nabla^2\delta\psi - (4\mu - \Omega^2 - \mu^2r^2)\delta\psi - \mu e^{-2i\Omega t}\delta\overline{\psi} = 0, \end{aligned} \quad (1.55)$$

for the perturbation $\delta\psi$. The soliton we are considering here has a similar time dependence as the soliton in the previous section (nonlinear Schrödinger). We, therefore, are going to follow the method used previously and assume $\delta\psi = \{u(x, y, z) + iv(x, y, z)\}e^{-i\Omega t + \lambda t}$ reducing equation (1.55) to the following two coupled differential equations for u and v :

$$-\nabla^2u + \mu^2r^2u = 5\mu u - \lambda^2u + 2\Omega\lambda v, \quad (1.56a)$$

$$-\nabla^2v + \mu^2r^2v = 3\mu v - \lambda^2v - 2\Omega\lambda u. \quad (1.56b)$$

With the form for the perturbation assumed, perturbations with $\lambda = 0$ will have the same time evolution as the solution ψ^s . Therefore the zero modes represent "stable" perturbations.

When $\lambda = 0$ equations (1.56a) and (1.56b) become equations for three-dimensional harmonic oscillators with energies $E = 5\mu$ and $E = 3\mu$, respectively. Both of these equations can then be reduced to three one-dimensional linear harmonic oscillators in x , y and z by the method of separation of variables. The three linear harmonic oscillators are then solved under the constraint that the total energy of the system is the sum of the energies for the three linear harmonic oscillators: $E = E_{n_x} + E_{n_y} + E_{n_z}$. For example, setting $\lambda = 0$ and assuming $u = X(x)Y(y)Z(z)$ reduces (1.56a) and (1.56b) to:

$$\begin{aligned} -\frac{d^2}{dx^2}X_{n_x} + \mu^2x^2X_{n_x} &= E_{n_x}X_{n_x} \\ -\frac{d^2}{dy^2}Y_{n_y} + \mu^2y^2Y_{n_y} &= E_{n_y}Y_{n_y} \\ -\frac{d^2}{dz^2}Z_{n_z} + \mu^2z^2Z_{n_z} &= E_{n_z}Z_{n_z}, \end{aligned} \quad (1.57)$$

three linear harmonic oscillators. These three harmonic oscillators are then solved with the constraints that the total energies are $E_{n_x} + E_{n_y} + E_{n_z} = 5\mu$ and $E_{n_x} + E_{n_y} + E_{n_z} = 3\mu$ for (1.56a) and (1.56b) respectively. The solutions to these linear harmonic oscillators (1.57) are well known [78] and are given by:

$$\begin{aligned} X_{n_x} &= H_{n_x}(\sqrt{\mu}x)e^{-\mu x^2/2} \\ Y_{n_y} &= H_{n_y}(\sqrt{\mu}y)e^{-\mu y^2/2} \\ Z_{n_z} &= H_{n_z}(\sqrt{\mu}z)e^{-\mu z^2/2}, \end{aligned}$$

with the energies

$$E_{n_x} = (2n_x + 1)\mu$$

$$E_{n_y} = (2n_y + 1)\mu$$

$$E_{n_z} = (2n_z + 1)\mu,$$

where n_x, n_y and n_z take on the values $0, 1, 2, \dots$ and $H_n(\xi)$ are the Hermite polynomials.

For the system (1.57) there are only three possible values of $\mathbf{n} \equiv (n_x, n_y, n_z)$ that correspond to a total energy of $E = 5\mu$, viz. $\mathbf{n} = (1, 0, 0)$, $\mathbf{n} = (0, 1, 0)$ and $\mathbf{n} = (0, 0, 1)$ and only one that corresponds to $E = 3\mu$, viz. $\mathbf{n} = (0, 0, 0)$. Thus the only three solutions to (1.56a) with $\lambda = 0$ are:

$$u_1 = X_1 Y_0 Z_0 = H_1(\sqrt{\mu}x)e^{-\mu(x^2+y^2+z^2)/2} = 2\sqrt{\mu}xe^{-\mu r^2/2} \quad (1.58a)$$

$$u_2 = X_0 Y_1 Z_0 = H_1(\sqrt{\mu}y)e^{-\mu(x^2+y^2+z^2)/2} = 2\sqrt{\mu}ye^{-\mu r^2/2} \quad (1.58b)$$

$$u_3 = X_0 Y_0 Z_1 = H_1(\sqrt{\mu}z)e^{-\mu(x^2+y^2+z^2)/2} = 2\sqrt{\mu}ze^{-\mu r^2/2}, \quad (1.58c)$$

and the single solution to (1.56b) is:

$$v_1 = X_0 Y_0 Z_0 = e^{-\mu x^2/2} e^{-\mu y^2/2} e^{-\mu z^2/2} = e^{-\mu r^2/2}. \quad (1.58d)$$

Thus the soliton solution ψ^s to the logarithmic Gausson's equation (1.53) has the four zero modes

$$\delta\psi_1 = 2\sqrt{\mu}xe^{-\mu r^2/2}e^{-i\Omega t}, \quad (1.59a)$$

$$\delta\psi_2 = 2\sqrt{\mu}ye^{-\mu r^2/2}e^{-i\Omega t}, \quad (1.59b)$$

$$\delta\psi_3 = 2\sqrt{\mu}ze^{-\mu r^2/2}e^{-i\Omega t}, \quad (1.59c)$$

$$\delta\psi_4 = ie^{-\mu r^2/2}e^{-i\Omega t}, \quad (1.59d)$$

only. Hence the largest family of solutions to which ψ^s belongs has only *four* continuous parameters. The first three zero modes (1.59a), (1.59b) and (1.59c) correspond to the translational degrees of freedom in the x, y and z directions:

$$\partial_x \psi_s = 2\mu x A e^{-\{i\Omega t + \mu r^2/2\}}$$

$$\partial_y \psi_s = 2\mu y A e^{-\{i\Omega t + \mu r^2/2\}}$$

$$\partial_z \psi_s = 2\mu z A e^{-\{i\Omega t + \mu r^2/2\}}$$

while the fourth (1.59d) corresponds to the global U(1) degree of freedom

$$\partial_\alpha (\varphi_s e^{i\alpha})|_{\alpha=0} = i A e^{-\{i\Omega t + \mu r^2/2\}}.$$

The final "toy" model that we are going to consider is the nonlinear O(3) σ -model. This is a field theoretic model in $(2+1)$ dimensions.

1.4 The Nonlinear O(3) σ -model

In this section we review the zero modes of the nonlinear O(3) σ -model closely following the formalism of Ivanov, Murav'ev and Sheka [79]. The action for the nonlinear O(3) σ -model is given by:

$$S = \int \{(\nabla n^a)^2 - (\partial_t n^a)^2\} d^3x, \quad (1.60)$$

where $\vec{n} = (n^1, n^2, n^3)$ is a three component field with unit length ($\vec{n}^2 = 1$). Since \vec{n} has unit length, it lies on a unit sphere in the *target* space and we can parametrise it as $\vec{n} = (\sin \theta \cos \phi, \sin \theta \sin \phi, \cos \theta)$ where θ and ϕ are the polar and azimuthal angles of the vector in the *target* space, respectively. With this parameterisation the action (1.60) becomes

$$S = \int \{(\nabla \theta)^2 - (\partial_t \theta)^2 + \sin^2 \theta [(\nabla \phi)^2 - (\partial_t \phi)^2]\} d^3x. \quad (1.61)$$

The two equations of motion

$$\begin{aligned} \partial_t^2 \theta - \nabla^2 \theta + \cos \theta \sin \theta [(\nabla \phi)^2 - (\partial_t \phi)^2] &= 0 \\ \sin^2 \theta [\partial_t^2 \phi - \nabla^2 \phi] + \sin(2\theta) [\partial_t \theta \partial_t \phi - \nabla \phi \cdot \nabla \theta] &= 0, \end{aligned} \quad (1.62)$$

are obtained from the action (1.61) by varying the action with respect to θ and ϕ , respectively. The simplest nontrivial solutions to these equations are the well-known Belavin-Polyakov (BP) solitons [11]:

$$\begin{aligned} \theta_0 &= 2 \arctan(r^{-|\nu|}) \\ \phi_0 &= \nu \chi, \end{aligned} \quad (1.63)$$

where (r, χ) are the polar coordinates in the *coordinate* space and ν is the topological charge of the soliton. When we linearise the equations of motion (1.62) about the BP soliton with topological charge ν we obtain

$$\begin{aligned} -\partial_t^2 \delta \theta + \nabla^2 \delta \theta - \cos(2\theta_0) \frac{\nu^2}{r^2} \delta \theta - \cos \theta_0 \frac{2\nu}{r^2} \partial_\chi (\sin \theta_0 \delta \phi) &= 0 \\ \sin^2 \theta_0 [\nabla^2 \delta \phi - \partial_t^2 \delta \phi] + \sin(2\theta_0) [\nabla \phi_0 \cdot \nabla \delta \theta + \nabla \theta_0 \cdot \nabla \delta \phi] &= 0. \end{aligned} \quad (1.64)$$

The boundary conditions for $\delta \theta$ and $\delta \phi$ are: $\delta \theta \rightarrow 0$ as $r \rightarrow \infty$ and $\delta \theta(0, \chi) = 0$ while $\delta \phi$ is regular everywhere. Under the substitution $\delta \theta = \vartheta$ and $\sin \theta_0 \delta \phi = \mu$ the above coupled differential equations simplify to:

$$\begin{aligned} \left[\partial_t^2 - \nabla_r^2 - \frac{1}{r^2} \partial_\chi^2 + \cos 2\theta_0 \frac{\nu^2}{r^2} \right] \vartheta + \cos \theta_0 \frac{2\nu}{r^2} \partial_\chi \mu &= 0 \\ \left[\partial_t^2 - \nabla_r^2 - \frac{1}{r^2} \partial_\chi^2 + \cot \theta_0 \nabla_r^2 \theta_0 - \left(\frac{d\theta_0}{dr} \right)^2 \right] \mu - \cos \theta_0 \frac{2\nu}{r^2} \partial_\chi \vartheta &= 0, \end{aligned} \quad (1.65)$$

where $\nabla_r \equiv \frac{1}{r} \partial_r (r \partial_r)$. The boundary conditions for ϑ are the same as for $\delta\theta$ while we now have that μ decays at infinity and behaves as $r^{2|\nu|-1}$ near the origin. This substitution allows us to combine the two real equations in (1.65) into a single complex differential equation for $\Psi = \vartheta + i\mu$

$$\left[\partial_t^2 - \nabla_r^2 - \frac{1}{r^2} \partial_\chi^2 + \frac{\nu^2}{r^2} \cos 2\theta_0 - i \frac{2\nu}{r^2} \cos \theta_0 \partial_\chi \right] \Psi = 0, \quad (1.66)$$

since the two potentials $U_1 = \cos(2\theta_0) \frac{\nu^2}{r^2}$ and $U_2 = \cot \theta_0 (\nabla_r \theta_0) - \left(\frac{d\theta_0}{dr} \right)^2$ are identical for BP solitons. A more physical understanding for the choice of substitution is obtained, when we introduce the coordinate system $\{\vec{e}_1, \vec{e}_2, \vec{e}_3\}$, as in [79]. The new coordinates are defined by

$$\begin{aligned} \vec{e}_3 &= (\sin \theta_0 \cos \phi_0, \sin \theta_0 \sin \phi_0, \cos \theta_0), \\ \vec{e}_2 &= (-\sin \phi_0, \cos \phi_0, 0), \\ \vec{e}_1 &= \vec{e}_2 \times \vec{e}_3 = (\cos \theta_0 \cos \phi_0, \cos \theta_0 \sin \phi_0, -\sin \theta_0). \end{aligned}$$

Note that $\vec{e}_3 = \vec{n}_0$. In these new coordinates we have that $\vartheta = \vec{n}' \cdot \vec{e}_1$ and $\mu = \vec{n}' \cdot \vec{e}_2$, where \vec{n}' is the perturbed solution. Therefore the ϑ and ν are components of the perturbed solution in the directions of the coordinate axes \vec{e}_1 and \vec{e}_2 , respectively.

We now seek separable solutions to (1.66) of the form $\Psi = f_m(r) e^{im\chi + i\omega t}$, where m is an integer, which reduces the equation to

$$\left[-\nabla_r + \frac{1}{r^2} (m^2 + 2m\nu \cos \theta_0 + \nu^2 \cos 2\theta_0) \right] f_m = \omega^2 f_m. \quad (1.67)$$

This is a radial eigenvalue problem for f_m with the boundary conditions: $f_m \rightarrow 0$ as $r \rightarrow \infty$ and $|f_m(0)| < \infty$. For the rest of the analysis we concentrate on solitons with a positive topological charge ($\nu > 0$). Since equation (1.67), for each ω^2 , is a second-order differential equation, there are two linearly independent solutions. One of the solutions to (1.67) with $\omega^2 = 0$, for positive ν ,

$$f_m = r^{-m} \sin \theta_0 = \frac{2r^{\nu-m}}{1+r^{2\nu}}, \quad (1.68)$$

is regular at the origin when $m \leq \nu$ and decays as $r \rightarrow \infty$ when $m \geq -\nu + 1$, thus $-\nu + 1 \leq m \leq \nu$ is the only range of m for which f_m satisfies both boundary conditions. The second, linearly independent, solution

$$\begin{aligned} g_m &= r^m \left(\frac{r^{2\nu}}{m+\nu} + \frac{2}{m} + \frac{r^{-2\nu}}{m-\nu} \right) \sin \theta_0 \\ &= \frac{1}{1+r^{2\nu}} \left(\frac{r^{m+3\nu}}{m+\nu} + \frac{2r^{m+\nu}}{m} + \frac{r^{m-\nu}}{m-\nu} \right), \end{aligned} \quad (1.69)$$

is only regular at the origin if $m > \nu$, but then grows as $r^{m+3\nu}$ as $r \rightarrow \infty$ and as such does not obey the required boundary conditions. Thus no solutions of this form are allowed.

The *only* eigenfunctions of (1.66) corresponding to $\omega^2 = 0$, are $f_m = r^{-m} \sin \theta$ (1.68) with m integer and $-\nu + 1 \leq m \leq \nu$. Hence there are 2ν eigenfunctions f_m , implying there are 4ν zero modes, for a soliton with topological charge ν . This follows because, if Ψ is a solution to (1.66) then so is $i\Psi$. We will now examine the single and double BP solitons.

1.4.1 Single BP soliton

First we consider the single soliton solution, i.e. the BP soliton with topological charge $\nu = 1$. In this case there are two solutions to (1.66) with $\omega^2 = 0$:

$$\Psi_1 = \sin \theta_0 \quad (1.70)$$

$$\Psi_2 = \frac{1}{r} \sin \theta_0 e^{i\chi}. \quad (1.71)$$

Thus there are four zero modes, since if Ψ is a solution then so is $i\Psi$. These four zero modes are:

$$\begin{aligned} (1) \quad \vartheta &= \sin \theta_0, & \mu &= 0 \\ (2) \quad \vartheta &= 0, & \mu &= \sin \theta_0 \\ (3) \quad \vartheta &= \frac{1}{r} \sin \theta_0 \cos \chi, & \mu &= \frac{1}{r} \sin \theta_0 \sin \chi \\ (4) \quad \vartheta &= \frac{1}{r} \sin \theta_0 \sin \chi, & \mu &= -\frac{1}{r} \sin \theta_0 \cos \chi. \end{aligned} \quad (1.72)$$

The first zero mode corresponds to a dilation degree of freedom in r , where the rescaled soliton is of the form $\tilde{\theta}_0 = 2 \arctan(R/r)$, $\tilde{\phi}_0 = \chi$. Taking the partial derivative with respect to the rescaling variable (R) we obtain

$$\partial_R \tilde{\theta}_0 = \frac{-2}{1 + (R/r)^2} \frac{1}{r} = \frac{1}{R} \sin \tilde{\theta}_0$$

$$\partial_R \tilde{\phi}_0 = 0,$$

thus

$$\vartheta|_{R=1} = \sin \theta_0, \quad \mu = 0. \quad (1.73)$$

This is, exactly, the first zero mode.

The second zero mode corresponds to a degree of freedom for rotations about the z -axis in the *target* space. Under a rotation through the angle φ_0 , the soliton becomes $\hat{\theta}_0 = 2 \arctan(1/r)$, $\hat{\phi}_0 = \chi + \varphi_0$. Taking the partial derivative with respect to φ_0 , we obtain

$$\vartheta = 0, \quad \mu = \sin \theta_0,$$

the second zero mode.

The third and fourth zero modes correspond to translational degrees of freedom in the

x and y directions, respectively. Taking the partial of the soliton with respect to x we obtain

$$\begin{aligned}\partial_x \theta_0 &= \frac{-2}{1 + (1/r)^2} \frac{1}{r^2} \partial_x r = -\frac{1}{r} \sin \theta_0 \cos \chi \\ \partial_x \phi_0 &= -\frac{y}{r^2} = -\frac{1}{r} \sin \chi.\end{aligned}$$

Thus

$$\vartheta = -\frac{1}{r} \sin \theta_0 \cos \chi, \quad \mu = -\frac{1}{r} \sin \theta_0 \sin \chi, \quad (1.74)$$

the third zero mode.

While taking the partial of the soliton with respect to y :

$$\begin{aligned}\partial_y \theta_0 &= \frac{-2}{1 + (1/r)^2} \frac{1}{r^2} \partial_y r = -\frac{1}{r} \sin \theta_0 \sin \chi \\ \partial_y \phi_0 &= \frac{x}{r^2} = \frac{1}{r} \cos \chi,\end{aligned}$$

gives us

$$\vartheta = -\frac{1}{r} \sin \theta_0 \sin \chi, \quad \mu = \frac{1}{r} \sin \theta_0 \cos \chi, \quad (1.75)$$

which is the fourth zero mode.

Since the BP soliton is a solution for the nonlinear $O(3)$ σ -model there should also be rotational degrees of freedom for rotations about the x and y -axis in the *target* space (we have already shown one exists for rotations about the z -axis). It turns out that these rotations are equivalent to translations in x and y in the *coordinate* space. This follows since the zero modes corresponding to these rotational degrees of freedom are just the third and fourth zero modes.

The matrix which generates a rotation around the x -axis by the angle α is given by

$$R_x = \begin{pmatrix} 1 & 0 & 0 \\ 0 & \cos \alpha & \sin \alpha \\ 0 & -\sin \alpha & \cos \alpha \end{pmatrix}$$

and the rotated soliton is given by $\vec{n}' = R_x \vec{n}$. We then have

$$\begin{aligned}\vartheta &= \vec{e}_1 \cdot (\partial_\alpha \vec{n}')|_{\alpha=0} = \sin \chi \\ \mu &= \vec{e}_2 \cdot (\partial_\alpha \vec{n}')|_{\alpha=0} = \cos \theta_0 \cos \chi\end{aligned}$$

which can be written as $\Psi_{n_x} = \sin \chi + i \cos \theta_0 \cos \chi$, since $\Psi = \vartheta + i\mu$. Repeating the above for rotations about the y -axis, using

$$R_y = \begin{pmatrix} \cos \alpha & 0 & \sin \alpha \\ 0 & 1 & 0 \\ -\sin \alpha & 0 & \cos \alpha \end{pmatrix},$$

gives $\Psi_{n_y} = \cos \chi - i \cos \theta_0 \sin \chi$. When we calculate $(\Psi_{n_x} - i\Psi_{n_y})$ and use the property that $1 - \cos \theta_0 = \frac{1}{r} \sin \theta_0$ we obtain

$$\vartheta = \frac{1}{r} \sin \theta_0 \sin \chi, \quad \mu = -\frac{1}{r} \sin \theta_0 \cos \chi,$$

which is exactly the fourth zero mode. And the combination $(i\Psi_{n_x} + \Psi_{n_y})$ gives

$$\vartheta = \frac{1}{r} \sin \theta_0 \cos \chi, \quad \mu = \frac{1}{r} \sin \theta_0 \sin \chi,$$

which is the third zero mode. Therefore rotations about the x and y axes in the *target* space can be represented by a finite series of translations in x and y in the *coordinate* space and vice versa.

Thus we have found that for the single BP soliton there are exactly *four zero modes*. The first zero mode corresponds to dilations in the *coordinate* space and the second to rotations about the z -axis in the *target* space. The third and fourth zero modes correspond to translations in x and y directions in the *coordinate* space or equivalently to rotations about the x and y axes in the *target* space.

1.4.2 Double BP soliton

We will now consider the configuration consisting of two solitons “on top” of each other at the origin i.e. the BP soliton with topological charge $\nu = 2$. For this BP soliton there are four solutions to (1.66):

$$\Psi_1 = f_{-1} e^{-i\chi} = r \sin \theta_0 e^{-i\chi} \quad (1.76)$$

$$\Psi_2 = f_0 = \sin \theta_0 \quad (1.77)$$

$$\Psi_3 = f_1 e^{i\chi} = \frac{1}{r} \sin \theta_0 e^{i\chi} \quad (1.78)$$

$$\Psi_4 = f_2 e^{2i\chi} = \frac{1}{r^2} \sin \theta_0 e^{2i\chi} \quad (1.79)$$

This actually gives us eight linearly independent pairs of ϑ and μ as solutions to equations (1.65) since if Ψ is a solution to (1.66) then so is $i\Psi$. The eight pairs of solutions to

equations 1.65) are

$$\begin{aligned}
(1) \quad \vartheta &= r \sin \theta_0 \cos \chi, & \mu &= -r \sin \theta_0 \sin \chi \\
(2) \quad \vartheta &= r \sin \theta_0 \sin \chi, & \mu &= r \sin \theta_0 \cos \chi \\
(3) \quad \vartheta &= \sin \theta_0, & \mu &= 0 \\
(4) \quad \vartheta &= 0, & \mu &= \sin \theta_0 \\
(5) \quad \vartheta &= \frac{1}{r} \sin \theta_0 \cos \chi, & \mu &= \frac{1}{r} \sin \theta_0 \sin \chi \\
(6) \quad \vartheta &= \frac{1}{r} \sin \theta_0 \sin \chi, & \mu &= -\frac{1}{r} \sin \theta_0 \cos \chi \\
(7) \quad \vartheta &= \frac{1}{r^2} \sin \theta_0 \cos \chi, & \mu &= \frac{1}{r^2} \sin \theta_0 \sin \chi \\
(8) \quad \vartheta &= \frac{1}{r^2} \sin \theta_0 \sin \chi, & \mu &= -\frac{1}{r^2} \sin \theta_0 \cos \chi.
\end{aligned} \tag{1.80}$$

Each of these linearly independent pairs of solutions corresponds to a zero mode.

The translation degrees of freedom in the x and y directions of the soliton is represented by the fifth and sixth zero modes respectively. Indeed, when we take the partial derivative of θ_0 and ϕ_0 with respect to x we obtain

$$\begin{aligned}
\partial_x \theta_0 &= \frac{-4}{1 + (1/r)^4} \frac{1}{r^3} \partial_x r = -\frac{2}{r} \sin \theta_0 \cos \chi \\
\partial_x \phi_0 &= -\frac{2y}{r^2} = -\frac{2}{r} \sin \chi.
\end{aligned}$$

This means that

$$\vartheta = -\frac{2}{r} \sin \theta_0 \cos \chi, \quad \mu = -\frac{2}{r} \sin \theta_0 \sin \chi, \tag{1.81}$$

which is just the fifth zero mode up to a factor of (-2) . Recall that if f is a solution to a linear differential eigenvalue problem then so is any scalar multiple of f . Taking the partial derivative with respect to y :

$$\begin{aligned}
\partial_y \theta_0 &= \frac{-4}{1 + (1/r)^4} \frac{1}{r^3} \partial_y r = -\frac{2}{r} \sin \theta_0 \sin \chi \\
\partial_y \phi_0 &= \frac{2x}{r^2} = \frac{2}{r} \cos \chi.
\end{aligned}$$

Thus

$$\vartheta = -\frac{2}{r} \sin \theta_0 \sin \chi, \quad \mu = \frac{2}{r} \sin \theta_0 \cos \chi, \tag{1.82}$$

which is the sixth zero mode up to a factor of (-2) .

The third zero mode corresponds to a dilation degree of freedom in r . The rescaled

soliton is of the form $\tilde{\theta}_0 = 2 \arctan(R^2/r^2)$, $\tilde{\phi}_0 = 2\chi$, where R is a constant. Taking the partial of the rescaled soliton with respect to the scaling variable (R) we obtain

$$\partial_R \tilde{\theta}_0 = \frac{-4R}{1 + (R/r)^4} = \frac{2}{R} \sin \tilde{\theta}_0$$

$$\partial_R \tilde{\phi}_0 = 0,$$

thus

$$\vartheta|_{R=1} = 2 \sin \theta_0, \quad \mu = 0. \quad (1.83)$$

This is the third zero mode up to a factor of 2.

The fourth zero mode corresponds to a degree of freedom for rotations about the z -axis in the *target* space. For a rotation about the z -axis the soliton becomes $\hat{\theta}_0 = 2 \arctan(1/r^2)$, $\hat{\phi}_0 = 2\chi + \varphi_0$, where φ_0 is a constant. Taking the partial of the rotated soliton with respect to the rotation variable φ_0 , we obtain

$$\vartheta = 0, \quad \mu = \sin \theta_0,$$

which is exactly the fourth zero mode.

The seventh and eighth zero modes correspond to degrees of freedom for rotations about the x and y axes in the *target* space. As in the single soliton case the rotated soliton is given by $\vec{n}' = R_x \vec{n}$. And we have

$$\vartheta = \vec{e}_1 \cdot (\partial_\alpha \vec{n}')|_{\alpha=0} = \sin 2\chi$$

$$\mu = \vec{e}_2 \cdot (\partial_\alpha \vec{n}')|_{\alpha=0} = \cos \theta_0 \cos 2\chi$$

which can be written as $\Psi_{n_x} = \sin 2\chi + i \cos \theta_0 \cos 2\chi$, since $\Psi = \vartheta + i\mu$. Repeating the above for rotations about the y -axis, we obtain $\Psi_{n_y} = \cos 2\chi - i \cos \theta_0 \sin 2\chi$. If we now calculate $\Psi_{n_x} - i\Psi_{n_y}$ and use the property that $1 - \cos \theta_0 = \frac{1}{r^2} \sin \theta_0$ we obtain

$$\vartheta = \frac{1}{r^2} \sin \theta_0 \sin 2\chi, \quad \mu = -\frac{1}{r^2} \sin \theta_0 \cos 2\chi,$$

which is the eighth zero mode, while $i\Psi_{n_x} + \Psi_{n_y}$ gives

$$\vartheta = \frac{1}{r^2} \sin \theta_0 \cos 2\chi, \quad \mu = \frac{1}{r^2} \sin \theta_0 \sin 2\chi,$$

the seventh zero mode.

We have managed to find the degrees of freedom corresponding to the last six zero modes, but unfortunately we have, as yet, been unable to find a symmetry corresponding to neither the first nor the second zero mode. It *may* be that these correspond to the splitting of the two solitons in the x and y directions in the *coordinate* space.

In conclusion, for the BP soliton with topological charge two there are eight zero modes. The fifth and sixth zero modes correspond to the translational degrees of freedom in x and y , respectively, while the third corresponds to a rescaling degree of freedom in the radius. We also concluded that the $O(3)$ σ -model is invariant under rotations about the z , x and y -axis (zero modes 3, 8 and 7 respectively) as expected. As stated above, we are still trying to determine the invariance corresponding to the first two zero modes.

1.5 Summary

Here is a brief summary of our results from this chapter.

- For both the φ^4 soliton and the kink of the sine-Gordon in (1+1)-dimensions the only degree of freedom which exists is the translational degree of freedom.
- For the lump of the massless cubic-quintic model in (2+1)-dimensions we were able to find the two expected translational degrees of freedom (in the x and y directions), but we note that a third degree of freedom might exist. What is certain though is that the largest family of solutions, which has the lump as a member, requires at most four parameters.
- The metastable solution to Rosen's model in (3+1)-dimensions has the three expected translational degrees of freedom as well as a scaling degree of freedom. We also note that a negative eigenvalue to the linearised operator exists. This is in agreement with the fact that the solutions is not stable.
- With the complex scalar field theories a new degree of freedom is introduced, a global $U(1)$ degree of freedom. This is evident with the soliton of the Klein-Gordon model in (1+1)-dimensions, which has the translational degree of freedom as well as a global $U(1)$ degree of freedom. The global $U(1)$ degree of freedom occurs since the actions for the complex scalar field theories are $U(1)$ invariant.
- For the nonlinear Schrödinger equation in (1+1)-dimensions we introduced a non-static soliton. Applying the formalism in (Section 1.3.2) we find two degrees of freedom; one translational and one global $U(1)$ degree of freedom.
- For the time-dependent logarithmic gaussian in (3+1)-dimensions we found four expected degrees of freedom; the three translational and the global $U(1)$ degree of freedom.
- Applying our formalism to the static Belavin-Polyakov solitons of the nonlinear $O(3)$ σ -model, in (2+1)-dimensions, we obtained the following results.
 - For the single soliton ($\nu = 1$), the dimension of the moduli space is four: One degree of freedom for dilations and three for the $O(3)$ invariance of the field theory. The translational degrees of freedom, one would expect to find in the theory, are in fact included amongst these degree of freedom. This is because rotations about the x and y axes in the *target* space are equivalent to translations in x and y in the *coordinate* space, for the single BP soliton.
 - For the double soliton ($\nu = 2$), there are eight degrees of freedom: One dilational degree of freedom, two translational, three for the $O(3)$ invariance of the field theory and two further degrees of freedom. In this case, as apposed to the single soliton, the translations and rotations are not equivalent. We conjecture that the last two degrees of freedom correspond to the splitting of the double soliton into two separated single solitons.

From these results it follows that for *static* solitons, *the number of zero modes gives the dimension of the moduli space of the soliton*. However, for time dependent solitons the formalism applied only gives the degrees of freedom corresponding to transformations that don't affect the time dependence of the soliton. In other words the degrees of freedom that correspond to transformations that only affect the location or the profile (modulus) of the soliton.

As an aside, we note that the energies of the static solitons of the models described in sections 1.2.1, 1.2.2 and 1.4 have *topological* lower bounds, while those of the other models discussed in this chapter do not.

Chapter 2

The Ginzburg-Landau Model

It is fairly widely known that Ginzburg-Landau model admits static coaxial multivortex solutions [14]. There are also recent indications that the Ginzburg-Landau model may admit non-coaxial multivortex solutions [81]. In this chapter we try to determine whether the axially-symmetric multivortices of the Ginzburg-Landau equation can be continuously deformed into a configuration of multiple vortices with finite separation. We attempt to achieve this by determining the degrees of freedom for the coaxial multivortex solutions. To determine the degrees of freedom, we consider the (2+0)-dimensional Ginzburg-Landau equation

$$\nabla^2\psi + (1 - |\psi|^2)\psi = 0, \quad (2.1)$$

as a reduction of the (2+1)-dimensional Higgs field equation

$$\psi_{tt} - \nabla^2\psi - (1 - |\psi|^2)\psi = 0. \quad (2.2)$$

Alternatively, we could have considered it as a reduction of the Gross-Pitaevskii equation [82], [83]:

$$i\psi_t + \nabla^2\psi + (1 - |\psi|^2)\psi = 0, \quad (2.3)$$

however, this generalisation gives rise to a *generalised* eigenvalue problem, when linearised about the vortex. Thus the relativistic generalisation is computationally advantageous. The static coaxial vortices we are interested in, were first discovered in [14] and are of the form $\Psi_n(r, \theta) = \Phi_n(r)e^{in\theta}$, where $\Phi_n(r) \rightarrow 1$ as $r \rightarrow \infty$. In this expression, the integer n is the topological charge (2) or, equivalently, the vorticity of the vortex Ψ_n . This ansatz, for the form of the vortices, reduces (2.2) to the equation

$$\left[-\nabla_r^2 + \frac{n^2}{r^2} - 1 + \Phi_n^2(r) \right] \Phi_n(r) = 0, \quad (2.4)$$

for the modulus $\Phi_n(r)$. Although this equation has been widely studied, no analytical solution is known.

It is clear from the form of equation (2.2) that any of its solutions will display at least three degrees of freedom; namely, two translational degrees of freedom and a global $U(1)$ degree of freedom (or, equivalently, rotations in the plane). Notice that, for the vortex Ψ_n , a rotation in the plane by an angle α has the same effect as changing the phase by $n\alpha$. In other words changing $\theta \rightarrow \theta + \alpha$ in Ψ_n is the same as multiplying Ψ_n

by $e^{in\alpha} \in U(1)$. The zero modes corresponding to these degrees of freedom were found in [81, 82, 84, 85].

What we would like to know, though, is whether these coaxial-vortices Ψ_n display any *other* degrees of freedom. Are there some degrees of freedom which correspond to the separation of the coaxial multivortices into a static configuration of multiple non-coaxial vortex states? We shall apply the approach laid out in chapter 1 and calculate the zero modes of the associated linear operator for the vortices Ψ_n .

2.1 Linearisation

First we linearise the relativistic generalisation of the Ginzburg-Landau equation (2.2) about one of the coaxial-vortex solutions Ψ_n . This results in the equation

$$(\delta\psi)_{tt} - \nabla^2 \delta\psi - \delta\psi + \Phi_n^2 e^{2in\theta} \delta\bar{\psi} + 2\Phi_n^2 \delta\psi = 0, \quad (2.5)$$

for the perturbation $\delta\psi$. Then assume a separable solution to this equation of the form $\delta\psi = \chi \cos \omega t$, reducing it to

$$[-\nabla^2 - 1 + 2\Phi_n^2] \chi + \Phi_n^2 e^{2in\theta} \bar{\chi} = \omega^2 \chi. \quad (2.6)$$

The explicit dependence on θ , in this equation, is removed by the transformation $\chi(r, \theta) = \varphi(r, \theta) e^{in\theta}$. Applying this transformation reduces the above equation to

$$-\nabla_r^2 \varphi - \frac{(\partial_\theta + in)^2}{r^2} \varphi - \varphi + \Phi_n^2 \bar{\varphi} + 2\Phi_n^2 \varphi = \omega^2 \varphi. \quad (2.7)$$

We will refer to this as an *eigenvalue* problem for the *complex* function φ , although technically (2.7) along with its complex conjugate form an eigenvalue problem for the vector $(\varphi, \bar{\varphi})$. To reduce this partial differential equation to a set of coupled ordinary differential eigenvalue problems we take a Fourier series expansion of φ in θ :

$$\varphi = \sum_{m=-\infty}^{\infty} \phi_m(r) e^{im\theta} = \sum_{m=-\infty}^{\infty} \{f_m(r) + ig_m(r)\} e^{im\theta}, \quad (2.8)$$

where $f_m(r)$ and $g_m(r)$ are real, radial functions. When this expansion is substituted into the eigenvalue problem (2.7) and coefficients of like harmonics are equated, the real part gives

$$\left[-\frac{d^2}{dr^2} - \frac{1}{r} \frac{d}{dr} + \frac{n^2 + m^2}{r^2} + (2\Phi_n^2 - 1) \right] f_m + \frac{2mn}{r^2} f_m + \Phi_n^2 f_{-m} = \omega^2 f_m \quad (2.9a)$$

$$\left[-\frac{d^2}{dr^2} - \frac{1}{r} \frac{d}{dr} + \frac{n^2 + m^2}{r^2} + (2\Phi_n^2 - 1) \right] f_{-m} - \frac{2mn}{r^2} f_{-m} + \Phi_n^2 f_m = \omega^2 f_{-m}. \quad (2.9b)$$

Adding (2.9a) and (2.9b) gives

$$\left[-\frac{d^2}{dr^2} - \frac{1}{r} \frac{d}{dr} + \frac{n^2 + m^2}{r^2} + 3\Phi_n^2 - 1 \right] u_m + \frac{2mn}{r^2} v_m = \omega^2 u_m, \quad (2.10)$$

while subtracting (2.9b) from (2.9a) produces

$$\left[-\frac{d^2}{dr^2} - \frac{1}{r} \frac{d}{dr} + \frac{n^2 + m^2}{r^2} + \Phi_n^2 - 1 \right] v_m + \frac{2mn}{r^2} u_m = \omega^2 v_m, \quad (2.11)$$

where u_m and v_m are defined as

$$u_m = f_m + f_{-m}, \quad v_m = f_m - f_{-m}.$$

Note that $m = 0$ is a special case and, here, $u_0 = 2f_0$ and $v_0 = 0$. For this case the eigenvalue problem

$$\left[-\frac{d^2}{dr^2} - \frac{1}{r} \frac{d}{dr} + \frac{n^2}{r^2} + 3\Phi_n^2 - 1 \right] u_0 = \omega^2 u_0, \quad (2.12)$$

determines u_0 . The two eigenvalue problems (2.10) and (2.11) can then be combined to give a single vector eigenvalue problem*

$$\mathcal{L} \begin{pmatrix} u_m \\ v_m \end{pmatrix} = \omega^2 \begin{pmatrix} u_m \\ v_m \end{pmatrix}, \quad (2.13a)$$

with the operator \mathcal{L} defined as

$$\mathcal{L} \equiv \begin{pmatrix} \mathcal{P} + 3\Phi_n^2 - 1 & \frac{2mn}{r^2} \\ \frac{2mn}{r^2} & \mathcal{P} + \Phi_n^2 - 1 \end{pmatrix}, \quad (2.13b)$$

where

$$\mathcal{P} \equiv -\frac{d^2}{dr^2} - \frac{1}{r} \frac{d}{dr} + \frac{n^2 + m^2}{r^2}.$$

We restrict ourselves to $m \geq 1$ as we only need u_m and v_m for positive m to reconstruct the f_m for all integer values of $m \neq 0$. When we consider the imaginary part after substituting the Fourier expansion (2.8) into the eigenvalue problem (2.7) we obtain the two coupled equations;

$$\left[-\frac{d^2}{dr^2} - \frac{1}{r} \frac{d}{dr} + \frac{n^2 + m^2}{r^2} + (2\Phi_n^2 - 1) \right] g_m + \frac{2mn}{r^2} g_m - \Phi_n^2 g_{-m} = \omega^2 g_m \quad (2.14)$$

$$\left[-\frac{d^2}{dr^2} - \frac{1}{r} \frac{d}{dr} + \frac{n^2 + m^2}{r^2} + (2\Phi_n^2 - 1) \right] g_{-m} - \frac{2mn}{r^2} g_{-m} - \Phi_n^2 g_m = \omega^2 g_{-m}. \quad (2.15)$$

Repeating the procedure as for the real part we obtain

$$\left[-\frac{d^2}{dr^2} - \frac{1}{r} \frac{d}{dr} + \frac{n^2 + m^2}{r^2} + \Phi_n^2 - 1 \right] \tilde{u}_m - \frac{2mn}{r^2} \tilde{v}_m = \omega^2 \tilde{u}_m \quad (2.16)$$

$$\left[-\frac{d^2}{dr^2} - \frac{1}{r} \frac{d}{dr} + \frac{n^2 + m^2}{r^2} + 3\Phi_n^2 - 1 \right] \tilde{v}_m - \frac{2mn}{r^2} \tilde{u}_m = \omega^2 \tilde{v}_m, \quad (2.17)$$

*Note that u_m and v_m carry a second, implicit index n . Its omission simplifies the notation.

with \tilde{u}_m and \tilde{v}_m are defined as

$$\tilde{u}_m = g_m + g_{-m}, \quad \tilde{v}_m = g_m - g_{-m}.$$

Note that, as with the real part, $m = 0$ is a special case and $\tilde{u}_0 = 2g_0$ and $\tilde{v}_0 = 0$. The eigenvalue problem which determines \tilde{u}_0 is:

$$\left[-\frac{d^2}{dr^2} - \frac{1}{r} \frac{d}{dr} + \frac{n^2}{r^2} + \Phi_n^2 - 1 \right] \tilde{u}_0 = \omega^2 \tilde{u}_0. \quad (2.18)$$

Again we can combine the two eigenvalue problems (2.16) and (2.17) into a single vector eigenvalue problem

$$\mathcal{L} \begin{pmatrix} \tilde{v}_m \\ \tilde{u}_m \end{pmatrix} = \omega^2 \begin{pmatrix} \tilde{v}_m \\ \tilde{u}_m \end{pmatrix}, \quad (2.19)$$

with \mathcal{L} as in (2.13b). We can also restrict this eigenvalue problem to $m \geq 1$ since we only need \tilde{u}_m and \tilde{v}_m for positive values of m to reconstruct the g_m for all $m \neq 0$.

This new formulation makes solving the system much simpler. Note from the form of (2.13) and (2.19) that if $(u_m, v_m)^T$ is an eigenfunction of (2.13) with eigenvalue ω_i^2 , then $(\tilde{v}_m, \tilde{u}_m)^T = \alpha(u_m, v_m)^T$ is an eigenfunction of (2.19) with the same eigenvalue ω_i^2 , where $\alpha \in \mathbb{R}$. Therefore there is a one-to-one correspondence between the solutions of (2.13) and those of (2.19) for $m \geq 1$. Note that the matrix in (2.13) becomes diagonal when $m = 0$ and the first row is just the eigenvalue problem that determines u_0 , while the second is the eigenvalue problem that determines \tilde{u}_0 . Thus the two special cases (2.12) and (2.18) are contained in (2.13) when $m = 0$, if we identify $\tilde{u}_0 = v_0$. Hence we need only solve (2.13) for $m \geq 0$ to know all the eigenfunctions of (2.7), and thus all the zero modes. From now on we will refer to the value of m as the *azimuthal quantum number*.

With the aid of the correspondence between u_m, v_m and \tilde{u}_m, \tilde{v}_m we can construct a general eigenfunction φ_m corresponding to a specific azimuthal quantum number m :

$$\varphi_m = \left(\phi_m e^{im\theta} + \phi_{-m} e^{-im\theta} \right) \quad (2.20a)$$

where the coefficients in the Fourier expansion are

$$\begin{aligned} \phi_m &= \frac{\beta}{2}(u_m + v_m) + i\frac{\alpha}{2}(u_m - v_m), \\ \phi_{-m} &= \frac{\beta}{2}(u_m - v_m) + i\frac{\alpha}{2}(v_m - u_m), \quad m \geq 1 \end{aligned} \quad (2.20b)$$

$$\phi_0 = \frac{\beta}{2}u_0 + i\frac{\alpha}{2}v_0. \quad (2.20c)$$

Recall that we identify v_0 with \tilde{u}_0 when solving (2.13) for $m = 0$. Choosing two linearly independent vectors $\begin{pmatrix} \beta \\ \alpha \end{pmatrix}$ gives two linearly independent eigenfunctions to (2.7). In this text we choose $\begin{pmatrix} \beta \\ \alpha \end{pmatrix} = \begin{pmatrix} 1 \\ 0 \end{pmatrix}$ and $\begin{pmatrix} \beta \\ \alpha \end{pmatrix} = \begin{pmatrix} 0 \\ 1 \end{pmatrix}$ as our two linearly independent vectors giving

$$\begin{aligned} \tilde{\varphi}_m &= \left(\frac{u_m + v_m}{2} e^{im\theta} + \frac{u_m - v_m}{2} e^{-im\theta} \right) = u_m \cos m\theta + iv_m \sin m\theta, \\ \hat{\varphi}_m &= i \left(\frac{u_m + v_m}{2} e^{im\theta} - \frac{u_m - v_m}{2} e^{-im\theta} \right) = -u_m \sin m\theta + iv_m \cos m\theta, \end{aligned} \quad (2.21)$$

as our two linearly independent eigenfunctions corresponding to azimuthal quantum number $m \geq 1$ and

$$\tilde{\varphi}_0 = u_0, \quad \hat{\varphi}_0 = iv_0, \quad (2.22)$$

Note that the eigenvalue problem (2.18) with $\omega^2 = 0$ has exactly the same form as equation (2.4). Therefore one of the eigenfunctions of (2.18) with $\omega^2 = 0$ is given by the modulus of the vortex: $\tilde{u}_0(r) = \Phi_n(r)$. Thus we already have one zero mode, given by $\varphi_0 = i\Phi_n e^{in\theta}$. This corresponds, as we have seen with the complex fields in Chapter 1, to a global $U(1)$ degree of freedom. Note that for the vortices $\Psi_n = \Phi_n(r)e^{in\theta}$ a $U(1)$ gauge transformation is equivalent to a rotation in the plane. This zero mode is one of the three which we expect to exist.

The other two zero modes we expect result from translational degrees of freedom in the x and y directions. It is expedient to know which azimuthal quantum numbers these zero modes correspond to. As we have learnt from the previous chapter, the zero mode of Ψ_n corresponding to translations in x is given by:

$$\begin{aligned} \partial_x[\Phi_n(r)e^{in\theta}] &= \left[\frac{d\Phi_n}{dr} \partial_x r + in\Phi_n \partial_x \theta \right] e^{in\theta} \\ &= \left[\frac{d\Phi_n}{dr} \cos \theta - i \frac{n\Phi_n}{r} \sin \theta \right] e^{in\theta}, \end{aligned} \quad (2.23)$$

and for translations in y , by:

$$\begin{aligned} \partial_y[\Phi_n(r)e^{i\theta}] &= \left[\frac{d\Phi_n}{dr} \partial_y r + in\Phi_n \partial_y \theta \right] e^{in\theta} \\ &= \left[\frac{d\Phi_n}{dr} \sin \theta + i \frac{n\Phi_n}{r} \cos \theta \right] e^{in\theta}. \end{aligned} \quad (2.24)$$

Recall that our ansatz for the perturbation is $\delta\psi(r, \theta, t) = \varphi(r, \theta)e^{in\theta} \cos \omega t$. Therefore, for zero modes ($\omega^2 = 0$) it is obvious from (2.21) that $\partial_x \Psi_n = -\tilde{\varphi}_1 e^{in\theta}$ and $\partial_y \Psi_n = \hat{\varphi}_1 e^{in\theta}$ for $u_1 = -\frac{d}{dr}(\Phi_n)$ and $v_1 = \frac{n\Phi_n}{r}$. Hence the zero modes for translational invariance correspond to the azimuthal quantum number $m = 1$.

The eigenvalue problem (2.13) is a second order differential equation in both $u_m(r)$ and $v_m(r)$ both of which have boundary conditions which they must satisfy at $r = 0$ and at $r = \infty$. Therefore there can be at most *one* solution $(u_m, v_m)^T$ to (2.13) for each value of m, n and ω^2 . This means that there can be at most two zero modes for *each* non-zero azimuthal quantum number m (2.21). In order to make the results more presentable, we make the previously implicit index explicit: $u_m \rightarrow u_{mn}$ and $v_m \rightarrow v_{mn}$ so as to distinguish between the eigenfunctions of the various coaxial vortices. We refer to them as the *components* u_{mn} and v_{mn} of the complex eigenfunction φ of (2.13).

As previously mentioned, no analytical solution for the coaxial-vortex Φ_n is known. Therefore, we have to proceed with solving the eigenvalue problem (2.13) numerically. In order to calculate the numerical solution of Φ_n , we initially implemented a shooting

method for $n = 1, 2$ and 3 (the single vortex, the coaxial double- and triple-vortex, respectively). However, with this method alone we were unable to extend the domain of the solution beyond a radius of $R = 20$. Since Φ_n approaches the value $\Phi_n(\infty) = 1$ slowly as $r \rightarrow \infty$, numerical calculations were very sensitive to the size of the domain. And a domain this small causes unacceptably large numerical errors in the calculations. Therefore, in order to improve the accuracy of our numerical calculations, we had to increase the size of the domain for which the coaxial multivortex was known. This was accomplished with the aid of the continuation software AUTO97. With this software, the three vortices were computed for the domain $0 \leq r \leq R = 80$.

It is necessary while calculating the zero modes numerically to impose boundary conditions. But, before we can do this, we need to know what boundary conditions are appropriate. To this end we will now analyse the asymptotics of $\tilde{\varphi}_{mn}$ for small and large r .

2.2 Asymptotic Behaviour of Zero Modes

2.2.1 Asymptotics for small r

To determine the boundary conditions of the zero modes at the origin, we first need to find the behaviour of the Φ_n at the origin. This is obtained by assuming an expansion of the form

$$\Phi_n(r) = r^l \left(\Phi^{(0)} + \Phi^{(1)}r + \Phi^{(2)}r^2 + \dots \right), \quad (2.25)$$

as $r \rightarrow 0$, and substituting it into equation (2.4). When terms of like powers of r are collected, the terms $\mathcal{O}(r^{l-2})$ yield $l = \pm n$. Therefore $\Phi_n \sim r^n$ for non-singularity of the vortex at the origin where n is positive.

In order to determine the boundary conditions of the eigenfunctions of (2.13) we assume an expansion of the form

$$\begin{aligned} u &= r^p \left[(u_0r + u_1r^1 + u_2r^2 + \dots) + \ln r (u'_0r + u'_1r^1 + u'_2r^2 + \dots) \right] \\ v &= r^p \left[(v_0r + v_1r^1 + v_2r^2 + \dots) + \ln r (v'_0r + v'_1r^1 + v'_2r^2 + \dots) \right], \end{aligned} \quad (2.26)$$

where u and v denote u_{mn} and v_{mn} , respectively. This expansion is then substituted into (2.13) and terms of like powers in r are collected, giving constraints on the parameters. The terms $\mathcal{O}(r^{p-2} \ln r)$ yield:

$$\begin{aligned} [n^2 + m^2 - p^2] u'_0 + 2mnv'_0 &= 0, \\ 2mnu'_0 + [n^2 + m^2 - p^2] v'_0 &= 0. \end{aligned} \quad (2.27)$$

To satisfy (2.27) either $\begin{pmatrix} u'_0 \\ v'_0 \end{pmatrix} = 0$ or the determinant of the system is zero:

$$(n^2 + m^2 - p^2)^2 - (2mn)^2 = 0,$$

which is equivalent to

$$[(m+n)^2 - p^2][(m-n)^2 - p^2] = 0.$$

This last equation implies that either $p = \pm(n-m)$ or $p = \pm(n+m)$ for $\begin{pmatrix} u'_0 \\ v'_0 \end{pmatrix} \neq 0$. If $p = \pm(n+m)$ then, from (2.27), $u'_0 = v'_0$ while $p = \pm(n-m)$ implies $u'_0 = -v'_0$. When the terms $\mathcal{O}(r^{p-2})$ are considered we find:

$$\begin{aligned} [n^2 + m^2 - p^2] u_0 + 2mnv_0 - 2pu'_0 &= 0, \\ 2mnu_0 + [n^2 + m^2 - p^2] v_0 - 2pv'_0 &= 0, \end{aligned} \quad (2.28)$$

which we can rearrange to give u_0 and v_0 in terms of u'_0 and v'_0 viz.

$$\begin{aligned} u_0 &= \frac{2p[(m^2 + n^2 - p^2)u'_0 - 2mnv'_0]}{(m+n-p)(m+n+p)(m-n+p)(m-n-p)}, \\ v_0 &= \frac{2p[(m^2 + n^2 - p^2)v'_0 - 2mnu'_0]}{(m+n-p)(m+n+p)(m-n+p)(m-n-p)}. \end{aligned} \quad (2.29)$$

But, from this it follows that if $p \neq 0$ and either $p = \pm(n-m)$ or $p = \pm(n+m)$ then u_0 and v_0 are infinite, which is not permitted. Thus for $\begin{pmatrix} u'_0 \\ v'_0 \end{pmatrix} \neq 0$ we must have $p = 0$. Since n and m are both positive, p can be zero only if $p = \pm(n-m)$ and $m = n$. In summary the coefficients u'_0 and v'_0 may only be non-zero when $p = 0$ and $m = n$.

If, however, $\begin{pmatrix} u'_0 \\ v'_0 \end{pmatrix} = 0$ then (2.28) yields that either $\begin{pmatrix} u_0 \\ v_0 \end{pmatrix} = 0$ or

$$[(m+n)^2 - p^2][(m-n)^2 - p^2] = 0,$$

in other words $p = \pm(n-m)$ or $p = \pm(n+m)$.

Consider next the terms $\mathcal{O}(r^{p-1} \ln r)$;

$$\begin{aligned} (2n^2 - 1)u'_1 + 2n^2v'_1 &= 0, \\ 2n^2u'_1 + (2n^2 - 1)v'_1 &= 0, \end{aligned} \quad (2.30)$$

for $\begin{pmatrix} u'_0 \\ v'_0 \end{pmatrix} \neq 0$ (i.e. $p = 0$ and $m = n$). This system has a zero determinant only for $n = \pm\frac{1}{2}$.

Since n is integer, the determinant of the system is never zero and hence $\begin{pmatrix} u'_1 \\ v'_1 \end{pmatrix} = 0$.

The terms of order $\mathcal{O}(r^{p-1})$ give:

$$\begin{aligned} [n^2 + m^2 - p^2 - 2p - 1] u_1 + 2mnv_1 &= 0, \\ 2mnu_1 + [n^2 + m^2 - p^2 - 2p - 1] v_1 &= 0. \end{aligned} \quad (2.31)$$

If $\begin{pmatrix} u_0 \\ v_0 \end{pmatrix} \neq 0$ then the determinant of the above system can only be zero if m or n take on half integer values and since m and n are integer the determinant is non-zero. Thus $\begin{pmatrix} u_1 \\ v_1 \end{pmatrix} = 0$ to satisfy (2.31), if $\begin{pmatrix} u_0 \\ v_0 \end{pmatrix} \neq 0$.

Therefore there are four linearly independent behaviours for the eigenfunctions of (2.13) as $r \rightarrow 0$:

$$\begin{aligned}
Z_1 &= r^{n+m}[1 + o(r)] \begin{pmatrix} 1 \\ 1 \end{pmatrix}; & Z_2 &= r^{-|n-m|}[1 + o(r)] \begin{pmatrix} 1 \\ -1 \end{pmatrix}; \\
Z_3 &= r^{-(n+m)}[1 + o(r)] \begin{pmatrix} 1 \\ 1 \end{pmatrix}; \\
Z_4 &= r^{|n-m|}[1 + o(r)] \begin{pmatrix} 1 \\ -1 \end{pmatrix}; & m &\neq n \\
Z_4 &= \ln r [1 + o(r)] \begin{pmatrix} 1 \\ -1 \end{pmatrix}, & m &= n
\end{aligned} \tag{2.32}$$

where the notation[†] $Z = (u_m, v_m)^T$ is used. Note that Z_1 and Z_2 are bounded at the origin for all m and n while Z_3 and Z_4 are not.

The boundary conditions, which we will impose during the numerical calculations, follow easily from the form of Z_1 and Z_2 . For $m \neq n \pm 1$ the first derivatives of the components $u_{mn}(r)$ and $v_{mn}(r)$ are equated to zero at the origin:

$$\frac{d}{dr} u_{mn}(0) = \frac{d}{dr} v_{mn}(0) = 0, \quad m \neq n \pm 1. \tag{2.33}$$

This is allowed since u and v are proportional to r only when $m = n \pm 1$. For this case, $m = n \pm 1$, the components themselves are equated to zero at the origin:

$$u_{n\pm 1, n}(0) = v_{n\pm 1, n}(0) = 0, \quad m = n \pm 1. \tag{2.34}$$

These boundary conditions reduce the possibility of the numerics giving ‘false’ eigenfunctions. Now that the boundary conditions at the origin are known we can consider the behaviour of the eigenfunctions as $r \rightarrow \infty$.

2.2.2 Asymptotics for large r

As with the asymptotics for small r , the asymptotic behaviour of Φ_n is needed before the boundary condition for the eigenfunctions can be determined. This time we use an expansion of the form:

$$\Phi_n(r) = 1 + \Phi^{(1)} r^{-1} + \Phi^{(2)} r^{-2} + \dots, \tag{2.35}$$

for $r \rightarrow \infty$. When this expansion is substituted into equation (2.4) and like powers of r are collected, we obtain the following conditions: From terms $\mathcal{O}(r^{-1})$ we obtain $\Phi^{(1)} = 0$; terms $\mathcal{O}(r^{-2})$ give $\Phi^{(2)} = \frac{-n^2}{2}$ and terms $\mathcal{O}(r^{-3})$ give $\Phi^{(3)} = 0$. Thus $\Phi_n \sim 1 - \frac{n^2}{2r^2} + \mathcal{O}(r^{-4})$ as $r \rightarrow \infty$. This asymptotic behaviour coincides with the one in [82] for the single vortex ($n = 1$).

[†]Here we have adopted the notation of [86]

When we consider the eigenvalue problem (2.13) we notice that positive eigenvalues ($\omega^2 > 0$) belong to the continuous spectrum. While trying to calculate the zero modes numerically, this is in fact problematic. Numerical methods do not obtain the zero eigenvalue exactly but produce a value within a small neighbourhood of zero. Hence, a means of discerning a true zero eigenvalue from a small positive eigenvalue (ω^2) is needed. To aid this and to determine the boundary conditions as $r \rightarrow \infty$, we assume an expansion of the form:

$$\begin{aligned} u &= \Re \left\{ e^{ikr} r^p [(u_0 + u_1 r^{-1} + u_2 r^{-2} + \dots) + \ln r (u'_0 + u'_1 r^{-1} + u'_2 r^{-2} + \dots)] \right\} \\ v &= \Re \left\{ e^{ikr} r^p [(v_0 + v_1 r^{-1} + v_2 r^{-2} + \dots) + \ln r (v'_0 + v'_1 r^{-1} + v'_2 r^{-2} + \dots)] \right\}, \end{aligned} \quad (2.36)$$

where p is real. We then substitute this into equation (2.13) and collect terms of like powers of r . This produces the following sets of equations:
for terms $\mathcal{O}(r^p \ln r)$:

$$\begin{aligned} (k^2 - \omega^2 + 2)u'_0 &= 0, \\ (k^2 - \omega^2)v'_0 &= 0, \end{aligned} \quad (2.37)$$

terms $\mathcal{O}(r^p)$:

$$\begin{aligned} (k^2 - \omega^2 + 2)u_0 &= 0, \\ (k^2 - \omega^2)v_0 &= 0, \end{aligned} \quad (2.38)$$

terms $\mathcal{O}(r^{p-1} \ln r)$:

$$\begin{aligned} -ik(1 + 2p)u'_0 + (k^2 - \omega^2 + 2)u'_1 &= 0, \\ -ik(1 + 2p)v'_0 + (k^2 - \omega^2)v'_1 &= 0, \end{aligned} \quad (2.39)$$

terms $\mathcal{O}(r^{p-1})$:

$$\begin{aligned} -ik(1 + 2p)u_0 + (k^2 - \omega^2 + 2)u_1 - 2iku'_0 &= 0, \\ -ik(1 + 2p)v_0 + (k^2 - \omega^2)v_1 - 2ikv'_0 &= 0, \end{aligned} \quad (2.40)$$

terms $\mathcal{O}(r^{p-2} \ln r)$:

$$\begin{aligned} (m^2 - 2n^2 - p^2)u'_0 + ik(1 - 2p)u'_1 + (k^2 - \omega^2 + 2)u'_2 + 2mnv'_0 &= 0, \\ (m^2 - p^2)v'_0 + ik(1 - 2p)v'_1 + (k^2 - \omega^2)v'_2 + 2mnu'_0 &= 0, \end{aligned} \quad (2.41)$$

terms $\mathcal{O}(r^{p-2})$:

$$\begin{aligned} (m^2 - 2n^2 - p^2)u_0 + ik(1 - 2p)u_1 + (k^2 - \omega^2 + 2)u_2 + 2mnv_0 - 2pu'_0 - 2iku'_1 &= 0, \\ (m^2 - p^2)v_0 + ik(1 - 2p)v_1 + (k^2 - \omega^2)v_2 + 2mnu_0 - 2pv'_0 - 2ikv'_1 &= 0, \end{aligned} \quad (2.42)$$

terms $\mathcal{O}(r^{p-3} \ln r)$:

$$\begin{aligned} (m^2 - 2n^2 - p^2 + 2p - 1)u'_1 + ik(3 - 2p)u'_2 + (k^2 - \omega^2 + 2)u'_3 + 2mnv'_1 &= 0, \\ (m^2 - p^2 + 2p - 1)v'_1 + ik(3 - 2p)v'_2 + (k^2 - \omega^2)v'_3 + 2mnu'_1 &= 0. \end{aligned} \quad (2.43)$$

Since at least one of the components u'_0 , u_0 , v'_0 and v_0 must be non-zero, we find that two cases follow from (2.37) and (2.38). In the first case (a), $k^2 = \omega^2 - 2$ and the components $v'_0 = v_0 = 0$ while u'_0 and u_0 are non-zero. And in the second case (b), $k^2 = \omega^2$ and the components $u'_0 = u_0 = 0$ and v'_0 and v_0 are non-zero.

(a) Consider the consequences of the first case. Here the terms $\mathcal{O}(r^{p-1} \ln r)$ (2.39) and $\mathcal{O}(r^{p-1})$ (2.40) reduce to:

$$ik(1 + 2p)u'_0 = 0, \quad 2v'_1 = 0, \quad (2.44)$$

and

$$ik(1 + 2p)u_0 + 2iku'_0 = 0, \quad 2v_1 = 0, \quad (2.45)$$

respectively. From these equations it follows that $v'_1 = v_1 = 0$. Also, for non-zero u'_0 , either $k = 0$ or $p = -\frac{1}{2}$. However, we are interested in zero modes and thus will only consider values of $\omega^2 \ll 2$. This means that we do not have to consider the sub-case $k = 0$ here. Recall that $k = \pm i\sqrt{2 - \omega^2}$ for this case. If we assume $p = -\frac{1}{2}$ then it follows that $u'_0 = 0$ from (2.45). And if we assume $p \neq -\frac{1}{2}$ then $u'_0 = u_0 = 0$ from (2.44) and (2.45). Thus the only possibility is $p = -\frac{1}{2}$, $u'_0 = 0$ and u_0 non-zero. This follows from the requirement that at least one of the components u_0 , v_0 , u'_0 and v'_0 in the expansion (2.36) is non-zero.

Proceeding to higher order terms we find that the terms $\mathcal{O}(r^{p-2} \ln r)$ (2.41) give $u'_1 = v'_2 = 0$, those $\mathcal{O}(r^{p-2})$ (2.42) result in

$$u_1 = \frac{i(2n^2 + (1/4) - m^2)}{2k}u_0, \quad v_2 = mnu_0,$$

and the terms $\mathcal{O}(r^{p-3} \ln r)$ (2.43) yield $u'_2 = v'_3 = 0$.

(b) For the second case $k^2 = \omega^2$, the terms of order $\mathcal{O}(r^{p-1} \ln r)$ (2.39) and $\mathcal{O}(r^{p-1})$ (2.40) reduce to:

$$2u'_1 = 0, \quad ik(1 + 2p)v'_0 = 0, \quad (2.46)$$

and

$$2u_1 = 0, \quad ik(1 + 2p)v_0 + 2ikv'_0 = 0, \quad (2.47)$$

respectively. In this case $u'_1 = u_1 = 0$ and either $v'_0 = 0$, $p = -\frac{1}{2}$ or $k = 0$. If $p = -\frac{1}{2}$ then (2.47) reduces to $kv'_0 = 0$. Hence case (b) splits into two sub-cases:

(bi) $p = -\frac{1}{2}$, $v'_0 = 0$ and k non-zero; and (bii) $k = 0 = (\omega)$.

For the case (bi) the terms $\mathcal{O}(r^{p-2} \ln r)$ (2.41) yield $u'_2 = v'_1 = 0$, terms $\mathcal{O}(r^{p-2})$ (2.42) give

$$u_2 = -mnv_0, \quad v_1 = \frac{im^2 - (1/4)}{2k}v_0,$$

while the terms $\mathcal{O}(r^{p-3} \ln r)$ (2.43) yield $u'_3 = v'_2 = 0$.

From the above results it follows that there are four asymptotic behaviours for non-zero k :

$$Y_{1,2} = \frac{e^{\pm i\omega r}}{\sqrt{r}} \begin{pmatrix} -\frac{mn}{r^2} + \mathcal{O}(\frac{1}{r^3}) \\ 1 \pm \frac{(1/4)-m^2}{2i\omega r} + \mathcal{O}(\frac{1}{r^2}) \end{pmatrix}; \quad (2.48)$$

$$Y_{3,4} = \frac{e^{\pm\sqrt{2-\omega^2} r}}{\sqrt{r}} \begin{pmatrix} 1 \pm \frac{2n^2+(1/4)-m^2}{2\sqrt{2-\omega^2} r} + \mathcal{O}(\frac{1}{r^2}) \\ \frac{mn}{r^2} + \mathcal{O}(\frac{1}{r^3}) \end{pmatrix} \quad (2.49)$$

Note that Y_1, Y_2 and Y_4 are bounded as $r \rightarrow \infty$ while Y_3 is unbounded [†].

We still need to consider the sub-case (bii) where $k = 0 = \omega$. In this case the terms $\mathcal{O}(r^{p-2} \ln r)$ (2.41) simplify to

$$u'_2 = -mnv'_0, \quad (m^2 - p^2)v'_0 = 0.$$

Thus, either $v'_0 = 0$ or $p = \pm m$. If we assume $p = \pm m$ then the terms $\mathcal{O}(r^{p-2})$ (2.42) reduce to

$$u_2 = -mnv_0, \quad mv'_0 = 0.$$

implying that either $m = 0$ or $v'_0 = 0$. If, however, we assume that $v'_0 = 0$ then (2.42) reduces to

$$u_2 = -mnv_0, \quad (m^2 - p^2)v_0 = 0,$$

which implies that $p = \pm m$ since $v_0 \neq 0$ as we require at least one of the components u'_0, v'_0, u_0 and v_0 to be non-zero. In summary; $p = \pm m$ and either $v'_0 = 0$ or $m = 0$. Considering terms $\mathcal{O}(r^{p-3} \ln r)$ (2.43) for $p = \pm m$ we find that $u'_3 = v'_2 = 0$. Therefore we have the following behaviours for $k^2 = \omega^2 = 0$:

$$Y_{1,2} = r^{\pm m} \begin{pmatrix} -\frac{mn}{r^2} + \mathcal{O}(\frac{1}{r^4}) \\ 1 + \mathcal{O}(\frac{1}{r^2}) \end{pmatrix} \quad m \neq 0$$

$$Y_1 = \ln r [1 + \mathcal{O}(\frac{1}{r^2})] \begin{pmatrix} 0 \\ 1 \end{pmatrix}; \quad Y_2 = [1 + \mathcal{O}(\frac{1}{r^2})] \begin{pmatrix} 0 \\ 1 \end{pmatrix} \quad m = 0. \quad (2.50)$$

Note that Y_1 is unbounded while Y_2 is bounded as $r \rightarrow \infty$.

Since the eigenfunctions decay to zero as $r \rightarrow \infty$ for $m \neq 0$ and the zero mode for $m = 0$ tends to a constant, we assume the following boundary conditions for the numerics at the right hand boundary: the first derivative of the components u_{mn} and v_{mn} are zero at $r = R$;

$$\frac{d}{dr} u_{mn}(R) = \frac{d}{dr} v_{mn}(R) = 0. \quad (2.51)$$

[†]Here we have adopted the notation consistent with [86]

A pertinent question to ask is, whether the eigenvalue $\omega^2 = 0$ exists or not, in other words, does there exist a bounded solution for $\omega^2 = 0$? First of all we note that each of the solutions Z_i can be expanded over the basis

$$Z_i(r) = \sum_{j=1}^4 T_{ij}^{(n,m)}(\omega) Y_j(r),$$

where the $T_{ij}^{(n,m)}$ are real coefficients. For all $0 < \omega^2 < 2$ we know that the linear combination $T_{23}^{(n,m)}(\omega) Z_1(r) - T_{13}^{(n,m)}(\omega) Z_2(r)$ is regular at the origin since Z_1 and Z_2 are. This linear combination is also bound at $r = \infty$ since it,

$$\begin{aligned} T_{23}^{(n,m)} Z_1 - T_{13}^{(n,m)} Z_2 &= T_{23}^{(n,m)} \left(T_{11}^{(n,m)} Y_1 + T_{12}^{(n,m)} Y_2 + T_{14}^{(n,m)} Y_4 \right) \\ &\quad - T_{13}^{(n,m)} \left(T_{21}^{(n,m)} Y_1 + T_{22}^{(n,m)} Y_2 + T_{24}^{(n,m)} Y_4 \right), \end{aligned}$$

is independent of the only unbounded solution Y_3 . Hence, we are guaranteed that an eigenfunction exists for all $0 < \omega^2 < 2$ and these eigenvalues belong to the continuous spectrum. But what about $\omega = 0$? For $\omega = 0$ the combination $c_1 Z_1(r) + c_2 Z_2(r)$, which is bounded at $r = 0$, is only bounded at $r = \infty$ if c_1 and c_2 satisfy the following *two* conditions: $c_1 T_{11}^{(n,m)}(0) + c_2 T_{21}^{(n,m)}(0) = 0$ and $c_1 T_{13}^{(n,m)}(0) + c_2 T_{23}^{(n,m)}(0) = 0$. This is because both Y_1 and Y_3 are unbounded when $\omega = 0$. The required conditions are only satisfied for non-zero c_1 and c_2 when

$$\begin{vmatrix} T_{11}^{(n,m)}(0) & T_{21}^{(n,m)}(0) \\ T_{13}^{(n,m)}(0) & T_{23}^{(n,m)}(0) \end{vmatrix} = 0,$$

which is not guaranteed to hold for all m and n . Hence, we have to calculate the eigenvalues directly to determine whether $\omega = 0$ is an eigenvalue.

The large r asymptotic analysis also gives a means for discerning true zero modes from eigenfunctions belonging to the continuum. First of all the eigenfunctions which belong to the continuum, $Y_{1,2}$ for $\omega^2 \neq 0$ (2.48), oscillate while zero modes (2.50) do not. However if the eigenvalue is small enough then the wavelength of the oscillation will be much larger than the domain $(0, R)$ and in such a case it will be difficult to observe the oscillations. In this case, eigenfunctions belonging to the continuum might be mistaken for zero modes. Fortunately there is another means of distinguishing zero modes from eigenfunctions belonging to the continuum. The zero modes behave as r^{-m} (2.50) while eigenfunctions from the continuum behave as $r^{-1/2}$ (2.48) as $r \rightarrow \infty$. This difference in behaviour for large r gives a means of discerning zero modes from eigenfunctions from the continuum with full certainty.

If the eigenfunction displays exponential decay such as Y_4 , then it definitely does not belong to the continuum and we will be able to determine if it is a zero mode by refining the grid in the numerics.

Now that we have a means to distinguish true zero modes from other eigenfunctions we can calculate the zero modes for $n = 1, 2$ and 3 numerically.

2.3 Numerical Calculation of the Zero Modes

A second-order finite difference scheme (see Appendix A) is used to convert the differential eigenvalue problem (2.13) to a matrix eigenvalue problem. For the finite differences we use a step size $\Delta r = 0.08$ for a domain of radius $R = 80$ (in other words, a grid with 1000 points). Once the matrix is obtained, numerical libraries in FORTRAN are used in order to compute the eigenvalues and eigenfunctions. A discussion of the results from the numerical calculations for $n = 1, 2$ and 3 follows.

2.3.1 Single vortex ($n = 1$)

First consider the single-vortex solution ($n = 1$), $\Psi_1 = \Phi_1 e^{i\theta}$. In this case, the numerical computations yield three eigenfunctions which are clearly zero modes. One occurs for azimuthal quantum number $m = 0$ and the other two for $m = 1$. We discuss the results for each azimuthal quantum number separately.

Firstly the results for azimuthal quantum number $m = 0$. The four smallest eigenvalues (ω^2) computed, for $m = 0$, are:

$$\omega_0^2 = -1.99 \times 10^{-7}; \omega_1^2 = 2.30 \times 10^{-3}; \omega_2^2 = 7.75 \times 10^{-3} \text{ and } \omega_3^2 = 1.63 \times 10^{-2}.$$

The smallest of these, ω_0^2 , has corresponding complex eigenfunctions $\varphi_{01} = u_{01}$ and $\hat{\varphi}_{01} = v_{01}$, where u_{01} is identically zero and v_{01} (Fig. 2.1) has exactly the same profile as the modulus of the vortex, Φ_1 . In other words there is only one eigenfunction: $\hat{\varphi}_{01} = v_{01}$. Note that the components u_{01} and v_{01} both satisfy the boundary conditions previously

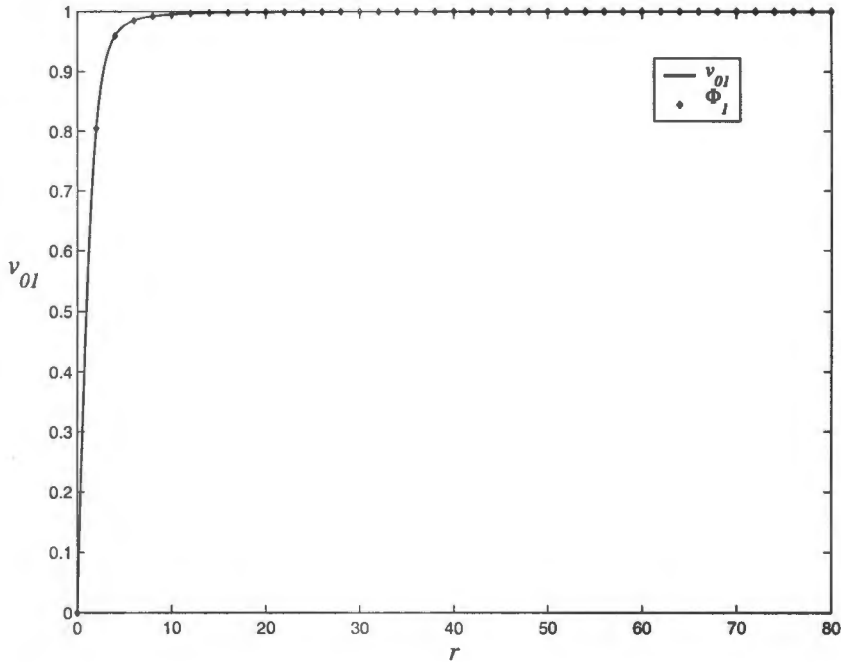


Figure 2.1: v_{01} , corresponding to ω_0^2 , and Φ_1 as functions of r

determined. They are zero at the origin and their first derivatives with respect to r

vanish as $r \rightarrow R$. Note also that \tilde{u}_{01} does not oscillate and hence the complex eigenfunction φ_{01} is a true zero mode. The next smallest eigenvalue (ω_1^2) has a corresponding eigenfunction with a function \tilde{u}_{01} which decays as $r^{-1/2}$ and which oscillates with wave number $k \sim \omega$, while the function u_{01} is still identically zero. This eigenfunction is therefore not a zero mode but corresponds to a small positive eigenvalue. Any eigenfunction with an eigenvalue ω^2 greater than ω_1^2 is therefore also not a zero mode. Thus, there is only one zero mode for vorticity $n = 1$ and azimuthal quantum number $m = 0$. This is one of the expected zero modes and corresponds to the global $U(1)$ degree of freedom or equivalently to rotations in the plane. That we are able to calculate this zero mode numerically is an indication that our numerical computations are correct.

For $m = 1$, the first four smallest eigenvalues computed are:

$$\omega_0^2 = -1.08 \times 10^{-4}; \omega_1^2 = 8.63 \times 10^{-4}; \omega_2^2 = 5.38 \times 10^{-3} \text{ and } \omega_3^2 = 1.30 \times 10^{-2}.$$

The components, u_{11} and v_{11} corresponding to the smallest eigenvalue (ω_0^2) are shown in Fig. 2.2 and Fig. 2.3, respectively. Note, again, that the components u_{11} and v_{11} obey the required boundary conditions. Also, these components display the asymptotic behaviour associated with $\omega^2 = 0$: $v_{11} \propto r^{-m}$, $u_{11} \rightarrow -v_{11}r^{-2}$ as $r \rightarrow \infty$. Hence we have two linearly independent zero modes, the complex eigenfunctions $\tilde{\varphi}_{11}$ and $\hat{\varphi}_{11}$.

More so, there are only two zero modes for $m = 1$. This results as the components v_{11} and u_{11} corresponding to eigenvalues $\omega^2 > \omega_0^2$ display the asymptotic behaviour associated with small positive eigenvalues: Both oscillate with wave number $k \sim \omega$ while v_{11} decays in absolute magnitude as $1/\sqrt{r}$ and $u_{11} \rightarrow -v_{11}/r^2$ as $r \rightarrow R$. This agrees with the previously mentioned fact that there can be at most two linearly independent zero modes to each specific azimuthal quantum number m .

The two zero modes $\tilde{\varphi}_{11}$ and $\hat{\varphi}_{11}$ correspond to translational degrees of freedom in the x and y directions, respectively. Recall that $\tilde{\varphi}_{11}$ corresponds to the zero mode for translation in x (2.23) and $\hat{\varphi}_{11}$ to the zero mode for translation in y (2.24), if the components u_{11} and v_{11} :

$$\begin{pmatrix} u_{11} \\ v_{11} \end{pmatrix} \propto \begin{pmatrix} -\frac{d\Phi_1}{dr} \\ \frac{\Phi_1}{r} \end{pmatrix}. \quad (2.52)$$

When we compare a normalised graph [†] of u_{11} and the first order finite difference approximation of $-\frac{d\Phi_1}{dr}$, we find they have the exact same profile (Fig. 2.2). And when a normalised graph of v_{11} is compared to $\frac{\Phi_1}{r}$ we observe that they are very similar (Fig. 2.3). The same normalisation constant was used for both u_{11} and v_{11} . Fig. 2.3 shows that a slight deviation occurs between $\frac{\Phi_1}{r}$ and v_{11} as $r \rightarrow R$; the bottom, dotted, curve is $\frac{\Phi_1}{r}$ while the top, solid, curve is $v_{11}(r)$ (normalised). We expect that the deviation between the two curves occurs as a result of setting the derivative of the function v_{11} to zero at $R = 80$, hence forcing the function v_{11} to ‘flatten’ out faster than it should. Because $\frac{\Phi_1}{r}$ decays very slowly to zero its derivative is not actually zero at $r = 80$ and, therefore, setting the derivative to zero is only an approximation to the true boundary condition.

[†]By normalise, we mean that the graph of $cf(r)$ is considered, for some real constant c

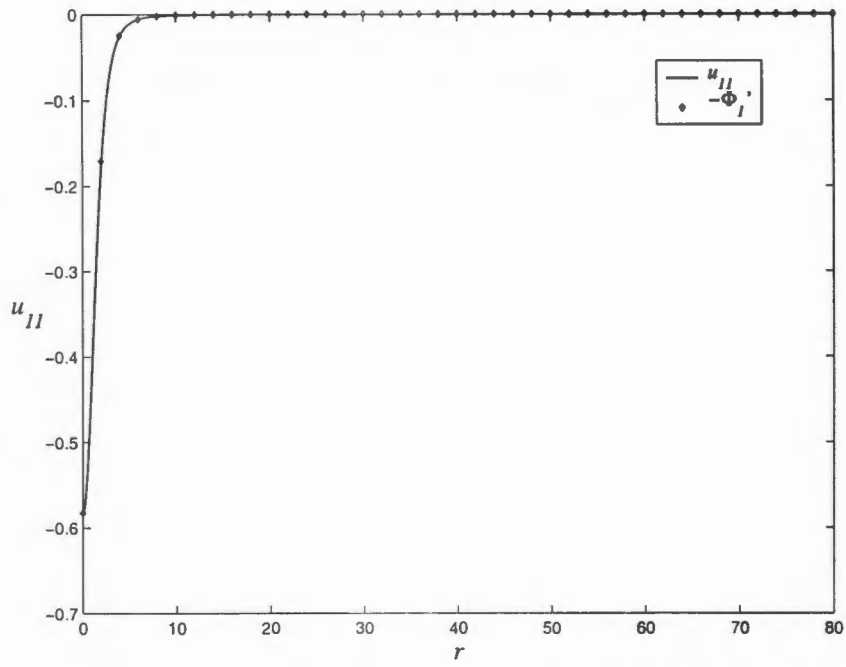


Figure 2.2: $u_{11}(r)$, corresponding to ω_0^2 , and $-\frac{d\Phi_1}{dr}$ as functions of r

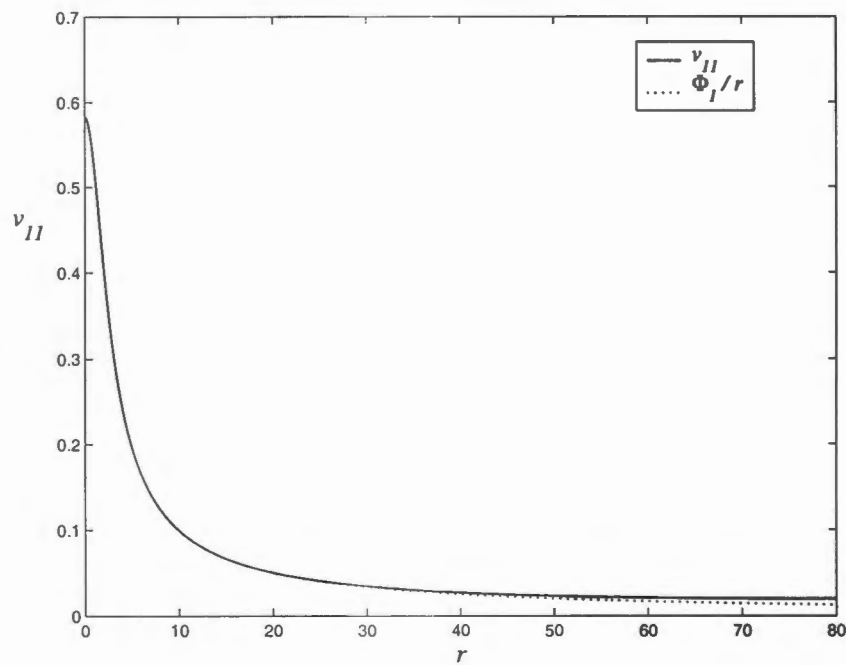


Figure 2.3: $v_{11}(r)$, corresponding to ω_0^2 , and Φ_1/r as functions of r

m	ω_0^2	ω_1^2	ω_2^2	ω_3^2
2	1.45×10^{-3}	7.00×10^{-3}	1.55×10^{-2}	2.70×10^{-2}
3	2.75×10^{-3}	1.00×10^{-2}	2.00×10^{-2}	3.31×10^{-2}
4	4.40×10^{-3}	1.34×10^{-2}	2.51×10^{-2}	3.97×10^{-2}
5	6.42×10^{-3}	1.72×10^{-2}	3.05×10^{-2}	4.67×10^{-2}

Table 2.1: The four smallest eigenvalues (ω^2) for $n = 1$ and $m = 2, 3, 4$ and 5

Thus far, only the three expected zero modes have been found. The question now is whether there are any other zero modes? To answer this we now discuss the results for the azimuthal quantum numbers $m = 2, 3, 4$ and 5 . The smallest eigenvalues for each azimuthal quantum number are given in Table 2.1. For these values of m , the components v_{m1} corresponding to the smallest computed eigenvalue (ω_0^2) initially grow but then flatten to non-zero values as they approach the boundary $r = R$ (Fig 2.4). Since this growth occurs for most of the domain, from $r = 0$ up to about $r = 55$ or $r = 65$, it appears as if the flattening is purely an effect of imposing the derivative to vanish at $r = 80$.

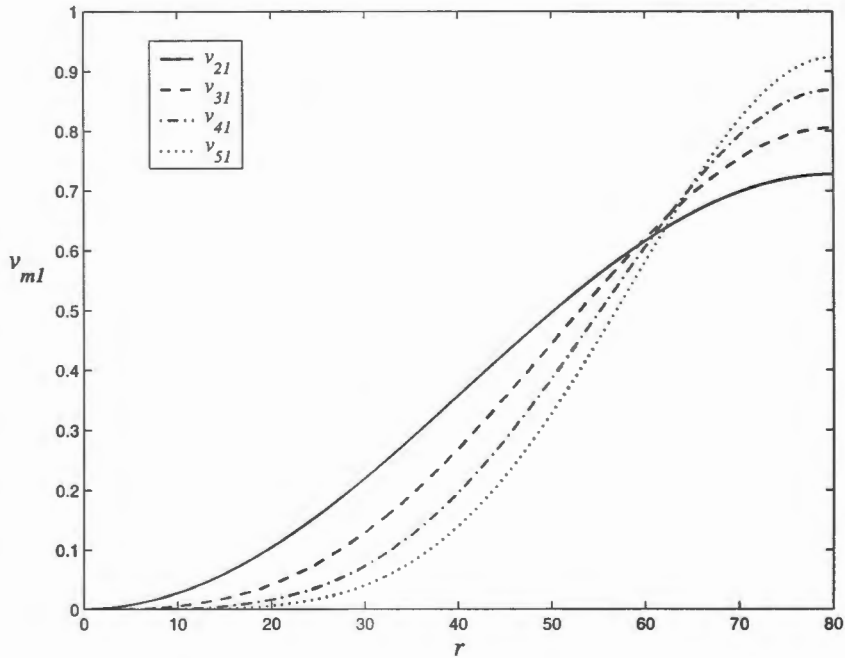


Figure 2.4: v_{21} , v_{31} , v_{41} and v_{51} , corresponding to ω_0^2 , as functions of r

Recall that the boundary conditions (2.50) for zero modes for large r require that $v_{m1} \sim r^{-m}$ and $u_{m1} \rightarrow -mv_{m1}/r^2$ as $r \rightarrow \infty$. The components v_{m1} for $m = 3, 4, 5$ clearly

do not satisfy these boundary conditions. Therefore these solutions do not correspond to zero modes. Also when we examine the eigenfunctions for eigenvalues $\omega^2 > \omega_0^2$, we find that their corresponding components v_{m1} oscillate with $k \sim \omega$ and hence correspond to small strictly positive eigenvalues. These results show that there are no zero modes for $m = 2, 3, 4$ and 5 for the single vortex. An analytic argument in [85] establishes that zero modes do not exist for $m \geq 2n$. Our results agree with this as there are no zero modes for $m \geq 2$ ($n=1$).

A pertinent question is whether the components for azimuthal quantum numbers $m = 2$ to 5 are in fact being artificially constrained at the right hand boundary? The analysis of the behaviour allowed by equation (2.13) for large r shows that the behaviours $v_{m1} \sim r^{\pm m}$ and $u_{m1} \rightarrow -mv_{m1}r^{-2}$, as $r \rightarrow \infty$, are allowed as solutions when $\omega^2 = 0$. When comparing the computed components v_{m1} for $m \geq 2$ to the graph of $c_1 r^m$, for some appropriate constant c_1 , we find that they follow each other closely and v deviates only as they approach $r = R$. The same occurs when comparing u_{m1} to $c_2 r^{m-2}$, for some appropriate constant c_2 . This seems to indicate that the computed components u_{m1} and v_{m1} are “trying to grow” as r^m and r^{m-2} , respectively. To check if this is indeed the case and that the flattening is purely due to the imposed boundary conditions, we perform the transformation $A(r) = u(r)r^{-(m-2)}$, $B(r) = v(r)r^{-m}$ in (2.13). We then solve this new eigenvalue problem numerically. If the components, u and v , calculated earlier are growing as described, then the transformed functions, $A(r)$ and $B(r)$, should tend to a constant as $r \rightarrow \infty$. The results from the numerical computations confirm that this is true. In fact the transformed functions A and B tend to constants very quickly. Therefore the original components u_{m1} and v_{m1} for $m = 2$ to 5 grow as $r \rightarrow \infty$.

In conclusion we find that for the single vortex solution there are only three zero modes; one corresponding to the global $U(1)$ degree of freedom (or equivalently rotations in the plane) and the other two due to the translational degrees of freedom in the x and y directions.

2.3.2 Double vortex ($n = 2$)

Next we examine the coaxial double-vortex case ($n = 2$), $\Psi_2 = \Phi_2 e^{2i\theta}$. As with the single vortex, our numerical computations only yield three zero modes, one for $m = 0$ and the other two for $m = 1$.

For $m = 0$, the four smallest eigenvalues in the spectrum are:

$$\omega_0^2 = 8.81 \times 10^{-8}; \omega_1^2 = 2.33 \times 10^{-3}; \omega_2^2 = 7.89 \times 10^{-3} \text{ and } \omega_3^2 = 1.67 \times 10^{-2}.$$

The smallest eigenvalue (ω_0^2) has corresponding complex eigenfunctions $\tilde{\varphi} = u_{02}$ and $\hat{\varphi} = v_{02}$ where the component u_{02} is identically zero and v_{02} has exactly the same profile as the modulus of the vortex, Φ_2 (Fig. (2.5)). Again, this means there is only the one eigenfunction $\hat{\varphi} = v_{02}$. This, as in the case of the single vortex ($n = 1$), is a zero mode. This is an expected zero mode and corresponds to the global $U(1)$ degree of freedom or equivalently to rotations in the plane. The components v_{02} corresponding to values of $\omega^2 > \omega_0^2$ all oscillate with $k \sim \omega$ while decaying in magnitude to zero as $1/\sqrt{r}$ as $r \rightarrow R$. The u_{02} are identically zero. Hence, the eigenfunctions corresponding to these larger eigenvalues display the behaviour associated with small positive eigenvalues of the continuous spectrum and are not zero modes. We conclude therefore that there is only

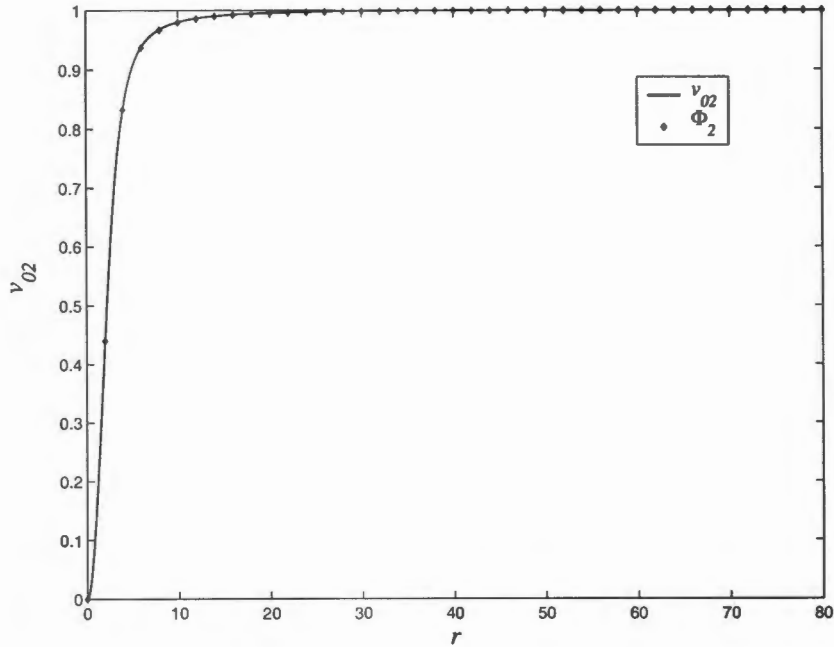


Figure 2.5: v_{02} , corresponding to ω_0^2 , and Φ_2 as functions of r

one zero mode for azimuthal quantum number $m = 0$, $\varphi = i\Phi_2(r)$.

For $m = 1$ the smallest computed eigenvalues in the spectrum are:

$$\omega_0^2 = -8.23 \times 10^{-5}; \omega_1^2 = 1.01 \times 10^{-3}; \omega_2^2 = 5.79 \times 10^{-3} \text{ and } \omega_3^2 = 1.38 \times 10^{-2}.$$

The complex eigenfunctions $\tilde{\varphi}$ and $\hat{\varphi}$ corresponding to ω_0^2 have components u_{12} and v_{12} as shown in Fig. 2.6 and Fig. 2.7, respectively. Both of these components obey the required boundary conditions as they are zero at the origin and have vanishing first derivatives at $r = 80$. The corresponding eigenfunctions $\tilde{\varphi}$ and $\hat{\varphi}$ (2.21) are zero modes since the components do not oscillate. Also $v_{12} \sim r^{-2}$ and $u_{12} \rightarrow -2v_{12}/r^2$ as $r \rightarrow \infty$. As with the single vortex, $\tilde{\varphi}$ corresponds to the translational degree of freedom in the x direction (2.23) and $\hat{\varphi}$ to the translational degree of freedom in the y direction (2.24). When we compare u_{12} to the finite difference approximation of $-\frac{d\Phi_2(r)}{dr}$ we observe that their profiles are identical. However, when v_{12} , normalised, is compared with the function $\frac{2}{r}\Phi_2(r)$ we see that they are not identical. The two curves deviate as they approach the right-hand boundary, $r = R$, (Fig. 2.7). The same normalisation constant was used for u_{12} and v_{12} . As with the single vortex ($n = 1$) the deviation is a result of setting the first derivative of v_{12} to zero at $r = 80$. Since the function $\frac{2}{r}\Phi_2(r)$ decreases slowly, the boundary condition imposed at $r = 80$ is, unfortunately, not the most appropriate approximation. When the values of ω^2 greater than ω_0^2 are considered the corresponding components v_{12} are found to oscillate implying that the eigenvalues are small positive eigenvalues. Therefore the eigenfunctions $\tilde{\varphi}_{12}$ and $\hat{\varphi}_{12}$ corresponding to $\omega^2 > \omega_0^2$ are *not* zero modes. Thus, we only have two zero modes for $m = 1$. They correspond to translational degrees of freedom in x and y .

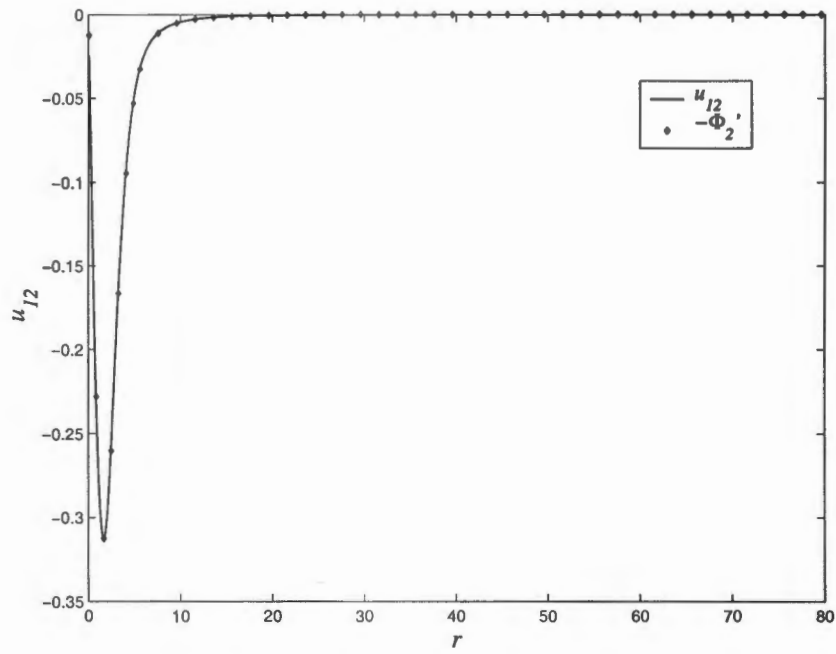


Figure 2.6: u_{12} , corresponding to ω_0^2 , and $-\frac{d\Phi_2}{dr}$ as functions of r

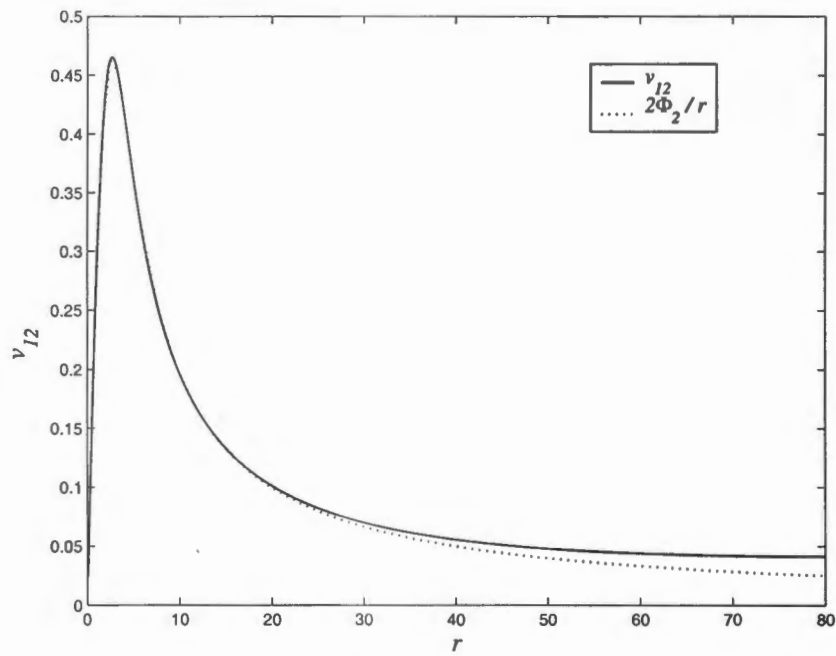


Figure 2.7: v_{12} , corresponding to ω_0^2 , and $\frac{2\Phi_2}{r}$ as a functions of r

What about the values of $m \geq 2$? Here the situation is very similar to the single vortex case. The components v_{m2} corresponding to the smallest computed values of $\omega^2 = \omega_0^2$, (given in Table 2.2) for $m = 2, 3, 4$ and 5, appear to grow with r (Fig. 2.8).

The components grow for most of the domain, up to about $r = 60$, but are forced to

m	ω_0^2	ω_1^2	ω_2^2	ω_3^2
2	1.45×10^{-3}	6.97×10^{-3}	1.54×10^{-2}	2.67×10^{-2}
3	2.75×10^{-3}	9.98×10^{-3}	2.00×10^{-2}	3.29×10^{-2}
4	4.40×10^{-3}	1.34×10^{-2}	2.50×10^{-2}	3.96×10^{-2}
5	6.41×10^{-3}	1.72×10^{-2}	3.04×10^{-2}	4.66×10^{-2}

Table 2.2: The four smallest eigenvalues (ω^2) for the double vortex for $m = 3, 4$ and 5

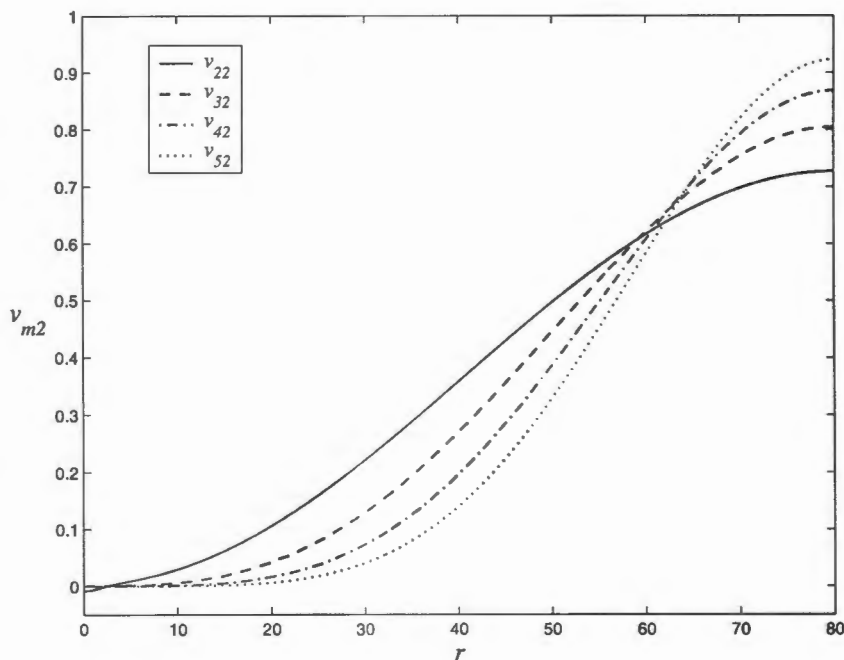


Figure 2.8: v_{22}, v_{32}, v_{42} and v_{52} , corresponding to ω_0^2 , as functions of r

flatten as they approach the right hand boundary. This is identical to the situation for the single vortex and again we suspect that this flattening is a result of the boundary condition imposed at $r = 80$. When we perform similar transformations, as with the single vortex, viz. $A(r) = u_{m2}(r)r^{-(m-2)}$ and $B(r) = v_{m2}(r)r^{-m}$ and then solve for the transformed functions $A(r)$ and $B(r)$, we find they decay very quickly to non-zero constants. This shows that the original components u_{m2} and v_{m2} do behave as r^{m-2} and

r^m , respectively, for $m \geq 2$. The flattening is purely a result of the imposed boundary conditions. Clearly these are not zero modes. When the eigenfunctions corresponding to the eigenvalues $\omega^2 \geq \omega_0^2$, for $m = 2$ to 5, are examined we find that all the components v_{m2} of the corresponding eigenfunctions oscillate and grow. Hence there are no zero modes for $m = 2, 3, 4$ and 5. Our results for $m = 4$ and 5 agree with the known result that zero modes cannot occur for $m \geq 2n = 4$ [85]. This fact and our results for $m = 2$ and 3 mean that there are no zero modes for $m \geq 2$.

There are however two eigenfunctions $\tilde{\varphi}$ and $\hat{\varphi}$ corresponding to a non-zero eigenvalue (ω^2) with components u and v which neither oscillate nor grow. These eigenfunctions occur for $m = 2$ and their corresponding eigenvalue is $\omega^2 = -0.419$. This is obviously not a zero mode, however it is still very interesting. Recall that a separable solution for the perturbation of the form $\delta\psi = \chi \cos \omega t$ was assumed. Therefore if ω^2 is negative then ω is purely imaginary, causing the perturbation to grow with time. Thus the vortex solution Ψ_2 is unstable. This agrees with the known fact that the double-coaxial vortex solution is unstable [82, 85]. This result was obtained in [82] by considering the energy of the vortices while [85] obtained the result by considering modes of the linearised equation of motion.

We conclude from our results that for the double vortex ($n = 2$) there are only three zero modes. One corresponds to a global $U(1)$ degree of freedom (or equivalently rotations in the plane) and the other two to translational degrees of freedom in the x and y directions.

2.3.3 Triple vortex ($n = 3$)

We shall now proceed with the coaxial triple-vortex solution ($n = 3$), $\Psi_3 = \Phi_3 e^{3i\theta}$. As with the two previous multivortices, the numerical computations only give three zero modes; one for $m = 0$ and the other two for $m = 1$.

For the azimuthal quantum number $m = 0$ the numerics give:

$$\omega_0^2 = -2.54 \times 10^{-7}; \omega_1^2 = 2.37 \times 10^{-3}; \omega_2^2 = 8.10 \times 10^{-3} \text{ and } \omega_3^2 = 1.71 \times 10^{-2}$$

as the four smallest computed eigenvalues. The complex eigenfunctions corresponding to the smallest eigenvalue ω_0^2 are $\tilde{\varphi} = u_{03}$ and $\hat{\varphi} = v_{03}$, where u_{03} is identically zero and $v_{03} \propto \Phi_3$ (Fig. 2.9). This is the same situation as occurs with the two previous vortex solutions. The eigenfunction $\tilde{\varphi}$ is the zero mode corresponding to a global $U(1)$ degree of freedom or equivalently a rotation in the plane, while $\hat{\varphi}$ is trivial. The complex eigenfunctions corresponding to eigenvalues $\omega^2 > \omega_0^2$ have components v_{03} which oscillate with wave number $k \sim \omega$ and decay as $1/r$ as $r \rightarrow \infty$, while the u_{03} are identically zero. These eigenfunctions are therefore not zero modes, as their components obey the behaviour associated with small positive eigenvalues (2.48). Thus there is only the one zero mode with $m = 0$ for the coaxial triple-vortex.

For the azimuthal quantum number $m = 1$ the smallest computed eigenvalues in the spectrum are:

$$\omega_0^2 = -8.83 \times 10^{-5}; \omega_1^2 = 1.11 \times 10^{-3}; \omega_2^2 = 6.12 \times 10^{-3} \text{ and } \omega_3^2 = 1.45 \times 10^{-2}.$$

The two complex eigenfunctions $\tilde{\varphi}$ and $\hat{\varphi}$ corresponding to ω_0^2 , have components u_{13} and

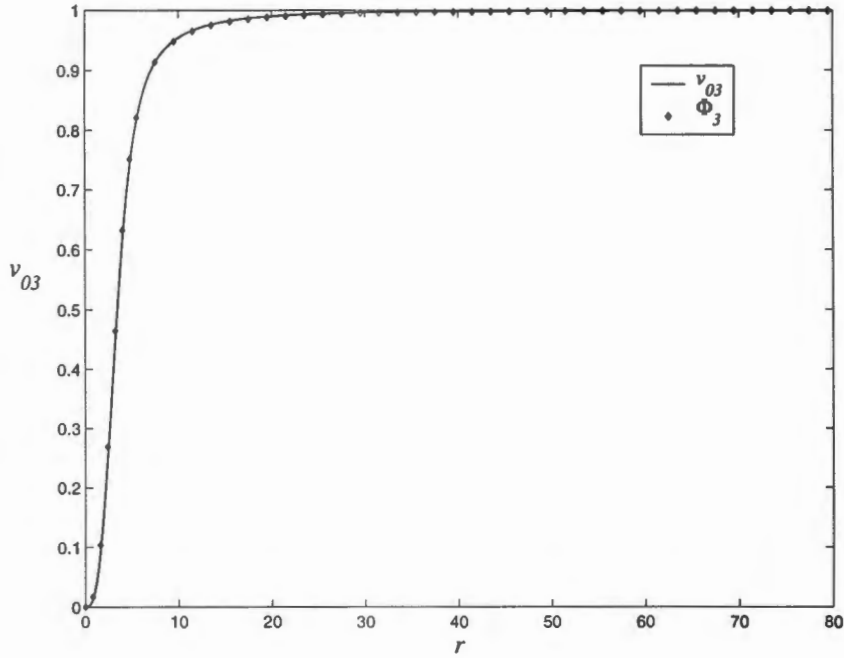


Figure 2.9: v_{03} , corresponding to ω_0^2 , and Φ_3 as functions of r

v_{13} as shown in Fig. 2.10 and Fig. 2.11, respectively. Note that both of these components obey the required boundary conditions (2.34) and (2.51), as their first derivatives vanish at the origin and as $r \rightarrow 80$. Since the components behave as in (2.50); $v_{13} \sim r^{-3}$ and $u_{13} \rightarrow -3v_{13}/r^2$ as $r \rightarrow \infty$ and they do not oscillate, their associated eigenvalue is the zero eigenvalue. Hence, the eigenfunctions $\tilde{\varphi}_{13}$ and $\hat{\varphi}_{13}$ corresponding to the smallest eigenvalue ω_0^2 are zero modes. As with the other vortices $\tilde{\varphi}_{13}$ corresponds to a translational degree of freedom in the x direction (2.23) and $\hat{\varphi}_{13}$ to a translational degree of freedom in the y direction (2.24).

This is confirmed by comparing the normalised graph of u_{13} to the finite difference approximation of $-\frac{d\Phi_3(r)}{dr}$ (Fig. 2.10) and a normalised graph of v_{13} to $\frac{3}{r}\Phi_3(r)$ (Fig. 2.11). The same normalisation constant was used for both u_{13} and v_{13} . Fig. 2.10 shows that the profiles of u_{13} and $-\frac{d\Phi_3(r)}{dr}$ are identical, while Fig. 2.11 shows that the curves of v_{13} and $\frac{3}{r}\Phi_3(r)$ deviate as they approach the right hand boundary, $r = R$. As with the other two vortices this deviation results from setting the first derivative of the components to zero at $r = 80$. Since the function $\frac{3}{r}\Phi_3(r)$ is a rationally decreasing function the boundary condition imposed at $r = 80$ is unfortunately not an extremely good approximation.

For the values of $\omega^2 > \omega_0^2$ the corresponding components v_{13} and u_{13} both oscillate and follow the behaviour in (2.48). This implies that these larger eigenvalues belong to positive eigenvalues and the corresponding eigenfunctions are not zero modes. Thus there are only two zero modes for $m = 1$ and $n = 3$. They correspond to translational degrees of freedom in the x and y directions.

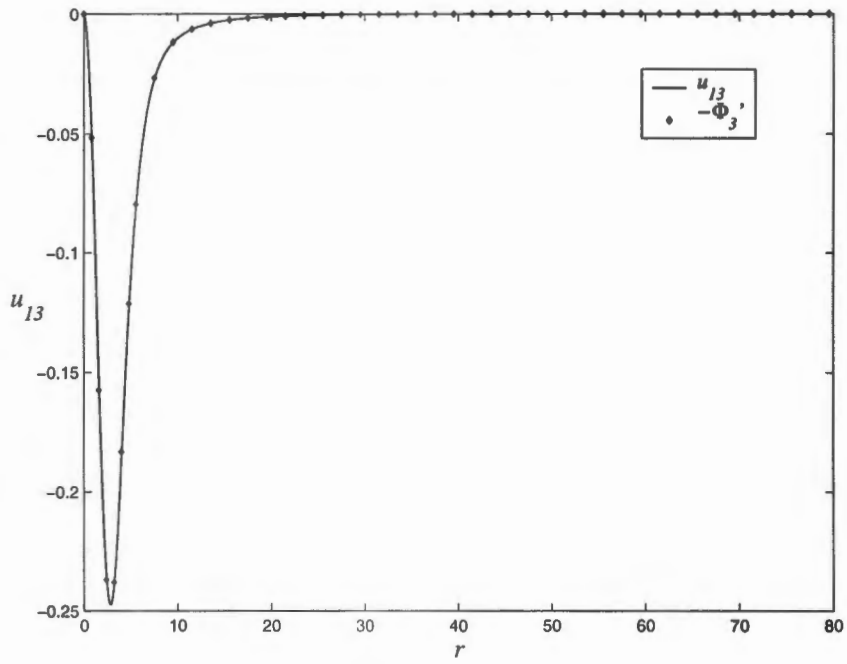


Figure 2.10: u_{13} , corresponding to ω_0^2 , and $-\frac{d\Phi_3}{dr}$ as functions of r

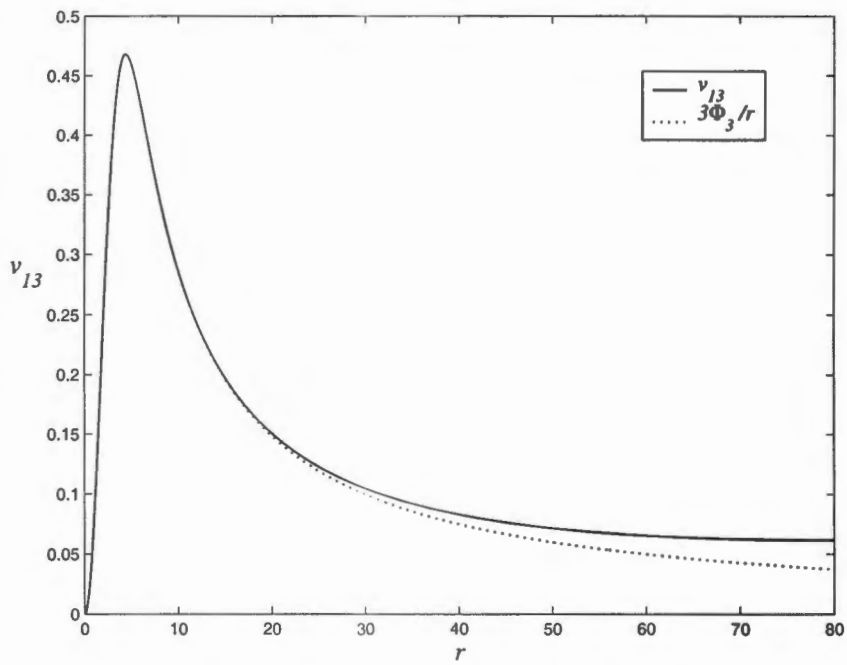


Figure 2.11: v_{13} , corresponding to ω_0^2 , and $\frac{3\Phi_3}{r}$ as functions of r

m	ω_0^2	ω_1^2	ω_2^2	ω_3^2
2	1.44×10^{-3}	6.92×10^{-3}	1.52×10^{-2}	2.64×10^{-2}
3	2.74×10^{-3}	9.93×10^{-3}	1.98×10^{-2}	3.26×10^{-2}
4	4.39×10^{-3}	1.34×10^{-2}	2.48×10^{-2}	3.93×10^{-2}
5	6.39×10^{-3}	1.72×10^{-2}	3.03×10^{-2}	4.63×10^{-2}

Table 2.3: The four smallest eigenvalues (ω^2) for the coaxial triple-vortex ($n = 3$) for $m = 2, 3, 4$ and 5

What about the values of $m \geq 2$? Again, the situation is similar as with the single vortex and coaxial double-vortices. The components v_{m3} corresponding to the smallest computed values of $\omega^2 = \omega_0^2$, (given in Table 2.3) for $m = 2, 3, 4$ and 5, appear to grow with r (Fig. 2.12). As is the case for the single vortex and the coaxial double-vortex

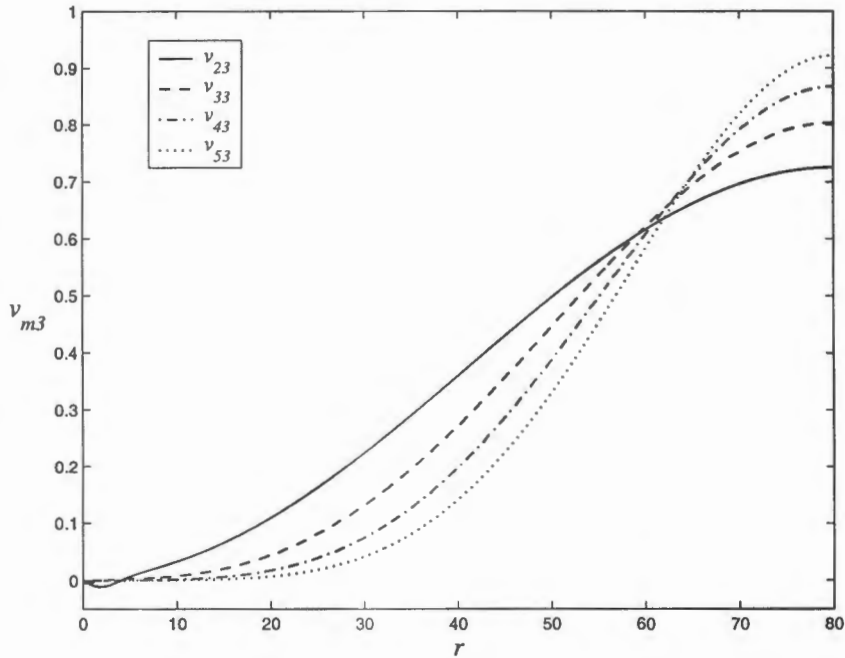


Figure 2.12: v_{23}, v_{33}, v_{43} and v_{53} , corresponding to ω_0^2 , as functions of r

the components grow for most of the domain and only flatten as they approach the right hand boundary $R = 80$. The fact that they approach a non-zero value as $r \rightarrow 80$ shows that the eigenfunctions are *not* zero modes. Performing similar transformations as with the other vortices viz. $A(r) = u_{m3}r^{-(m-2)}$ and $B(r) = v_{m3}(r)r^{-m}$ and solving for the transformed functions $A(r)$ and $B(r)$, we find that $A(r)$ and $B(r)$ decay to non-zero constants very quickly as $r \rightarrow 80$. Thus the original components u_{m2} and v_{m2} actually

grow as r^{m-2} and r^m , respectively, for $m \geq 2$. The flattening is purely a result of the imposed boundary conditions (2.51). Also the eigenfunctions corresponding to the eigenvalues $\omega^2 > \omega_0^2$, for all $m = 2$ to 5, have components which oscillate. Thus, there are no zero modes for azimuthal quantum numbers $m = 2, 3, 4$ and 5. These results along with the fact that there are no zero modes for $m \geq 3n = 6$ [85] implies that there are no zero modes for $m \geq 2$.

There are however six eigenfunctions, $\tilde{\varphi}_{m3}$ and $\hat{\varphi}_{m3}$ for $m = 2, 3, 4$, with components u and v which neither oscillate nor grow. These eigenfunctions correspond to the eigenvalues $\omega^2 = -0.256$, $\omega^2 = -0.658$ and $\omega^2 = -0.241$ for $m = 2, 3$ and 4, respectively. These are obviously not zero modes, however, they are still very interesting. As with the double-coaxial vortex, these negative eigenvalues imply that the vortex is unstable. Again, this agrees with the known fact that coaxial-vortices with $n > 1$ are unstable [82, 85].

We conclude from our results that for the coaxial triple-vortex ($n = 3$) there are only three zero modes. One corresponding to a global $U(1)$ degree of freedom (or equivalently rotations in the plane) and the other two to translational degrees of freedom in the x and y directions.

2.4 Summary

We were unable to determine whether the eigenvalue $\omega^2 = 0$ exists or not, by simply looking at the asymptotics of the eigenfunctions. Therefore we had to compute the eigenvalues directly in order to determine whether any zero modes do in fact exist. Unfortunately, the eigenvalues $\omega^2 > 0$ belong to the continuous spectrum. This means that if the numerics give a small positive eigenvalue, it could either be a numerical approximation of the zero eigenvalue or be an eigenvalue in its own right. Thus we needed a means to distinguish whether the numerically computed eigenfunctions corresponded to positive eigenvalues or were in fact zero modes. This was provided by the analysis of the asymptotic behaviours of the eigenfunctions. With this information in hand we then proceeded to calculate the zero modes numerically.

From our results it follows that for all the multivortex solutions ($n = 1, 2$ and 3) the only degrees of freedom that exist are those expected from the form of the equation of motion (2.2). Namely, the zero modes corresponding to a global $U(1)$ degree of freedom and the two translational degrees of freedom. From these results we conclude that it is *not possible to continuously* deform either the coaxial triple- or double-vortex solutions into non-coaxial vortex bound states.

We also confirmed that the coaxial double- and triple-vortices are unstable.

Chapter 3

Complex Sine-Gordon-1

The complex sine-Gordon-1 equation in two euclidean dimensions,

$$\nabla^2\psi + \frac{(\nabla\psi)^2}{1-|\psi|^2}\bar{\psi} + \psi(1-|\psi|^2) = 0, \quad (3.1)$$

is an equation for a complex scalar field ψ . It originally appeared in its (1+1)-dimensional (Minkowski space) formulation:

$$\psi_{xx} - \psi_{tt} + \frac{(\psi_x^2 - \psi_t^2)}{1-|\psi|^2}\bar{\psi} + \psi(1-|\psi|^2) = 0, \quad (3.2)$$

as a reduction of the $O(4)$ nonlinear σ -model [87] and in a theory of dual strings interacting through a massless scalar field [88]. This last theory is equivalent to a relativistic theory of vortex motion in a superfluid. The Minkowski complex sine-Gordon has also appeared in the study of classical massless Fermi fields with symmetric couplings [89] and in hydrodynamics [90] where an evolution equation for a vortex line is shown to be equivalent to the Lund-Regge equation. The Lund-Regge equation [88]

$$\alpha_{xx} - \alpha_{tt} - \frac{\sin\alpha}{\cos^3\alpha}(\chi_x^2 - \chi_t^2) + \sin\alpha \cos\alpha = 0, \quad (\chi_x \tan^2\alpha)_x = (\chi_t \tan^2\alpha)_t, \quad (3.3)$$

is just another formulation of the Minkowski complex sine-Gordon equation. The two equations, (3.2) and (3.3), are related via $\psi = \sin\alpha e^{i\chi}$. The term "complex sine-Gordon" follows from the fact that by setting $\chi = 0$ and rescaling $\alpha \rightarrow \alpha/2$, $x \rightarrow x/\sqrt{2}$ and $t \rightarrow t/\sqrt{2}$, these equations of motion reduce to the well known real sine-Gordon equation (eq. (1.15)). This complex sine-Gordon equation has also appeared in the description of stimulated Raman scattering in nonlinear optics [91]. The Euclidean form of the complex sine-Gordon equation (3.1) may be obtained as a symmetry reduction of the self-dual Yang-Mills over a self-dual manifold [92].

More recently, interest in the Euclidean and Minkowski complex sine-Gordon models [93, 94] was expressed when it was realised that they may be interpreted as integrable deformations of the $SU(2)/U(1)$ coset model [95, 96]. Unlike the Ginzburg-Landau both the Minkowski [87, 97, 98, 99] and the Euclidean [100] versions of the complex sine-Gordon are completely integrable (in the sense that they admit the Lax representation).

The Euclidean complex sine-Gordon equation (3.1) is known to admit coaxial multi-vortex solutions as one of its families of static solutions [67]. These multivortex solutions are of the form $\Psi_n = \Phi_n(r)e^{in\theta}$, where the Φ_n 's are expressed as ratios of the modified Bessel functions and n is the vorticity (2). The equation which the modulus $\Phi_n(r)$ must satisfy

$$\frac{d^2\Phi_n}{dr^2} + \frac{1}{r} \frac{d\Phi_n}{dr} + \frac{\Phi_n}{1 - \Phi_n^2} \left[\left(\frac{d\Phi_n}{dr} \right)^2 - \frac{n^2}{r^2} \right] + \Phi_n(1 - \Phi_n^2) = 0, \quad (3.4)$$

is obtained by substituting $\psi = \Phi_n(r)e^{in\theta}$ into (3.1).

As with the Ginzburg-Landau model, it is clear from the form of the equation (3.5) that all of its solutions will have a global $U(1)$ degree of freedom (or, equivalently, a degree of freedom for rotations in the plane) as well as two translational degrees of freedom. However, it is of interest to know whether these coaxial multivortex solutions display any other degrees of freedom. If they do, then these vortex solutions belong to a larger family of solutions to (3.5), possibly a family including non-coaxial vortex states.

To determine whether any other degrees of freedom exist, we are going to consider equation (3.1) as a reduction of a (2+1)-dimensional theory

$$\psi_{tt} - \nabla^2\psi - \frac{(\nabla\psi)^2}{1 - |\psi|^2} \bar{\psi} - \psi(1 - |\psi|^2) = 0, \quad (3.5)$$

when calculating the zero modes. This particular generalisation is chosen because it produces an eigenvalue problem similar to the one in the case of the Ginzburg-Landau model. Note that this generalisation is not relevant, physically (since the equation is not Lorentz invariant), therefore negative eigenvalues will not have much meaning here. If we had chosen a Lorentz invariant generalisation we would obtain a *generalised* eigenvalue problem, increasing the computational complexity of the problem unnecessarily. We now proceed with calculating the zero modes for the coaxial multivortices of the complex sine-Gordon-1 equation.

3.1 Linearisation

Firstly, we linearise the complex sine-Gordon equation of motion (3.5) about a coaxial n -vortex, Ψ_n . This gives the equation

$$\begin{aligned} (\delta\psi)_{tt} - \nabla^2\delta\psi - \frac{2\nabla\Psi_n\bar{\Psi}_n}{1 - |\Psi_n|^2} \nabla(\delta\psi) - \frac{(\nabla\Psi_n)^2}{1 - |\Psi_n|^2} \delta\bar{\psi} \\ - \frac{(\nabla\Psi_n)^2\bar{\Psi}_n}{(1 - |\Psi_n|^2)^2} [\Psi_n\delta\bar{\psi} + \bar{\Psi}_n\delta\psi] - \delta\psi + 2|\Psi_n|^2\delta\psi + \Psi_n^2\delta\bar{\psi} = 0, \end{aligned} \quad (3.6)$$

for the perturbation $\delta\psi$. Then, by assuming a separable solution to this equation of the form $\delta\psi(r, \theta) = \varphi(r, \theta)e^{in\theta} \cos \omega t$, (3.6) can be reduced to

$$\begin{aligned} -\nabla_r^2\varphi - \frac{1}{r^2}\partial_\theta^2\varphi - \frac{2\Phi_n'\Phi_n}{1 - \Phi_n^2}\partial_r\varphi - \frac{2in}{r^2}\frac{1}{1 - \Phi_n^2}\partial_\theta\varphi \\ + \left[\frac{(n^2/r^2) - (\Phi_n')^2\Phi_n^2}{(1 - \Phi_n^2)^2} + 2\Phi_n^2 - 1 \right] \varphi + \left[\Phi_n^2 + \frac{n^2\Phi_n^2 - (\Phi_n')^2}{(1 - \Phi_n^2)^2} \right] \bar{\varphi} = \omega^2\varphi, \end{aligned} \quad (3.7)$$

where a prime denotes a derivative with respect to r . We shall refer to this as an eigenvalue problem for the complex eigenfunction φ , although formally equation (3.7) along with its complex conjugate form an eigenvalue problem for the vector $(\varphi, \bar{\varphi})^T$. To convert this partial differential eigenvalue problem to a set of coupled ordinary differential eigenvalue problems we take the Fourier series expansion of φ in θ :

$$\varphi(r, \theta) = \sum_{m=-\infty}^{\infty} \phi_m(r) e^{im\theta} = \sum_{m=-\infty}^{\infty} \{f_m(r) + ig_m(r)\} e^{im\theta}, \quad (3.8)$$

where $f_m(r)$ and $g_m(r)$ are real, radial functions. When this expansion is substituted into (3.7) and coefficients of like harmonics are equated, the real part yields

$$\left[-\frac{d^2}{dr^2} + B_n(r) \frac{d}{dr} + \frac{m^2}{r^2} + C_n(r) \right] f_m + mA_n(r)f_m + D_n(r)f_{-m} = \omega^2 f_m, \quad (3.9a)$$

$$\left[-\frac{d^2}{dr^2} + B_n(r) \frac{d}{dr} + \frac{m^2}{r^2} + C_n(r) \right] f_{-m} - mA_n(r)f_{-m} + D_n(r)f_m = \omega^2 f_{-m}. \quad (3.9b)$$

The potentials in the above differential equations are:

$$\begin{aligned} A_n(r) &= \frac{2n}{r^2} \frac{1}{1 - \Phi_n^2}, \\ B_n(r) &= \frac{2n}{r} \frac{\Phi_n^2}{1 - \Phi_n^2} - 2\Phi_n \Phi_{n-1} - \frac{1}{r}, \\ C_n(r) &= 2\Phi_n^2 - \Phi_n^2 \Phi_{n-1}^2 - 1 + \frac{n^2}{r^2} \frac{1 + \Phi_n^2}{1 - \Phi_n^2} + \frac{2n}{r} \frac{\Phi_{n-1} \Phi_n^3}{1 - \Phi_n^2}, \\ D_n(r) &= \Phi_n^2 - \Phi_{n-1}^2 + \frac{2n}{r} \frac{\Phi_n \Phi_{n-1}}{1 - \Phi_n^2}, \end{aligned} \quad (3.10)$$

which are obtained by using the relation

$$\frac{d}{dr} \Phi_n + \frac{n}{r} \Phi_n = (1 - \Phi_n^2) \Phi_{n-1}, \quad (3.11)$$

to eliminate derivatives of Φ_n [67]. This relation follows from a Bäcklund transformation for the complex sine-Gordon-1. Adding equations (3.9a) and (3.9b) and subtracting (3.9b) from (3.9a) yields:

$$\left[-\frac{d^2}{dr^2} + B_n(r) \frac{d}{dr} + \frac{m^2}{r^2} + C_n(r) + D_n(r) \right] u_m + mA_n(r)v_m = \omega^2 u_m \quad (3.12a)$$

and

$$\left[-\frac{d^2}{dr^2} + B_n(r) \frac{d}{dr} + \frac{m^2}{r^2} + C_n(r) - D_n(r) \right] v_m + mA_n(r)u_m = \omega^2 v_m, \quad (3.12b)$$

respectively, where u_m and v_m are defined as

$$u_m = f_m + f_{-m}, \quad v_m = f_m - f_{-m}. \quad (3.13)$$

Note that $m = 0$ is a special case; $u_0 = 2f_0$ while $v_0 = 0$ and the eigenvalue problem

$$\left[-\frac{d^2}{dr^2} + B_n(r)\frac{d}{dr} + C_n(r) + D_n(r) \right] u_0 = \omega^2 u_0, \quad (3.14)$$

determines u_0 . The two coupled eigenvalue problems (3.12a) and (3.12b) can be combined into a single matrix eigenvalue Problem*

$$\mathcal{L}_{mn} \begin{pmatrix} u_m \\ v_m \end{pmatrix} = \omega^2 \begin{pmatrix} u_m \\ v_m \end{pmatrix}, \quad (3.15)$$

where the operator \mathcal{L}_{mn} is defined as

$$\mathcal{L}_{mn} \equiv \begin{pmatrix} \mathcal{P} + D_n(r) & mA_n(r) \\ mA_n(r) & \mathcal{P} - D_n(r) \end{pmatrix}, \quad (3.16)$$

with

$$\mathcal{P} = -\frac{d^2}{dr^2} + B_n(r)\frac{d}{dr} + \frac{m^2}{r^2} + C_n(r).$$

We restrict ourselves to $m \geq 1$ as we only need u_m and v_m for positive m to reconstruct the components f_k for all non-zero integer values of k .

Similarly the imaginary part, after substituting the Fourier expansion (3.8) into (3.7), yields

$$\left[-\frac{d^2}{dr^2} + B_n(r)\frac{d}{dr} + \frac{m^2}{r^2} + C_n(r) \right] g_m + mA_n(r)g_m - D_n(r)g_{-m} = \omega^2 g_m, \quad (3.17a)$$

$$\left[-\frac{d^2}{dr^2} + B_n(r)\frac{d}{dr} + \frac{m^2}{r^2} + C_n(r) \right] g_{-m} - mA_n(r)g_{-m} - D_n(r)g_m = \omega^2 g_{-m}. \quad (3.17b)$$

Following the same procedure as with the real part, we add (3.17a) to (3.17b) and subtract (3.17b) from (3.17a) obtaining

$$\left[-\frac{d^2}{dr^2} + B_n(r)\frac{d}{dr} + \frac{m^2}{r^2} + C_n(r) + D_n(r) \right] \tilde{v}_m + mA_n(r)\tilde{u}_m = \omega^2 \tilde{v}_m, \quad (3.18a)$$

$$\left[-\frac{d^2}{dr^2} + B_n(r)\frac{d}{dr} + \frac{m^2}{r^2} + C_n(r) - D_n(r) \right] \tilde{u}_m + mA_n(r)\tilde{v}_m = \omega^2 \tilde{u}_m, \quad (3.18b)$$

where \tilde{u}_m and \tilde{v}_m are defined as

$$\tilde{u}_m = g_m + g_{-m}, \quad \tilde{v}_m = g_m - g_{-m}. \quad (3.19)$$

Note that, as with the real case, $m = 0$ is a special case: $\tilde{u}_0 = 2g_0$ and $\tilde{v}_0 = 0$. Here, \tilde{u}_0 satisfies the eigenvalue problem

$$\left[-\frac{d^2}{dr^2} + B_n(r)\frac{d}{dr} + C_n(r) - D_n(r) \right] \tilde{u}_0 = \omega^2 \tilde{u}_0. \quad (3.20)$$

*Note that u_m and v_m carry a second, implicit index n . Its omission simplifies the notation.

Similarly, (3.18a) and (3.18b) can be combined to give a single eigenvalue problem

$$\mathcal{L}_{mn} \begin{pmatrix} \tilde{v}_m \\ \tilde{u}_m \end{pmatrix} = \omega^2 \begin{pmatrix} \tilde{v}_m \\ \tilde{u}_m \end{pmatrix}, \quad (3.21)$$

with \mathcal{L}_{mn} as in (3.16). Again, we restrict ourselves to $m \geq 1$ since \tilde{u}_m and \tilde{v}_m are only needed for positive m to reconstruct the g_k 's for all non-zero integer values of k .

This new formulation simplifies the system. From the form of (3.15) and (3.21) it follows that if there is an eigenfunction of (3.15) with eigenvalue ω_i^2 then there is an eigenfunction of (3.21) corresponding to the same eigenvalue ω_i^2 . This eigenfunction is $(\tilde{v}_m, \tilde{u}_m)^T = \alpha_1 (u_m, v_m)^T$, where $(u_m, v_m)^T$ is the known eigenfunction of (3.15) with $\alpha \in \mathbb{R}$. Therefore, there is a one-to-one correspondence between the solutions of (3.15) and those of (3.21) for each value of n , ω^2 and $m \geq 1$. When $m = 0$ the matrix eigenvalue problem (3.15) decouples and contains the two special cases (3.14) and (3.20), if v_0 is identified with $\alpha \tilde{u}_0$, $\alpha \in \mathbb{R}$. Thus, by solving (3.15) explicitly for $m \geq 0$ we can reconstruct all the solutions and, hence, know all the zero modes.

As with the Ginzburg-Landau model (Chapter 2), we refer to m as the *azimuthal quantum number*. With the aid of the correspondence between $(u_m, v_m)^T$ and $(\tilde{v}_m, \tilde{u}_m)^T$, we can construct the most general complex eigenfunction with azimuthal quantum number m :

$$\varphi = \left\{ \phi_m e^{im\theta} + \phi_{-m} e^{-im\theta} \right\}, \quad (3.22)$$

where the coefficients in the Fourier expansion are

$$\begin{aligned} \phi_m &= \frac{\beta}{2}(u_m + v_m) + i\frac{\alpha}{2}(u_m - v_m), \\ \phi_{-m} &= \frac{\beta}{2}(u_m - v_m) + i\frac{\alpha}{2}(v_m - u_m), \quad m \geq 1 \\ \phi_0 &= \frac{\beta}{2}u_0 + i\frac{\alpha}{2}v_0. \end{aligned} \quad (3.23)$$

Choosing two linearly independent constant vectors $\begin{pmatrix} \beta \\ \alpha \end{pmatrix}$ gives rise to two linearly independent eigenfunctions. In this text we choose $\begin{pmatrix} \beta \\ \alpha \end{pmatrix} = \begin{pmatrix} 1 \\ 0 \end{pmatrix}$ and $\begin{pmatrix} \beta \\ \alpha \end{pmatrix} = \begin{pmatrix} 0 \\ 1 \end{pmatrix}$ as our two linearly independent vectors. This choice then gives

$$\tilde{\varphi} = \left(\frac{u_m + v_m}{2} e^{im\theta} + \frac{u_m - v_m}{2} e^{-im\theta} \right) = u_m \cos m\theta + iv_m \sin m\theta, \quad (3.24a)$$

$$\hat{\varphi} = i \left(\frac{u_m + v_m}{2} e^{im\theta} - \frac{u_m - v_m}{2} e^{-im\theta} \right) = -u_m \sin m\theta + iv_m \cos m\theta, \quad (3.24b)$$

as our two linearly independent eigenfunctions with *non-zero* azimuthal quantum number m and

$$\tilde{\varphi} = \left(\frac{u_0 + v_0}{2} + \frac{u_0 - v_0}{2} \right) = u_0, \quad (3.25a)$$

$$\hat{\varphi} = i \left(\frac{u_0 + v_0}{2} - \frac{u_0 - v_0}{2} \right) = iv_0, \quad (3.25b)$$

for azimuthal quantum number $m = 0$. Recall that when solving (3.15), v_0 is identified with \tilde{u}_0 .

We can already write down one of the zero modes for azimuthal quantum number $m = 0$ viz. $\varphi = i\Phi_n$. This follows since the second row of (3.15), the eigenvalue problem for v_0 , with $\omega^2 = 0$ has exactly the same form as (3.4). By rewriting (3.4) as

$$\left\{ \frac{d^2}{dr^2} + \left[\frac{1}{r} + \frac{2\Phi_n}{1-\Phi_n^2} \frac{d\Phi_n}{dr} \right] \frac{d}{dr} - \frac{1}{1-\Phi_n^2} \left[\left(\frac{d\Phi_n}{dr} \right)^2 + \frac{n^2}{r^2} \right] + (1-\Phi_n) \right\} \Phi_n = 0, \quad (3.26)$$

and using relation (3.11), (3.26) reduces to (3.20) with $\omega^2 = 0$;

$$\left[-\frac{d^2}{dr^2} + B(r) \frac{d}{dr} + C(r) - D(r) \right] \Phi_n = 0. \quad (3.27)$$

This zero mode, $\varphi = i\Phi_n$, is one of the three we were expecting and corresponds to the global $U(1)$ degree of freedom (or equivalently rotations in the plane).

It is pertinent at this stage to ask which azimuthal quantum numbers correspond to the other expected zero modes. These are the two zero modes resulting from translational degrees of freedom in the x and y directions. We know that the zero mode from the translational degree of freedom in the x direction is given by:

$$\begin{aligned} \partial_x[\Phi_n(r)e^{in\theta}] &= \left[\frac{d\Phi_n}{dr} \partial_x r + in\Phi_n \partial_x \theta \right] e^{in\theta} \\ &= - \left[-\frac{d\Phi_n}{dr} \cos \theta + i \frac{n\Phi_n}{r} \sin \theta \right] e^{in\theta}, \end{aligned} \quad (3.28a)$$

and in the y direction by:

$$\begin{aligned} \partial_y[\Phi_n(r)e^{in\theta}] &= \left[\frac{d\Phi_n}{dr} \partial_y r + in\Phi_n \partial_y \theta \right] e^{in\theta} \\ &= \left[\frac{d\Phi_n}{dr} \sin \theta + i \frac{n\Phi_n}{r} \cos \theta \right] e^{in\theta}. \end{aligned} \quad (3.28b)$$

From the comparison of (3.28a) and (3.28b) to (3.24) it is evident that $\partial_x \Psi_n = -\tilde{\varphi}_1 e^{in\theta}$ and $\partial_y \Psi_n = \tilde{\varphi}_1 e^{in\theta}$ when $u_1 = -\frac{d}{dr} \Phi_n$ and $v_1 = \frac{n}{r} \Phi_n$. Therefore the zero modes corresponding to the translational degrees of freedom have azimuthal quantum number $m = 1$.

The eigenvalue problem (3.15) consists of a set of coupled, second order differential equations for u_m and v_m , both of which have two boundary conditions they must satisfy. The one set of boundary conditions is at $r = 0$ and the other at $r = \infty$. Thus there can be at most one solution $(u_m, v_m)^T$ to (3.15) for each value of $m \geq 1$, n and ω^2 . This implies that there can be at most two complex eigenfunctions φ for each $m \geq 1$. When $m = 0$, the equations decouple and then there can be at most one solution to each equation, implying that there can be at most two complex eigenfunctions. Hence, for each vortex Ψ_n , there can be at most two zero modes to each azimuthal quantum number $m \geq 0$.

In order to make the results more legible, the previously implicit index is made explicit: $u_m \rightarrow u_{mn}$ and $v_m \rightarrow v_{mn}$. This distinguishes between the eigenfunctions of the various coaxial vortices. We shall refer to them as the *components* u_{mn} and v_{mn} associated with the complex eigenfunction φ_{mn} of (3.7).

We know that there are at least three zero modes for each n , one corresponding to the global $U(1)$ degree of freedom and two to the two translational degrees of freedom. But an important question to ask is whether are there any other zero modes? The answer to this question will help to decide whether non-coaxial vortices are admitted by the complex sine-Gordon equation. Although the complex sine-Gordon equation is completely integrable and has analytic solutions, the potentials (3.10) of the eigenvalue problem (3.15) are in terms of modified Bessel functions. Thus it might prove difficult to solve the system analytically and for this reason we will solve it numerically. If we find any extra zero modes numerically then we have a motive for attempting to solve the system analytically.

As was evident with the Ginzburg-Landau model, it is necessary to impose boundary conditions while performing the numerical computations. However, before we can do this we first need to know what boundary conditions the eigenfunctions should observe. In order to determine these boundary conditions we will now analyse the asymptotics of eigenfunctions of the eigenvalue problem (3.15).

3.2 Asymptotic Behaviour of Zero Modes

3.2.1 Asymptotics for small r

For small r we assume an expansion of the form

$$\begin{aligned} u &= r^p [(u_0 r + u_1 r^1 + u_2 r^2 + \dots) + \ln r (u'_0 r + u'_1 r^1 + u'_2 r^2 + \dots)] \\ v &= r^p [(v_0 r + v_1 r^1 + v_2 r^2 + \dots) + \ln r (v'_0 r + v'_1 r^1 + v'_2 r^2 + \dots)], \end{aligned} \quad (3.29)$$

where p is a real constant and u and v denote u_{mn} and v_{mn} , respectively. Then we substitute this expansion along with the Taylor expansions for the potentials:

$$\begin{aligned} A_n(r) &= \frac{2n}{r^2} + \frac{2n}{(2^n n!)^2} r^{2n-2} + \mathcal{O}(r^{2n}), \\ B_n(r) &= -\frac{1}{r} - \frac{2n}{(2^n n!)^2} r^{2n-1} + \mathcal{O}(r^{2n+1}), \\ C_n(r) &= \frac{n^2}{r^2} - 1 + \frac{2n^2}{(2^n n!)^2} r^{2n-2} + \mathcal{O}(r^{2n}), \\ D_n(r) &= \mathcal{O}(r^{2n}), \end{aligned}$$

into the eigenvalue problem (3.15). These Taylor expansions, for the potentials, are obtained from the known behaviour of Φ_n at the origin [67]

$$\Phi_n \sim \frac{1}{2^n n!} r^n - \frac{1}{2^{n+2} (n+1)!} r^{n+2} + \mathcal{O}(r^{n+4}). \quad (3.30)$$

After substitution, we then collect terms of like powers of r to obtain constraints on the coefficients in the expansion.

Up to and including terms $\mathcal{O}(r^{p-1})$, the expansion for eigenvalue problem (3.15) is identical to that of the eigenvalue problem (2.4) for the Ginzburg-Landau model (§2.2.1). Therefore, following the formalism in §2.2.1, we know the eigenfunctions of (3.15) obey the following four, linearly independent behaviours as $r \rightarrow 0$:

$$\begin{aligned}
Z_1 &= r^{n+m}[1 + o(r)] \begin{pmatrix} 1 \\ 1 \end{pmatrix}; & Z_2 &= r^{-|n-m|}[1 + o(r)] \begin{pmatrix} 1 \\ -1 \end{pmatrix}; \\
Z_3 &= r^{-(n+m)}[1 + o(r)] \begin{pmatrix} 1 \\ 1 \end{pmatrix}; \\
Z_4 &= r^{|n-m|}[1 + o(r)] \begin{pmatrix} 1 \\ -1 \end{pmatrix}; & m &\neq n \\
Z_4 &= \ln r[1 + o(r)] \begin{pmatrix} 1 \\ -1 \end{pmatrix}, & m &= n
\end{aligned} \tag{3.31}$$

where we have used the notation[†] $Z = (u_m, v_m)^T$. Note that Z_1 and Z_2 are bounded at the origin for all m and n while Z_3 and Z_4 are not.

The boundary conditions imposed in the numerical calculations follow easily from the form of Z_1 and Z_2 . For $m \neq n \pm 1$ the first derivatives of the components $u_{mn}(r)$ and $v_{mn}(r)$ are equated to zero at the origin:

$$\frac{d}{dr}u_{mn}(0) = \frac{d}{dr}v_{mn}(0) = 0, \quad m \neq n \pm 1. \tag{3.32a}$$

This is allowed since u and v are proportional to r only when $m = n \pm 1$. For the case, $m = n \pm 1$, the components themselves are equated to zero at the origin:

$$u_{n\pm 1, n}(0) = v_{n\pm 1, n}(0) = 0, \quad m = n \pm 1. \tag{3.32b}$$

These boundary conditions reduce the possibility of the numerics giving ‘false’ eigenfunctions. Now that the boundary conditions at the origin are known we can consider the behaviour of the eigenfunctions as $r \rightarrow \infty$.

3.2.2 Asymptotics for large r

When we consider the eigenvalue problem (3.15) for large r we find that the eigenvalues $\omega^2 > 0$ belong to the continuous spectrum. Unfortunately, this gives rise to difficulties while solving for zero modes numerically, as the numerics do not obtain the zero eigenvalue ($\omega^2 = 0$) exactly, but a value of ω^2 in a small neighbourhood of zero. Now if the numerics give a small positive value for ω^2 then it may be an approximation of the zero eigenvalue or it may be a “true” eigenvalue in its own right. Therefore a means of distinguishing zero modes from eigenfunctions corresponding to small positive eigenvalues (ω^2) is needed.

[†]Here we have adopted the notation consistent with [86]

In order, to help determine this method and to determine the boundary conditions at $r = \infty$ we assume an expansion for the functions u and v of the form

$$\begin{aligned} u &= \Re \left\{ e^{ikr} r^p \left[\left(u_0 + \frac{u_1}{r} + \frac{u_2}{r^2} + \frac{u_3}{r^3} + \dots \right) + \ln r \left(\frac{u'_1}{r} + \frac{u'_2}{r^2} + \frac{u'_3}{r^3} \dots \right) \right] \right\} \\ v &= \Re \left\{ e^{ikr} r^p \left[\left(v_0 + \frac{v_1}{r} + \frac{v_2}{r^2} + \frac{v_3}{r^3} + \dots \right) + \ln r \left(\frac{v'_1}{r} + \frac{v'_2}{r^2} + \frac{v'_3}{r^3} \dots \right) \right] \right\}, \end{aligned} \quad (3.33)$$

where $p, k, u_j, v_j, u'_j, v'_j \in \mathbb{C}$. We then substitute this expansion along with the asymptotic form of the potentials (3.10) as $r \rightarrow \infty$ into equation (3.15). The asymptotic form of the potentials is derived from the behaviour of Φ_n as $r \rightarrow \infty$

$$\Phi_n(r) = 1 - \frac{n}{2r} - \frac{n^2}{8r^2} - \frac{n(n^2+1)}{16r^3} - \frac{5n^2(n^2+4)}{128r^4} - \frac{n(7n^4+70n^2+27)}{256r^5} + \mathcal{O}(r^{-6}) \quad (3.34)$$

which is readily determined from relation (3.11). The asymptotics of these potentials, for all n , are then:

$$\begin{aligned} A_n(r) &= \frac{2}{r} - \frac{1}{4r^3} - \frac{n}{2r^4} + \mathcal{O}(r^{-5}), \\ B_n(r) &= -\frac{2}{r} - \frac{1}{4r^3} - \frac{3n}{4r^4} + \mathcal{O}(r^{-5}), \\ C_n(r) &= 2 - \frac{2n}{r} - \frac{1}{2r^2} - \frac{3n}{4r^3} - \frac{\frac{1}{2} + \frac{5}{4}n^2}{r^4} + \mathcal{O}(r^{-5}), \\ D_n(r) &= 2 - \frac{2n}{r} - \frac{1}{2r^2} - \frac{3n}{4r^3} - \frac{\frac{1}{2} + n^2}{r^4} + \mathcal{O}(r^{-5}). \end{aligned} \quad (3.35)$$

After substituting the expansions (3.33) and (3.35) into equation (3.15) we collect terms of like powers of r . This gives various constraints on the coefficients and the constants in the expansions of u and v .

The terms $\mathcal{O}(r^p)$ yield the equations:

$$(k^2 + 4 - \omega^2)u_0 = 0, \quad (3.36a)$$

$$(k^2 - \omega^2)v_0 = 0, \quad (3.36b)$$

and the terms $\mathcal{O}(r^{p-1} \ln r)$ yield:

$$(k^2 + 4 - \omega^2)u'_1 = 0, \quad (3.37a)$$

$$(k^2 - \omega^2)v'_1 = 0. \quad (3.37b)$$

These present us with two possible cases; either (a) $k^2 = \omega^2 - 4$, $v_0 = v'_1 = 0$ and u_0 and u'_1 are arbitrary or else (b) $k^2 = \omega^2$, $u_0 = u'_1 = 0$ and v_0 and v'_1 are arbitrary.

We now continue with the terms of higher order. The terms $\mathcal{O}(r^{p-1})$ yield:

$$2mv_0 - \{4n + 2ik(p+1)\}u_0 + (k^2 + 4 - \omega^2)u_1 = 0, \quad (3.38a)$$

$$2mu_0 - 2ik(p+1)v_0 + (k^2 - \omega^2)v_1 = 0, \quad (3.38b)$$

and those $\mathcal{O}(r^{p-2} \ln r)$ yield:

$$2mv'_1 - (4n + 2ikp)u'_1 + (k^2 + 4 - \omega^2)u'_2 = 0, \quad (3.39a)$$

$$2mu'_1 - 2ikpv'_1 + (k^2 - \omega^2)v'_2 = 0. \quad (3.39b)$$

The terms $\mathcal{O}(r^{p-2})$ yield:

$$(k^2 + 4 - \omega^2)u_2 - (4n + 2ikp)u_1 + (m^2 - p^2 - p - 1)u_0 + 2mv_1 - 2iku'_1 = 0, \quad (3.40a)$$

$$(k^2 - \omega^2)v_2 - 2ikpv_1 + (m^2 - p^2 - p)v_0 + 2mu_1 - 2ikpv'_1 = 0 \quad (3.40b)$$

and finally the terms $\mathcal{O}(r^{p-3} \ln r)$ give:

$$(k^2 + 4 - \omega^2)u'_3 - (4n + 2ik(p-1))u'_2 + (m^2 - p^2 + p - 1)u'_1 + 2mv'_2 = 0, \quad (3.41a)$$

$$(k^2 - \omega^2)v'_3 - 2ik(p-1)v'_2 + (m^2 - p^2 + p)v'_1 + 2mu'_2 = 0. \quad (3.41b)$$

Firstly, we will consider case (a). For this case equations (3.38) become

$$\{4n + 2ik(p+1)\}u_0 = 0, \quad (3.42a)$$

$$2mu_0 - 4v_1 = 0, \quad (3.42b)$$

thus $v_1 = \frac{m}{2}u_0$ and either $p = -\frac{4n}{2ik} - 1$ or $u_0 = 0$. Also equations (3.39) reduce to

$$(4n + 2ikp)u'_1 = 0, \quad (3.43a)$$

$$2mu'_1 - 4v'_2 = 0, \quad (3.43b)$$

implying $v'_2 = \frac{m}{2}u'_1$ and either $p = -\frac{4n}{2ik}$ or $u'_1 = 0$. From these results it follows that case (a) separates into two sub-cases. In the first sub-case (a.i) $p = -\frac{4n}{2ik} - 1$ and $u'_1 = 0 \Rightarrow v'_2 = 0$ and in the second (a.ii) $p = -\frac{4n}{2ik}$ and $u_0 = 0 \Rightarrow v_1 = 0$. Note that in the first case the series begins with a term independent of $\ln r$ while in the second it begins with a term dependent on $\ln r$. When we continue examining these two possibilities we find that for case (a.ii) equation (3.40b) gives $u'_1 = 0$. Thus for case (a.ii) the coefficients u_0, v_0, u'_1 and v'_1 are all zero, hence case (a.ii) is *disallowed*.

However when we consider the terms up to order $\mathcal{O}(r^{p-3} \ln r)$ for case (a.i) we find the following:

$$\begin{aligned} u'_2 &= 0, & v'_3 &= 0, \\ u_1 &= \frac{2m^2 - p^2 - p - 1}{2ikp + 4n}, \\ v_2 &= \frac{m}{2}u_1 - \frac{imkp}{4}u_0. \end{aligned} \quad (3.44)$$

Note that since we are interested in zero modes we can restrict ourselves to the region $\omega^2 < 4$. In this region $k \neq 0$ and therefore the power $p = -\frac{4n}{2ik} - 1$ and the coefficients are analytic. Therefore from case (a) we obtain two behaviours:

$$Y_{3,4} = e^{\pm\sqrt{4-\omega^2}r} r^p \left(\begin{aligned} &1 \mp \frac{2m^2 - p^2 - p - 1}{2\sqrt{4-\omega^2}r} + \mathcal{O}\left(\frac{1}{r^2}\right) \\ &\frac{m}{2r} \mp \frac{m}{4} \left(\frac{2m^2 - p^2 - p - 1 - (4-\omega^2)}{\sqrt{4-\omega^2}} \mp 2n \right) \frac{1}{r^2} + \mathcal{O}\left(\frac{1}{r^3}\right) \end{aligned} \right), \quad (3.45)$$

where $p = \mp \frac{2n}{\sqrt{4-\omega^2}} - 1$. Note that Y_3 is bounded as $r \rightarrow \infty$ while Y_4 is not[†].

We now continue with analysing case (b). Remember that for this case $k^2 = \omega^2$, $u_0 = u'_1 = 0$ and v_0 and v'_1 are arbitrary. Under these conditions equations (3.38) reduce to:

$$2mv_0 + 4u_1 = 0, \quad (3.46a)$$

$$2ik(p+1)v_0 = 0, \quad (3.46b)$$

and equations (3.39) to:

$$2mv'_1 + 4u'_2 = 0, \quad (3.47a)$$

$$2ikpv'_1 = 0. \quad (3.47b)$$

From these two sets of equations it is obvious that $u_1 = -\frac{m}{2}v_0$ and $u'_2 = -\frac{m}{2}v'_1$. Also we find that case (b) splits into three separate sub-cases: (b.i) $k = 0$ and v_0 and v'_1 are arbitrary, (b.ii) $p = -1$, $v'_1 = 0$ and v_0 is arbitrary and (b.iii) $p = 0$, $v_0 = 0$ and v'_1 is arbitrary. As previously we will examine the various cases separately.

Firstly, for case (b.i) ($k = 0$, v_0 and v_1 arbitrary), the equations (3.40) reduce to:

$$4u_2 + 2nmv_0 + 2mv_1 = 0, \quad (3.48a)$$

$$p(p+1)v_0 = 0, \quad (3.48b)$$

while the equations (3.41) become:

$$4u'_3 + 2nmv'_1 + 2mv'_2 = 0, \quad (3.49a)$$

$$p(p-1)v'_1 = 0. \quad (3.49b)$$

From these two sets of equations it follows that $u_2 = -\frac{mn}{2}v_0 - \frac{m}{2}v_1$ and either $p = 0$ and both v_0 and v'_1 are arbitrary or $p = -1$, $v'_1 = 0$ and v_0 is arbitrary or $p = 1$, $v_0 = 0$ and v'_1 is arbitrary. To examine these various options we have to consider the terms $\mathcal{O}(r^{p-3})$. Under the conditions of case (b.i) the terms $\mathcal{O}(r^{p-3})$ reduce to

$$4u_3 + \frac{m}{4}(8n^2 - 2m^2 + 2p^2 - 2p + 1)v_0 + 2mnv_1 + 2mv_2 = 0, \quad (3.50a)$$

$$-p(p-1)v_1 - m^2nv_0 + (1-2p)v'_1 = 0. \quad (3.50b)$$

When we substitute $p = 0$ into equation (3.50b) we find $v'_1 = m^2nv_0$ while substituting $p = -1$ gives $v_1 = -\frac{m^2n}{2}v_0$. However, if we substitute $p = 1$ into (3.50b) we find that $v'_1 = 0$. Recall that for $p = 1$ we also know that $v_0 = 0$. Thus, $p = 1$ is not allowed since for all the sub-cases of (b) we have $u_0 = u'_1 = 0$. Therefore, only values of $p = -1$ and $p = 0$ are allowed in case (b.i). Finally from terms $\mathcal{O}(r^{p-3} \ln r)$ and $\mathcal{O}(r^{p-4})$ it follows that $v'_2 = 0$ for $p = -1$.

[†]Here we have adopted the notation consistent with [86]

Therefore from case (b.i) we have two possible behaviours for $k = \omega = 0$:

$$Y_1 = \frac{1}{r} \left(-\frac{m}{2r} - \frac{mn(2+m^2)}{4r^2} + \mathcal{O}\left(\frac{\ln r}{r^3}\right) \right);$$

$$Y_2 = \left(-\frac{m}{2r} - \frac{m^3 n \ln r}{2r^2} + \mathcal{O}\left(\frac{1}{r^2}\right) \right) \cdot \quad (3.51)$$

Secondly, for case (b.ii) (k and v_0 arbitrary, $p = -1$, $v'_1 = 0$), the equations (3.40) and (3.41) reduce to

$$4u_2 + (2n - ik)mv_0 + 2mv_1 = 0, \quad (3.52a)$$

$$2ikv_1 = 0, \quad (3.52b)$$

and

$$4u'_3 + 2mv'_2 = 0, \quad (3.53a)$$

$$2ikv'_2 = 0, \quad (3.53b)$$

respectively. From these we deduce that $v_1 = v'_2 = u'_3 = 0$ and $u_2 = \frac{m(ik-2n)}{4}v_0$. This gives two possible behaviours for $k^2 = \omega^2 \neq 0$:

$$Y_{1,2} = \Re \left\{ \frac{e^{\pm i\omega r}}{r} \left(-\frac{m}{2r} - \frac{m(2n \mp i\omega)}{4r^2} + \mathcal{O}\left(\frac{1}{r^3}\right) \right) \right\}. \quad (3.54)$$

Note that for all ω , Y_1 and Y_2 are bounded.

Finally, for case (b.iii) (k and v'_1 are arbitrary and $p = v_0 = 0$), the equations (3.40) reduce to

$$4u_2 + 2mv_1 = 0, \quad (3.55a)$$

$$2ikv'_1 = 0. \quad (3.55b)$$

From this it follows that $v'_1 = 0$, but for this case we also have $v_0 = u_0 = u'_1 = 0$, hence case (b.iii) is *disallowed*. Therefore we are left with four possible behaviours; Y_1 , Y_2 , Y_3 and Y_4 ; (3.51), (3.54) and (3.45). Of these only Y_1 , Y_2 and Y_4 are bounded as $r \rightarrow \infty$.

From the asymptotics it follows that, for eigenfunctions, the components u_{mn} and v_{mn} all tend to a constant as $r \rightarrow \infty$. Therefore to give the numerics as much "freedom" as possible the boundary condition of vanishing first derivatives at right hand boundary ($r = R$) is imposed:

$$\frac{d}{dr}u_{mn}(R) = \frac{d}{dr}v_{mn}(R) = 0. \quad (3.56)$$

A pertinent question to ask is if we can determine at this stage whether the zero eigenvalue $\omega^2 = 0$ exists or not? To answer this we first note that each of the solutions Z_i can be expanded over the basis

$$Z_i(r) = \sum_{j=1}^4 T_{ij}^{(n,m)}(\omega) Y_j(r),$$

where the $T_{ij}^{(n,m)}$ are real coefficients. Then for all $\omega^2 < 4$ we know that the linear combination $T_{23}^{(n,m)}(\omega)Z_1(r) - T_{13}^{(n,m)}(\omega)Z_2(r)$ is regular at the origin since Z_1 and Z_2 are. This linear combination is also bound at $r = \infty$ since

$$T_{23}^{(n,m)}Z_1 - T_{13}^{(n,m)}Z_2 = T_{23}^{(n,m)} \left(T_{11}^{(n,m)}Y_1 + T_{12}^{(n,m)}Y_2 + T_{14}^{(n,m)}Y_4 \right) \\ - T_{13}^{(n,m)} \left(T_{21}^{(n,m)}Y_1 + T_{22}^{(n,m)}Y_2 + T_{24}^{(n,m)}Y_4 \right),$$

is independent of the only unbounded solution Y_3 . Hence, we are guaranteed that an eigenfunction exists for all $\omega^2 > 0$. Hence the zero eigenvalue ($\omega^2 = 0$) does exist.

This is a very important fact as it guarantees that for each azimuthal quantum number m there is at least one zero mode. Hence the coaxial multivortices of the complex sine-Gordon model have infinitely many zero modes as $0 \leq m \leq \infty$. And thus they belong to a infinite parameter family of solutions.

Note that we have also obtained a means of distinguishing true zero modes from eigenfunctions corresponding to small positive eigenvalues. If the computed eigenfunction has components v_{mn} and u_{mn} which oscillate with wavenumber $k \sim \omega$ and approach zero as r^{-1} and r^{-2} , respectively, then the eigenfunction is not a zero mode. The components then have the same behaviour as in (3.54) and correspond to a *positive* eigenvalue ω^2 . If the components v_{mn} and u_{mn} do not oscillate and v_{mn} tends to a constant as $r \rightarrow \infty$ while $u_{mn} \rightarrow -mv_{mn}/2$, then the eigenfunction is a zero mode. If, however, the eigenfunction has functions u_{mn} and v_{mn} which decay to zero exponentially as $r \rightarrow \infty$ then the eigenfunction belongs to a discrete eigenvalue and we can tell whether it is a true zero mode by refining the grid.

Now that we know the boundary conditions for the eigenfunctions and have a means of identifying true zero modes we can proceed with computing the zero modes.

3.3 The Numerical Solutions

A second order finite difference method (A) is used to convert the differential eigenvalue problem (3.15) into a banded-matrix eigenvalue problem. Numerical libraries in FORTRAN are then used to calculate the eigenvalues and eigenfunctions for this matrix eigenvalue problem.

As previously mentioned we examine the coaxial vortices Ψ_1 , Ψ_2 and Ψ_3 (the single vortex and the double and triple coaxial-vortices, respectively). These coaxial vortex solutions are of the form:

$$\Psi_n = \Phi_n e^{in\theta}, \quad (3.57)$$

where

$$\Phi_1 = \frac{I_1(r)}{I_0(r)}, \quad (3.58a)$$

$$\Phi_2 = \frac{I_1^2(r) - I_0(r)I_2(r)}{I_0^2(r) - I_1^2(r)}, \quad (3.58b)$$

$$\Phi_3 = \frac{(I_3(r) - I_1(r))(I_0^2(r) - I_1^2(r)) + I_1(r)(I_0(r) - I_2(r))^2}{(I_0(r) - I_2(r))(I_0(r)I_2(r) - 2I_1^2(r) + I_0^2(r))}, \quad (3.58c)$$

and $I_n(r)$ is the modified Bessel function of the n -th order [67].

There are fast and efficient routines available for finding the eigenvalues and eigenvectors of symmetric banded matrices. However, the banded matrix obtained from (3.15) using the finite difference method is non-symmetric. This is because the finite difference equations for the first derivatives in the eigenvalue problem (3.15) are non-symmetric. If the matrix obtained from (3.15) can be reduced to a symmetric matrix by means of a suitable transformation, the faster and more efficient routines can be used. The transformation needed is merely an integrating factor which eliminates the first derivatives in the eigenvalue problem (3.15) viz.

$$\eta_{mn} = u_{mn}e^{-\frac{1}{2} \int B_n(r)dr}, \quad \zeta_{mn} = v_{mn}e^{-\frac{1}{2} \int B_n(r)dr}, \quad (3.59)$$

with $B_n(r)$ as in (3.10). With the aid of the relation (3.11), the integral in (3.59) is simple to perform and the integrating factor has the surprisingly simple form:

$$e^{-\frac{1}{2} \int B_n(r)dr} = \frac{\sqrt{r}}{\sqrt{1 - \Phi_n(r)^2}}. \quad (3.60)$$

Under the transformation (3.59) the original eigenvalue problem (3.15) reduces to

$$\begin{pmatrix} \mathcal{P}'_n + D_n(r) & mA_n(r) \\ mA_n(r) & \mathcal{P}'_n - D_n(r) \end{pmatrix} \begin{pmatrix} \eta_{mn} \\ \zeta_{mn} \end{pmatrix} = \omega^2 \begin{pmatrix} \eta_{mn} \\ \zeta_{mn} \end{pmatrix}, \quad (3.61)$$

where the new operator \mathcal{P}'_n is defined as

$$\mathcal{P}'_n \equiv -\frac{d^2}{dr^2} + \left[\frac{1}{4}B_n^2(r) - \frac{1}{2} \frac{dB_n(r)}{dr} + \frac{m^2}{r^2} + C_n(r) \right] \quad (3.62)$$

with the potentials given in (3.10). The only derivatives of the functions η_{mn} and ζ_{mn} which occur in this new eigenvalue problem are of second order. Therefore the finite differences convert (3.61) to a matrix eigenvalue problem with a real, symmetric, banded matrix. This means that the transformed functions η_{mn} and ζ_{mn} are computed in a far shorter time than is necessary to compute the corresponding u_{mn} and v_{mn} directly from (3.15). It would be helpful if this transformation worked for all values of m and n , but unfortunately this is not the case. The transformation (3.59) is not suitable in two cases, firstly when $m = n$ and secondly when v_{mn} tends to a non-zero constant as $r \rightarrow \infty$. This can be understood from the asymptotics of the transformed functions η_{mn} and ζ_{mn} .

Recall from the analysis of the eigenfunctions for small r that for $m = n$ the functions u_{nn} and v_{nn} may be non-zero at the origin (Z_2 in (3.31)). Since the integrating factor

(3.60) behaves as \sqrt{r} , at the origin, this implies that $\zeta_{nn} \sim \sqrt{r}$ and $\xi_{nn} \rightarrow -\zeta_{nn}$ as $r \rightarrow 0$. Thus these functions have an infinite gradient at the origin, resulting in large errors in the numerical calculations.

For the second case, recall that the coefficients v_{mn} of the zero modes may tend to a non-zero constant as $r \rightarrow \infty$ (3.51). This means that they have the asymptotic form $c_1 + \frac{c_2}{r} + \mathcal{O}(r^{-2})$ for some constants c_1 and c_2 . Since the integrating factor (3.60) has the asymptotic form $\frac{r}{\sqrt{n}} + \mathcal{O}(r^{-1})$, the corresponding ζ_{mn} will then grow as $\frac{1}{\sqrt{n}}(c_1 r + c_2)$, as $r \rightarrow \infty$. This boundary condition, $\zeta_{mn} \sim \frac{1}{\sqrt{n}}(c_1 r + c_2)$ at $r = R$, cannot be written as a homogeneous boundary condition involving only ζ_{mn} and $\frac{d}{dr}\zeta_{mn}$. Since only homogeneous boundary conditions can be imposed in the numerics, we cannot impose the correct boundary condition here.

For these reasons we adopt the following approach while computing the eigenfunctions numerically. If $m = n$ then we solve the non-symmetric eigenvalue problem (3.15) for a grid with 1600 points. While for $m \neq n$ we initially solve (3.15) for a relatively coarse grid of 1000 points. Then, if for a specific m there are solutions to these coarse computations, where one of the v_{mn} 's tend to a non-zero constant as $r \rightarrow R$, then we solve the nonsymmetric eigenvalue problem (3.15) for a grid with 1600 points. If, however, there are no components v_{mn} which tend to a non-zero constant then we solve the symmetric system (3.61) with a grid of 4000 points.

When solving (3.15) explicitly we use a domain radius of $R = 160$ and step size of $\Delta r = 0.1$. While when solving the symmetric system (3.61) we use a domain radius of $R = 200$ and step size of $\Delta r = 0.05$.

When it is possible to solve the symmetric system (3.61) we impose the following boundary conditions: At the origin we equate the functions η_{mn} and ζ_{mn} to zero and at the right hand boundary ($r = R$) we equate their derivatives to zero:

$$\begin{aligned} \eta_{mn}(0) &= \zeta_{mn}(0) = 0, \\ \frac{d}{dr}\eta_{mn}(R) &= \frac{d}{dr}\zeta_{mn}(R) = 0. \end{aligned} \tag{3.63}$$

These follow from the asymptotics of u_{mn} and v_{mn} and the asymptotics of the integrating factor. Near the origin the integrating factor behaves as \sqrt{r} and functions u_{mn} and v_{mn} are zero for $m \neq n$. Therefore, transformed functions η_{mn} and ζ_{mn} are zero at the origin for $m \neq n$. For large r the transformation is only used if component v_{mn} tends to zero as $r \rightarrow \infty$. Thus the corresponding ζ_{mn} will tend to a constant as $r \rightarrow \infty$ and $\eta_{mn} \rightarrow \zeta_{mn}/r$.

The manner in which the results are presented may seem unusual but it will become clear later as to the reasons for the chosen form. Firstly, the results for azimuthal quantum number $m = 0$ for each vortex ($n = 1, 2$ and 3) are discussed. Secondly, the results for $m = 1$ for each vortex are discussed and finally the results for each vortex are discussed separately for azimuthal quantum numbers $2 \leq m \leq 5$.

3.3.1 Azimuthal quantum number $m = 0$

For $m = 0$, all three vortices have an eigenfunction whose component v_{0n} tends to a non-zero constant as $r \rightarrow R$. Thus the transformation (3.59) is inappropriate and the functions u_{mn} and v_{mn} are obtained by solving the non-symmetric system (3.15) directly.

The four smallest eigenvalues computed for each vortex solution are given in Table 3.1.

n	ω_0^2	ω_1^2	ω_2^2	ω_3^2
1	3.69×10^{-7}	7.94×10^{-4}	2.35×10^{-3}	4.68×10^{-3}
2	7.45×10^{-7}	8.00×10^{-4}	2.36×10^{-3}	4.71×10^{-3}
3	1.13×10^{-6}	8.05×10^{-4}	2.38×10^{-3}	4.74×10^{-3}

Table 3.1: Table of four smallest eigenvalues (ω^2) for azimuthal quantum number $m = 0$.

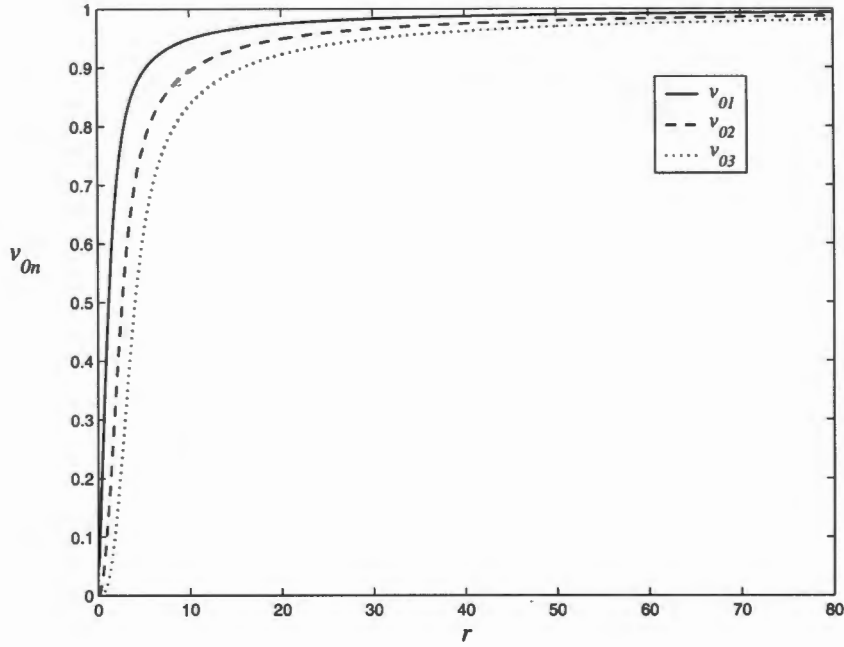


Figure 3.1: v_{01} , v_{02} and v_{03} as functions of r

When we consider the eigenfunctions $\hat{\varphi}_{0n} = iv_{0n}$ (3.25) corresponding to the smallest eigenvalue ω_0^2 , we find $v_{0n} \propto \Phi_n$. The graphs of v_{0n} versus r are given in Fig. 3.1 for $n = 1, 2$ and 3. Note that the components v_{0n} obey the correct boundary conditions as their first derivatives vanish as $r \rightarrow R$ and also v_{01} is zero at the origin (3.32b) while the first derivatives of v_{02} and v_{03} vanish at the origin (3.32a). Now, recall that v_{0n} may only tend to a non-zero constant as $r \rightarrow \infty$ when $\omega^2 = 0$ (3.51). Therefore, since these components do tend to non-zero constants, the corresponding eigenfunctions $\hat{\varphi}_{0n}$ are zero modes. However, the eigenfunctions $\hat{\varphi}_{0n}$, corresponding to eigenvalues $\omega^2 > \omega_0^2$, have components v_{0n} which oscillate with wavenumber $k \sim \omega$ and approach zero like $\frac{1}{r}$. These eigenfunctions therefore correspond to strictly positive eigenvalues $\omega^2 > 0$ (3.54). Hence they are not zero modes.

When we consider the coefficients u_{0n} , we find that they are identically zero for all eigenvalues $\omega^2 < 3.5 \times 10^{-2}$. It is possible that u_{0n} is not identically zero for higher eigenvalues, but $\omega^2 = 3.5 \times 10^{-2}$ is already too large to be considered as a numerical approximation of the zero eigenvalue. Therefore, the eigenfunctions $\tilde{\varphi}_{0n} = u_{0n}$ corresponding to eigenvalues in a small neighbourhood of zero are trivial eigenfunctions. Hence, there is only one zero mode for azimuthal quantum number $m = 0$ for each vortex solution: $\hat{\varphi}_{0n}$ corresponding to ω_0^2 . In each case the zero mode corresponds to a global $U(1)$ degree of freedom (or equivalently, rotations in the plane). The fact that this expected zero mode is reproduced indicates that the numerics are correct. We now continue with the results for zero modes of azimuthal quantum number $m = 1$.

3.3.2 Azimuthal quantum number $m = 1$

For the double and triple coaxial-vortices, we use the symmetric matrix eigenvalue problem (3.61) along with the inverse of the transformation (3.59) to obtain the components u_{1n} and v_{1n} . Unfortunately however, for the single vortex ($n = 1$), we must solve the non-symmetric eigenvalue problem (3.15) to obtain u_{11} and v_{11} directly. This is because, for the single vortex, $n = m$ implying that the transformation (3.59) is inappropriate.

The four smallest eigenvalues computed for the vortices Ψ_1 , Ψ_2 and Ψ_3 are given in Table 3.2. And the components u_{1n} and v_{1n} corresponding to ω_0^2 are given in Figs. 3.2-3.3, Figs. 3.4-3.5 and Figs. 3.6-3.7 for $n = 1, 2$ and 3 , respectively.

n	ω_0^2	ω_1^2	ω_2^2	ω_3^2
1	-5.82×10^{-5}	3.17×10^{-4}	1.51×10^{-3}	3.49×10^{-3}
2	-1.54×10^{-7}	2.63×10^{-4}	1.04×10^{-3}	2.33×10^{-3}
3	1.60×10^{-7}	2.71×10^{-4}	1.07×10^{-3}	2.38×10^{-3}

Table 3.2: Table of four smallest eigenvalues (ω^2) for azimuthal quantum number $m = 1$.

When we consider the components u_{1n} and v_{1n} corresponding to ω_0^2 , we find they display the correct behaviour at the origin (3.31) and the asymptotic form associated with the eigenvalue $\omega^2 = 0$ for large r (3.51). Therefore the corresponding complex eigenfunctions $\tilde{\varphi}_{1n}$ and $\hat{\varphi}_{1n}$ (3.24) are zero modes.

Previously we showed that the zero modes from the translational degrees of freedom correspond to the azimuthal quantum number $m = 1$ (3.28). To check that the computed components do in fact correspond to translational zero modes we must show:

$$\begin{pmatrix} u_{1n} \\ v_{1n} \end{pmatrix} \propto \begin{pmatrix} -\frac{d\Phi_n}{dr} \\ \frac{n\Phi_n}{r} \end{pmatrix}. \quad (3.64)$$

When $c_1 u_{11}$ (Fig. 3.2) is compared with $-\frac{d\Phi_1}{dr} \Phi_1$, for some constant c_1 , we observe that they are identical. Also, when $c_1 v_{11}$ is compared to $\frac{\Phi_1}{r}$ (Fig. 3.3), for the same c_1 , we discover that they are very similar but that a slight deviation in the shape of the two curves occurs as $r \rightarrow R$. This deviation is a result of imposing the boundary condition

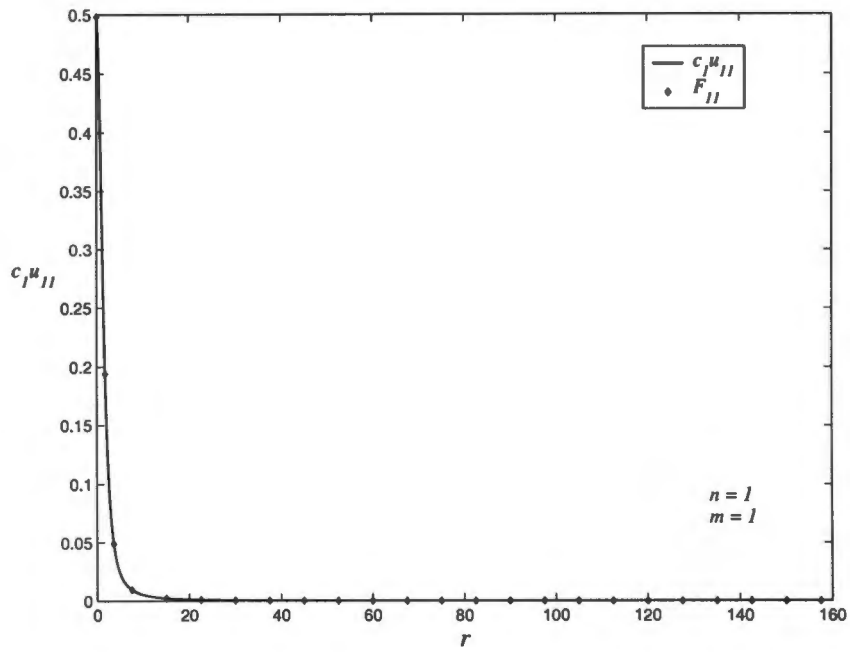


Figure 3.2: $c_1 u_{11}$ and $-\frac{d}{dr}\Phi_1$ as functions of r

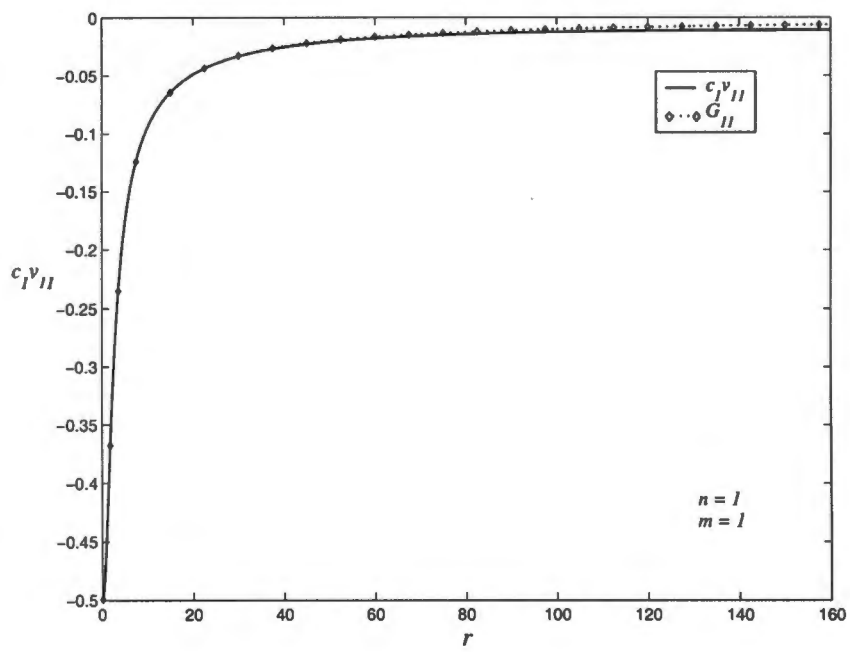


Figure 3.3: $c_1 v_{11}$ and $\frac{\Phi_1}{r}$ as functions of r

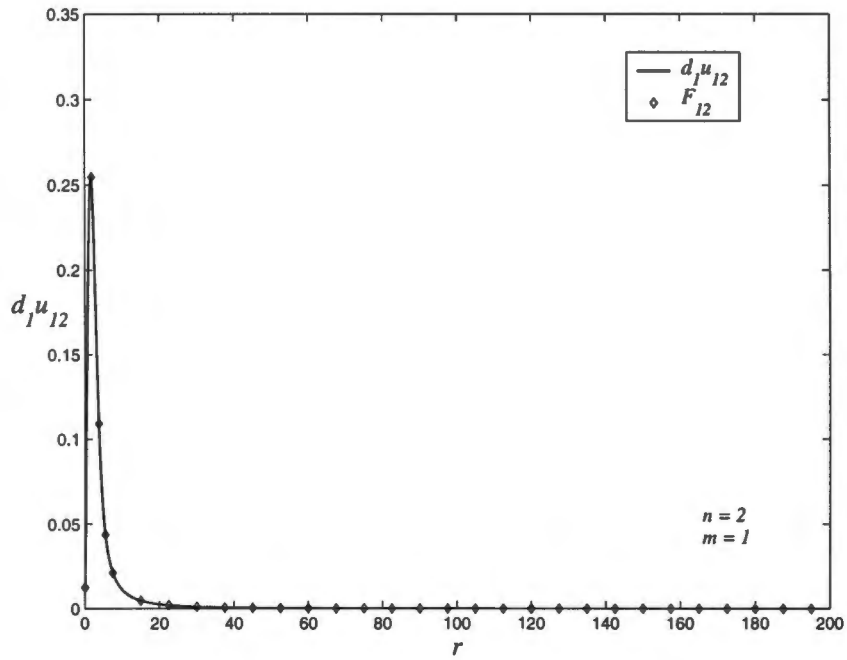


Figure 3.4: $d_1 u_{12}$ and $-\frac{d}{dr} \Phi_2$ as functions of r

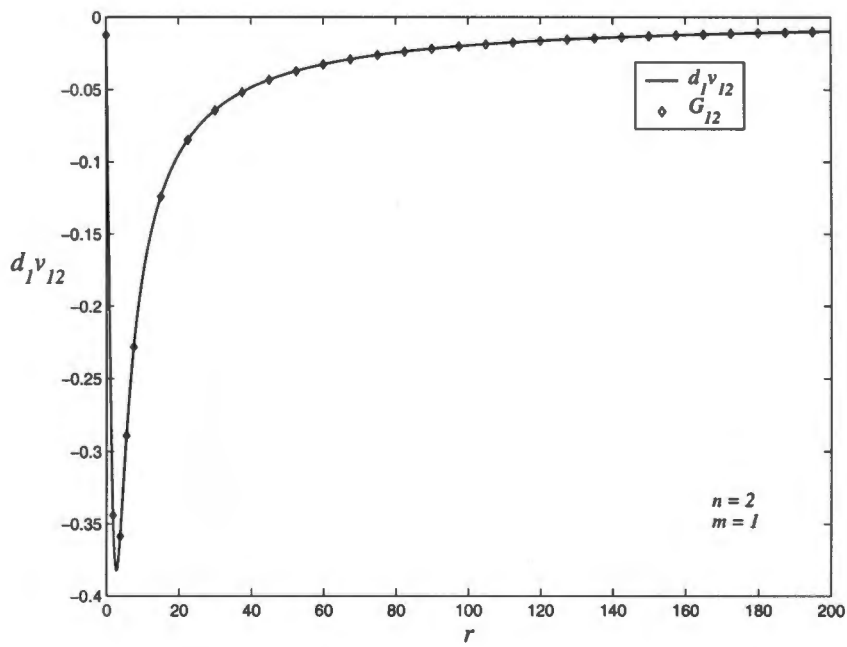


Figure 3.5: $d_1 v_{12}$ and $\frac{\Phi_2}{r}$ as functions of r

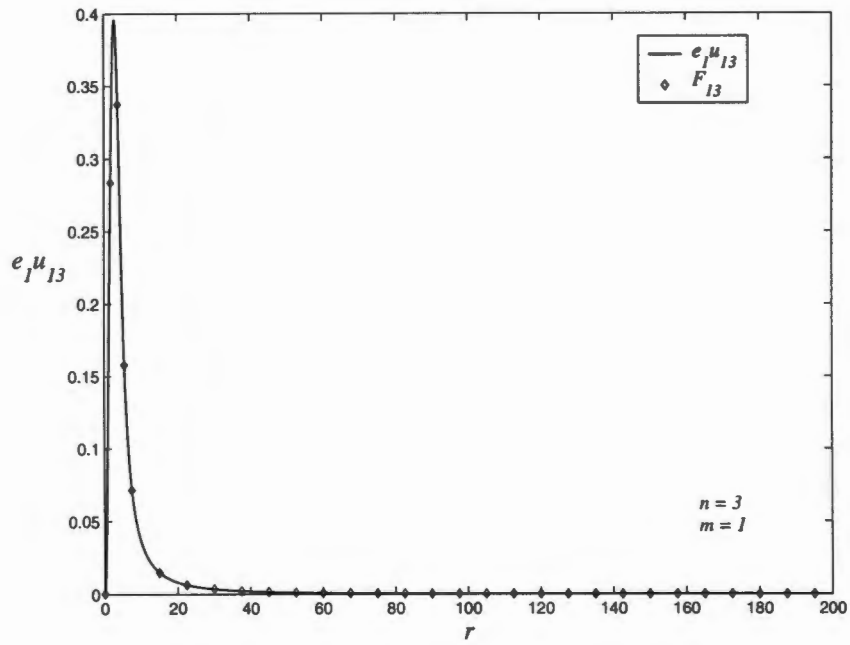


Figure 3.6: $e_1 u_{13}$ and $-c \frac{d}{dr} \Phi_3$ as functions of r

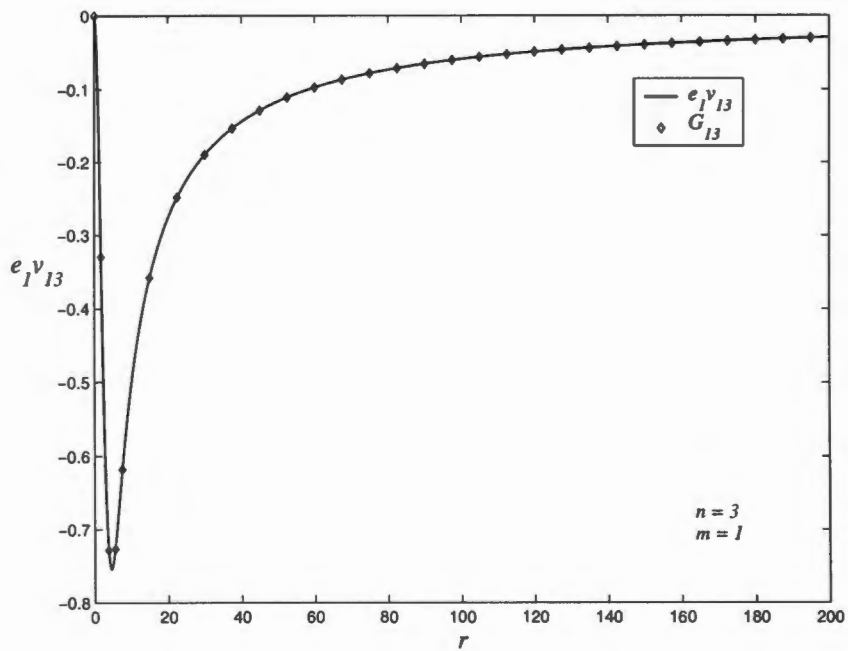


Figure 3.7: $e_1 v_{13}$ and $c \frac{\Phi_3}{r}$ as functions of r

$\frac{d}{dr}v_{11}(R) = 0$ (the nonsymmetric eigenvalue problem was used for the single vortex). This, unfortunately, is not the most accurate approximation to the true boundary condition at $r = R$ as the function $\frac{\Phi_1}{r}$ decays slowly to zero as $r \rightarrow \infty$. Therefore, it is clear from (3.28a) and (3.28b) that for ω_0^2 , the zero mode $\tilde{\varphi}_{11}$ corresponds to a translational degree of freedom in the x direction and $\hat{\varphi}_{11}$ to one in the y direction.

Considering the double coaxial-vortex Ψ_2 , we observe that the complex eigenfunctions $\tilde{\varphi}_{12}$ and $\hat{\varphi}_{12}$ have components $d_1 u_{12} = -\frac{d\Phi_2}{dr}$ (Fig. 3.4) and $d_1 v_{12} = \frac{2\Phi_2}{r}$ (Fig. 3.5), for some constant d_1 . Hence, these zero modes are the modes corresponding to translational degrees of freedom in the x and y directions for the double coaxial-vortex.

Similarly, the components $e_1 u_{13} = -\frac{d\Phi_3}{dr}$ (Fig. 3.6) and $e_1 v_{13} = \frac{3\Phi_3}{r}$ (Fig. 3.7), for some constant e_3 . Thus the eigenfunctions $\tilde{\varphi}_{13}$ and $\hat{\varphi}_{13}$ corresponding to ω_0^2 are zero modes from Ψ_3 's translational degrees of freedom in the x and y directions.

When we consider, for all three vortices, the eigenfunctions corresponding to eigenvalues $\omega^2 > \omega_0^2$ we discover that their components u_{1n} and v_{1n} oscillate with wavenumber $k \sim \omega$. Therefore they correspond to positive eigenvalues $\omega^2 > 0$ (3.54) and are not zero modes. This agrees with our earlier statement that there can be at most two zero modes to each azimuthal quantum number per vortex.

Hence for $m = 1$ there are only two zero modes for each of the single, double and triple coaxial-vortices. In each case the zero modes correspond to translational degrees of freedom in the x and y directions.

Up until now we have only reproduced the three expected zero modes for each vortex. We know however, from studying the asymptotics (§3.2), that other zero modes do exist. Recall that the asymptotics show that the eigenvalue $\omega^2 = 0$ does exist and belongs to the continuous spectrum. What we would like to know, is to what these other degrees of freedom correspond? To establish that they in fact correspond to the continuous parameters of a recently discovered infinite parameter solution [86], we will now discuss the results obtained for higher azimuthal quantum numbers. The results for each of the three vortices (Ψ_1 , Ψ_2 and Ψ_3) are discussed separately for azimuthal quantum numbers $m = 2$ to 5.

3.3.3 Excitations of the single vortex with azimuthal quantum numbers $m \geq 2$

As mentioned we compute the eigenfunctions for azimuthal quantum numbers $m = 2$ to 5 for the single vortex. To calculate the zero modes, we first solve the symmetric matrix eigenvalue problem from (3.61) for η_{m1} and ζ_{m1} . Thereafter, we use the inverse of the transformation (3.59) to obtain the components u_{m1} and v_{m1} . The four smallest eigenvalues ω^2 computed for each value of m are displayed in Table 3.3. And the components for azimuthal quantum numbers $m = 2, 3, 4$ and 5 corresponding to the smallest eigenvalues ω_0^2 are given in Figs. 3.8-3.9, Figs. 3.10-3.11, Figs. 3.12-3.13 and Figs. 3.14-3.15, respectively.

Observe that the components corresponding to the smallest eigenvalues (ω_0^2) display the asymptotics associated with zero modes both at the origin (3.31) and for large r (3.51). Therefore the eigenfunctions $\tilde{\varphi}_{m1}$ and $\hat{\varphi}_{m1}$ (3.24), corresponding to ω_0^2 , are zero modes. When we consider the eigenfunctions corresponding to eigenvalues $\omega^2 > \omega_0^2$ we

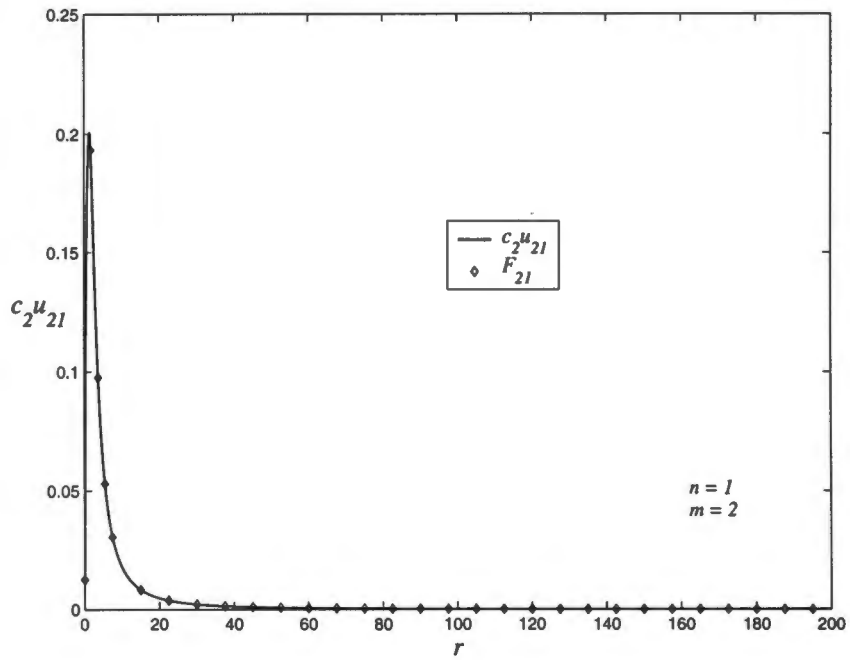


Figure 3.8: $c_2 u_{21}$ and F_{21} as functions of r

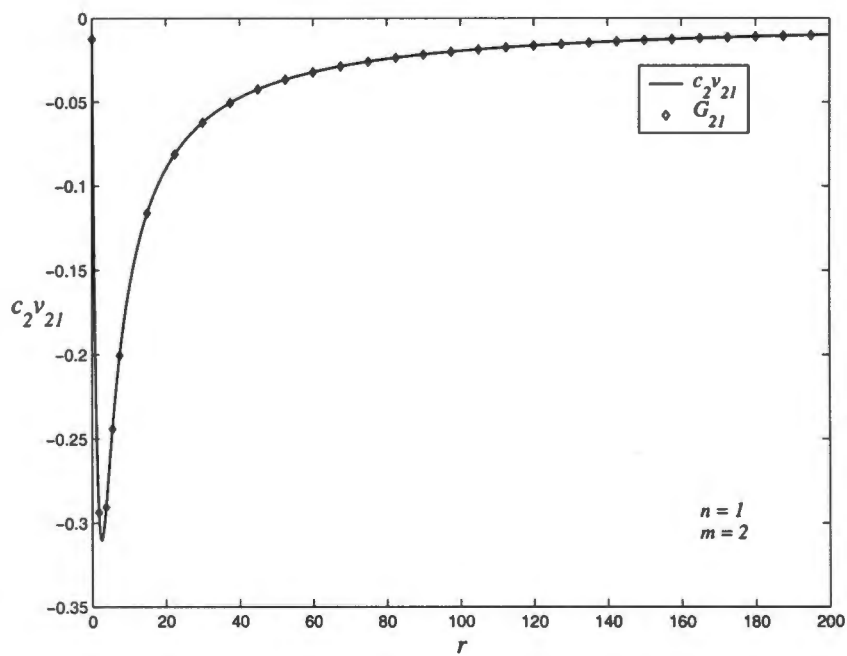


Figure 3.9: $c_2 v_{21}$ and G_{21} as functions of r

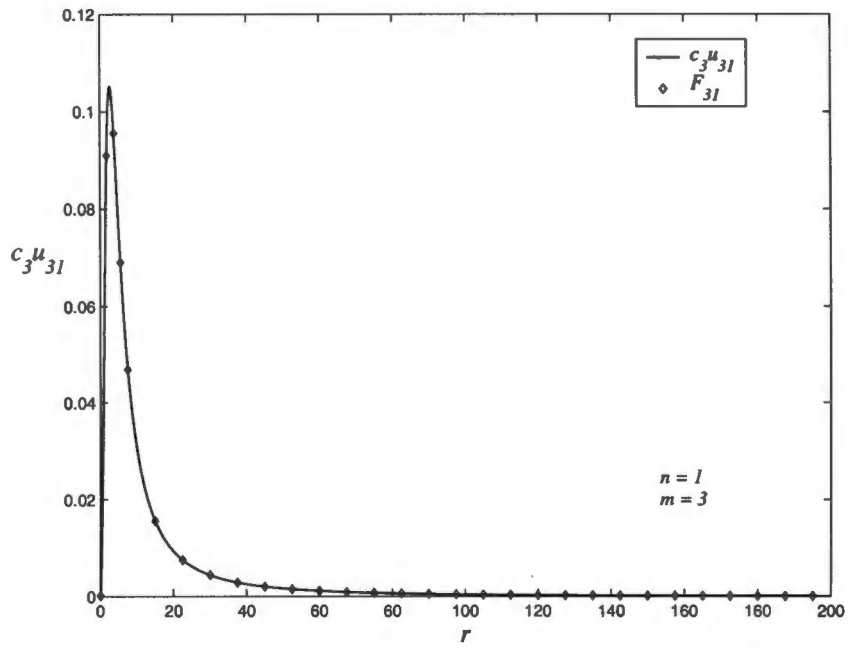


Figure 3.10: $c_3^{\mu_{31}}$ and F_{31} as functions of r

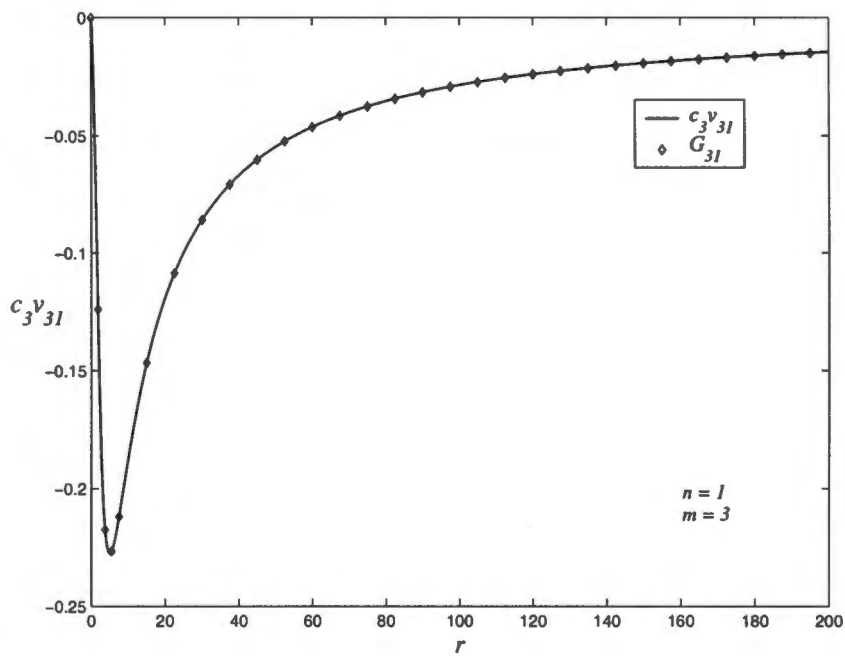


Figure 3.11: $c_3^{\nu_{31}}$ and G_{31} as functions of r

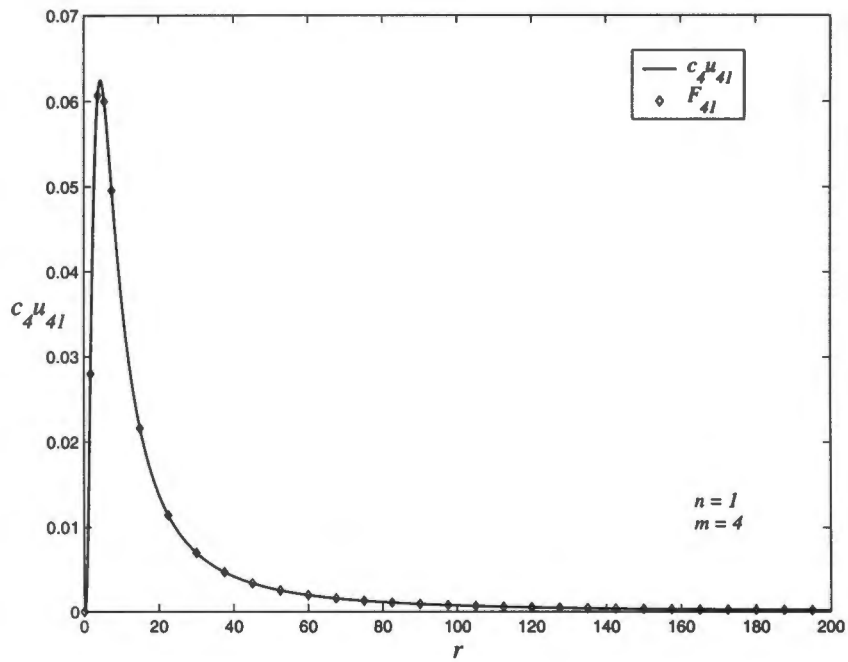


Figure 3.12: $c_4^\mu{}_{41}$ and F_{41} as functions of r

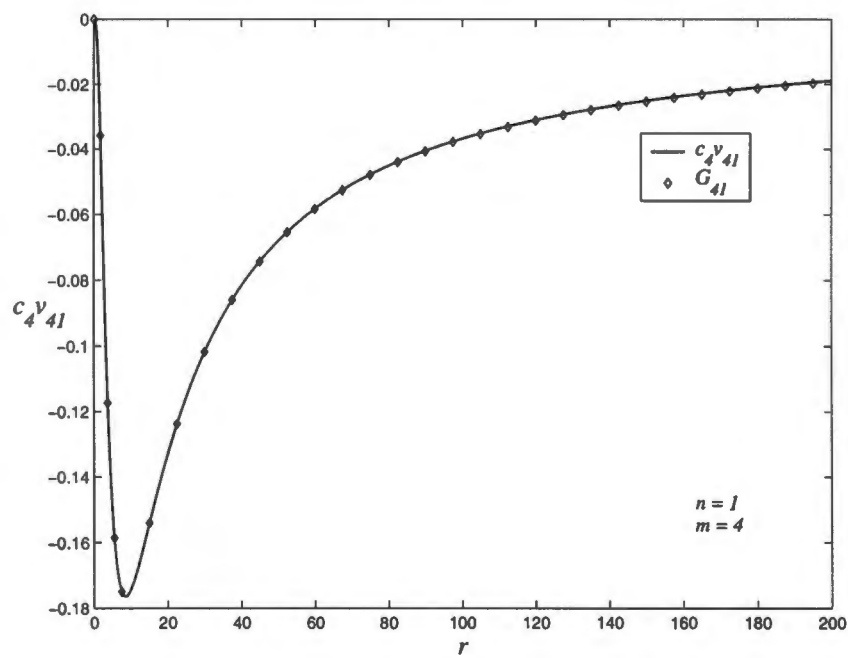


Figure 3.13: $c_4^\nu{}_{41}$ and G_{41} as functions of r

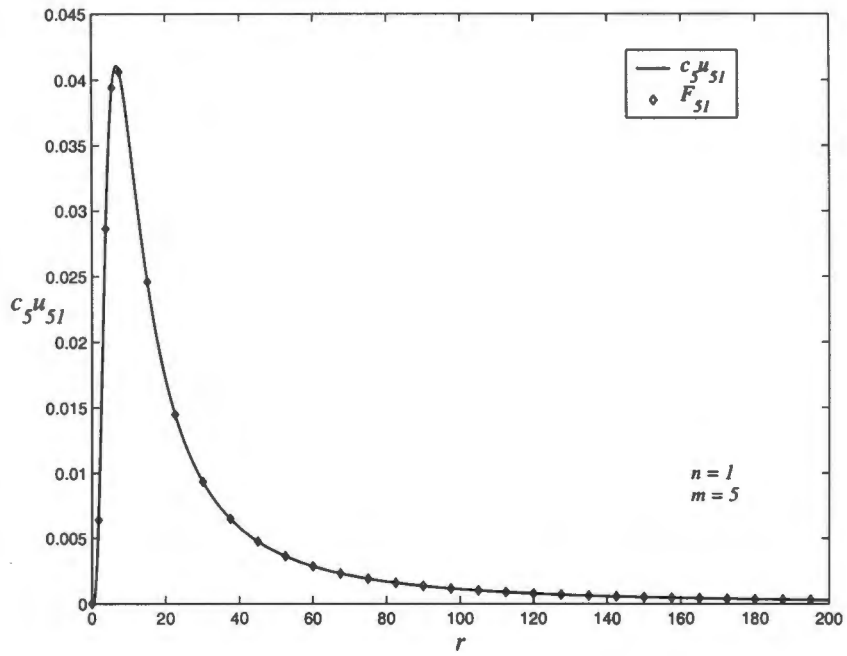


Figure 3.14: $c_5 u_{51}$ and F_{51} as functions of r

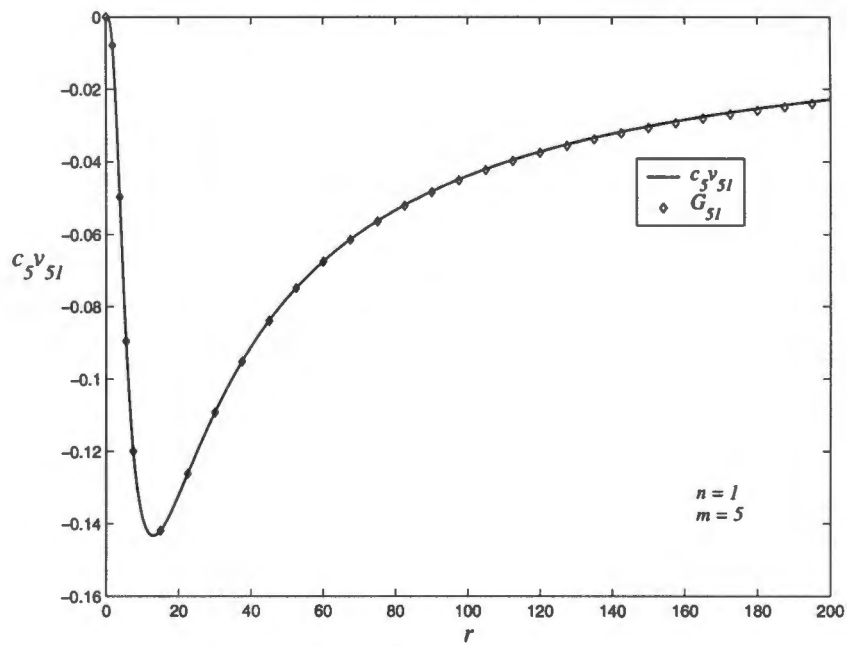


Figure 3.15: $c_5 v_{51}$ and G_{51} as functions of r

m	ω_0^2	ω_1^2	ω_2^2	ω_3^2
2	1.25×10^{-7}	2.72×10^{-4}	1.06×10^{-3}	2.37×10^{-3}
3	6.28×10^{-7}	2.91×10^{-4}	1.12×10^{-3}	2.47×10^{-3}
4	1.20×10^{-6}	3.12×10^{-4}	1.18×10^{-3}	2.57×10^{-3}
5	2.00×10^{-5}	3.53×10^{-4}	1.24×10^{-3}	4.65×10^{-3}

Table 3.3: Table of smallest eigenvalues (ω^2) for the single vortex ($n = 1$) for azimuthal quantum numbers $m = 2$ to 5.

find that they have components u_{m1} and v_{m1} which oscillate with the wavenumber $k \sim \omega$. Therefore, there are only two zero modes, $\tilde{\varphi}_{m1}$ and $\hat{\varphi}_{m1}$, corresponding to $\omega^2 = 0$, for each azimuthal quantum number $m = 2, 3, 4$ and 5.

Now the question of the origin of these zero modes, arises. The answer to this is found on examining a recently obtained, exact solution to the complex sine-Gordon model [86]. This solution describes bound states of non-coaxial vortices. In particular, we will consider the vortex state with vorticity $n = 1$. This solution is of the form:

$$\hat{\Psi}_1 = \frac{Z_1}{Z_0}, \quad (3.65)$$

where

$$Z_k = \sum_{m=0}^{\infty} (\gamma_m \xi_{m+k} + \bar{\gamma}_m \xi_{-m+k}),$$

$$\xi_s = I_s(r) e^{is\theta}, \quad \gamma_m = \frac{\beta_m}{2} e^{i\delta_m}.$$

In the above equation, $I_s(r)$ is the modified Bessel function of order s and β_m and δ_m are real constants. We do not have complete freedom while choosing the values for the β_m 's. For example, the constraint $\beta_0 \neq 0$ is required to ensure the non-singularity of the vortex at the origin. In this text we will choose $\beta_0 = 1$ and with this choice the inequality $\sum_{m \geq 1} |\beta_m| \leq 1$ ensures regularity of $\hat{\Psi}_1$ everywhere.

With the use of the relation $I_s(r) = I_{-s}(r)$, Z_k can be rewritten in a simpler form:

$$Z_k = I_k + \sum_{m \geq 1} \frac{\beta_m}{2} \left(I_{m+k} e^{i(m\theta + \delta_m)} + I_{m-k} e^{-i(m\theta + \delta_m)} \right) e^{ik\theta}. \quad (3.66)$$

Note that by setting $\beta_m = 0$ in (3.66), the vortex (3.65) reduces to the single vortex (3.58a).

To determine the zero modes of the non-coaxial multivortex $\hat{\Psi}_1$, we take the partial derivative with respect to β_m and then let $\beta_i = 0$ for all i :

$$\left. \frac{\partial \hat{\Psi}_1}{\partial \beta_m} \right|_{\beta=0} = \{ F_{m1}(r) \cos(m\theta + \delta_m) + i G_{m1}(r) \sin(m\theta + \delta_m) \} e^{i\theta}, \quad (3.67)$$

where

$$F_{m1} = \frac{d}{dr} \left(\frac{I_m}{I_0} \right),$$

$$G_{m1} = -\frac{m I_m}{r I_0}. \quad (3.68)$$

Note that these zero modes have azimuthal quantum number m . Therefore, we expect the computed zero modes $\tilde{\varphi}_{m1} e^{i\theta}$ and $\tilde{\varphi}_{m1} e^{i\theta}$ to correspond to $\frac{\partial \hat{\Psi}_1}{\partial \beta_m} |_{\beta_m}$ with two different values of δ_m . From the form of $\tilde{\varphi}_{m1}$ and $\tilde{\varphi}_{m1}$ (3.24) it follows that the zero modes coincide if

$$\begin{pmatrix} u_{m1} \\ v_{m1} \end{pmatrix} \propto \begin{pmatrix} F_{m1} \\ G_{m1} \end{pmatrix} \quad (3.69)$$

and δ_m takes the values 0 and $\frac{\pi}{2}$.

When the graphs of $c_m u_{m1}$, for some constants c_m , are compared to those of F_{m1} for azimuthal quantum numbers $m = 2$ to 5, we find that they are identical. The graphs for $m = 2, 3, 4, 5$ are given in Figs. 3.8, 3.10, 3.12 and 3.14, respectively. Similarly, when we compare the graphs of $c_m v_{m1}$, for the same c_m , to the functions G_{m1} , we observe that they are also identical Figs. 3.8, 3.10, 3.12 and 3.14. Table 3.4 lists the relative differences between $c_m u_{m1}$ and F_{m1} and between $c_m v_{m1}$ and G_{m1} at the right hand boundary.

m	c_m	$\left 1 - \frac{F_{m1}(R)}{c_m u_{m1}(R)} \right \times 100\%$	$\left 1 - \frac{G_{m1}(R)}{c_m v_{m1}(R)} \right \times 100\%$
1	3.19	42.6	42.5
2	120	0.314	0.314
3	173	0.166	0.166
4	219	0.242	0.242
5	258	0.343	0.343

Table 3.4: Table of relative differences at $r = R$ for $m = 1, 2, 3, 4$ and 5 for the single vortex.

We conclude that the extra zero modes for the single vortex Ψ_1 are the zero modes that result from the parameters in $\hat{\Psi}_1$. We conjecture that this is true for all azimuthal quantum numbers even for $m > 5$. In this case all the extra zero modes of the single vortex are accounted for. Hence, $\hat{\Psi}_1$ is the largest continuous parameter family of solutions to the complex sine-Gordon model which has the single vortex Ψ_1 as one of its members.

3.3.4 Excitations of the double coaxial-vortex with azimuthal quantum numbers $m \geq 2$

As for the single vortex, the eigenfunctions for azimuthal quantum numbers $m = 2$ to 5 are computed for the double coaxial-vortex ($n = 2$). The nonsymmetric eigenvalue problem (3.15) is solved directly for the functions u_{22} and v_{22} since for $m = 2$, $m = n$. For the other azimuthal quantum numbers the symmetric eigenvalue problem (3.61) is first solved for η_{m2} and ζ_{m2} , then the inverse of (3.59) is used to obtain the functions

u_{m2} and v_{m2} . The four, smallest computed eigenvalues, ω^2 , for each azimuthal quantum number m are displayed in Table 3.5. The components u_{m2} and v_{m2} , for $m = 2, 3, 4$

m	ω_0^2	ω_1^2	ω_2^2	ω_3^2
2	-6.07×10^{-5}	3.80×10^{-4}	1.70×10^{-3}	3.85×10^{-3}
3	1.36×10^{-6}	3.23×10^{-4}	1.21×10^{-3}	2.64×10^{-3}
4	2.77×10^{-6}	3.63×10^{-4}	1.32×10^{-3}	2.83×10^{-3}
5	4.86×10^{-6}	4.08×10^{-4}	1.43×10^{-3}	3.04×10^{-3}

Table 3.5: Table of smallest eigenvalues (ω^2) for the double coaxial-vortex for $m = 2$ to 5.

and 5 corresponding to the smallest eigenvalues, ω_0^2 , are given in Figs. 3.16-3.17, Figs. 3.18-3.19, Figs. 3.20-3.21 and Figs. 3.22-3.23, respectively.

Observe that these components exhibit the behaviour associated with zero modes at the origin (3.31) and as they approach the right hand boundary (3.51). When examining the eigenfunctions which correspond to eigenvalues $\omega^2 > \omega_0^2$, their components u_{m2} and v_{m2} are found to oscillate with wavenumber $k \sim \omega$. The eigenfunctions corresponding to eigenvalues $\omega^2 > \omega_0^2$ are not zero modes. Therefore, there are only two zero modes, $\hat{\varphi}_{m2}$ and $\tilde{\varphi}_{m2}$ corresponding to ω_0^2 , for each azimuthal quantum number $2 \leq m \leq 5$.

Again, as with the single vortex, we would like to know what these zero modes correspond to. In this case we discover the origin of these zero modes by examining the recently obtained non-coaxial multivortex $\hat{\Psi}_2$ [86]. This multivortex has vorticity 2 (2) and is described by:

$$\hat{\Psi}_2 = \frac{Z_1^2 - Z_2 Z_0}{Z_0^2 - Z_{-1} Z_1}, \quad (3.70)$$

with Z_k as in (3.66). The same restriction for the β_m 's holds as for $\hat{\Psi}_1$: $\sum_{m \geq 1} |\beta_m| \leq 1$. Note that this non-coaxial multivortex $\hat{\Psi}_2$ reduces to the double coaxial-vortex (3.58b) when $\beta_m = 0$ for $m \geq 1$.

To determine the zero modes of this non-coaxial multivortex, take the partial derivative of (3.65) with respect to β_m and then set $\beta_j = 0$ for all $j \geq 1$. This gives

$$\left. \frac{\partial \hat{\Psi}_2}{\partial \beta_m} \right|_{\beta=0} = \left[F_{m2}(r) \cos(m\theta + \delta_m) + iG_{m2}(r) \sin(m\theta + \delta_m) \right] e^{2i\theta}, \quad (3.71)$$

where

$$\begin{aligned}
F_{m2} &= \frac{1}{I_0^2 - I_1^2} \left\{ I_1(I_{m+1} + I_{m-1}) - \frac{1}{2}I_0(I_{m+2} + I_{m-2}) + I_2I_m \right. \\
&\quad \left. - \frac{I_1^2 - I_0I_2}{I_0^2 - I_1^2} \left[2I_mI_0 - I_1(I_{m+1} + I_{m-1}) \right] \right\}, \\
G_{m2} &= \frac{I_1(I_{m+1} - I_{m-1}) - \frac{1}{2}I_0(I_{m+2} - I_{m-2})}{I_0^2 - I_1^2}. \tag{3.72}
\end{aligned}$$

If for the computed zero modes

$$\begin{pmatrix} u_{m2} \\ v_{m2} \end{pmatrix} \propto \begin{pmatrix} F_{m2} \\ G_{m2} \end{pmatrix} \tag{3.73}$$

then $\tilde{\varphi}_{m2}e^{2i\theta}$ and $\hat{\varphi}_{m2}e^{2i\theta}$ are given by $\frac{\partial \hat{\Psi}_2}{\partial \beta_m} \Big|_{\beta_m}$ with $\delta_m = 0$ and $\delta_m = \frac{\pi}{2}$, respectively.

In other words the computed zero modes will correspond to the zero modes of $\hat{\Psi}_2$.

When the graph of $d_m u_{m2}$, $d_m \in \mathbb{R}$, is compared to the function F_{m2} we find that they are identical. Also, when comparing the graphs of the functions $d_m v_{m2}$ to those of G_{m2} , for the same d_m , we find that they are identical except when $m = n = 2$. For the azimuthal quantum number $m = 2$ there is a slight deviation between the two curves as $r \rightarrow R$ (Fig. 3.17). This is because the boundary condition (3.56) imposed for the eigenvalue problem (3.15) forces the coefficient v_{m2} to flatten too quickly as $r \rightarrow R$. This is the same situation as occurs with the single vortex and azimuthal quantum number $m = 1$. The relative differences between the various functions at $r = R$ are given in Table 3.6.

As with the single vortex we conjecture that the non-coaxial multivortex $\hat{\Psi}_2$ is the largest continuous parameter family of solutions with the coaxial double-vortex Ψ_2 as a member.

m	d_m	$\left 1 - \frac{F_{m2}(R)}{d_m u_{m2}(R)} \right \times 100\%$	$\left 1 - \frac{G_{m2}(R)}{d_m v_{m2}(R)} \right \times 100\%$
1	86.5	0.458	0.458
2	4.59	40.6	40.4
3	227	0.352	0.352
4	276	0.412	0.412
5	310	0.541	0.541

Table 3.6: Table of relative differences at $r = R$ for $m = 1, 2, 3, 4$ and 5 for the coaxial double-vortex.

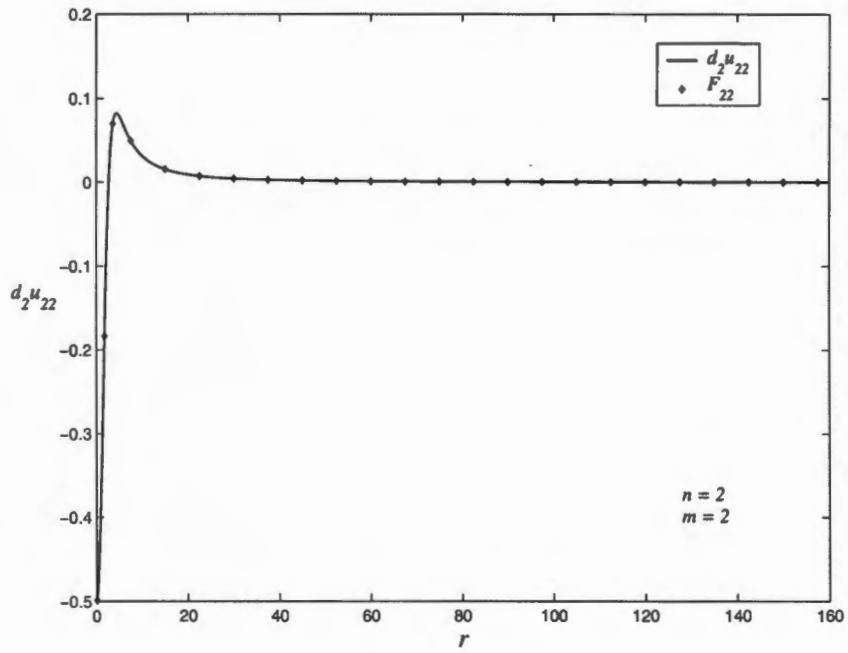


Figure 3.16: $d_2^u_{22}$ and F_{22} as functions of r

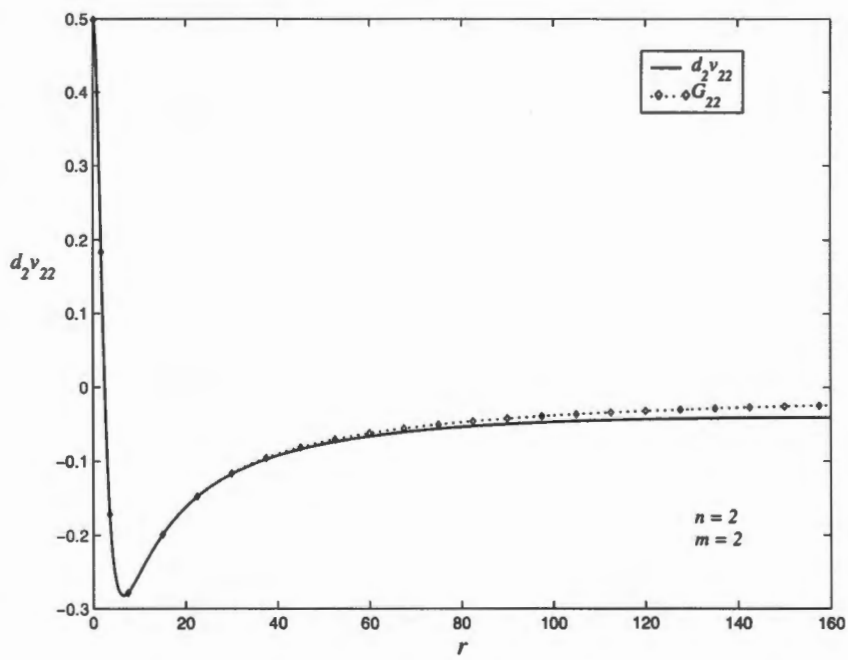


Figure 3.17: $d_2^v_{22}$ and G_{22} as functions of r

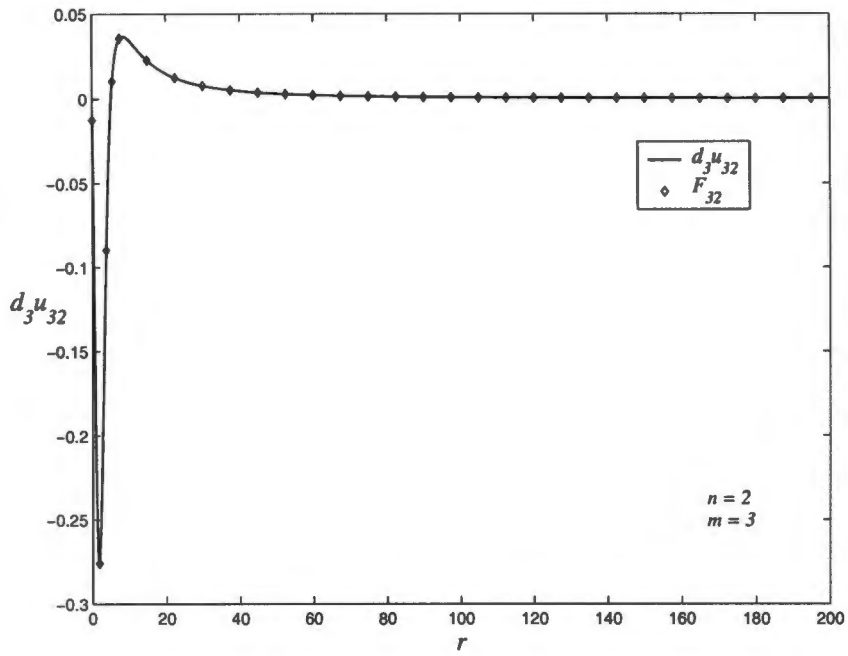


Figure 3.18: d_3u_{32} and F_{32} as functions of r

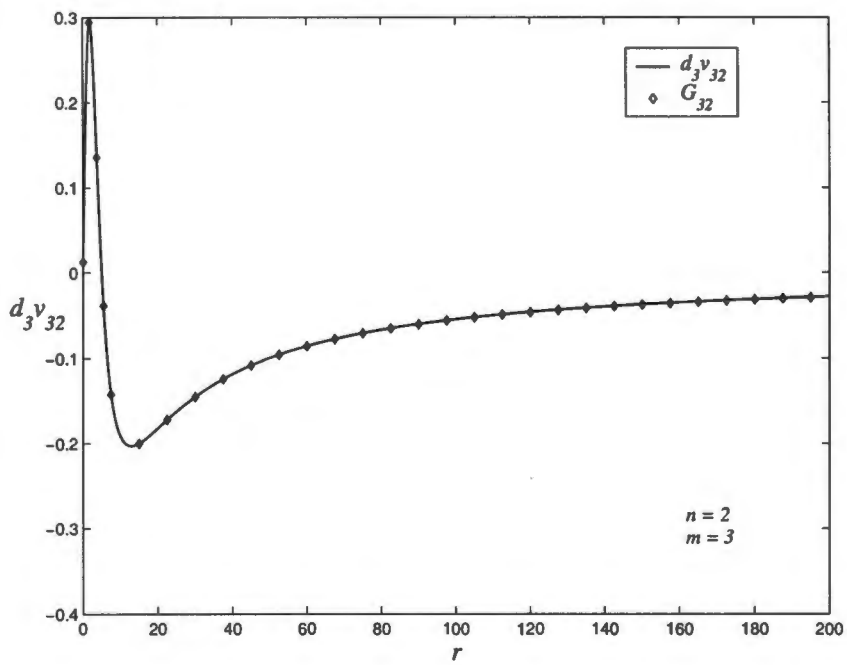


Figure 3.19: d_3v_{32} and G_{32} as functions of r

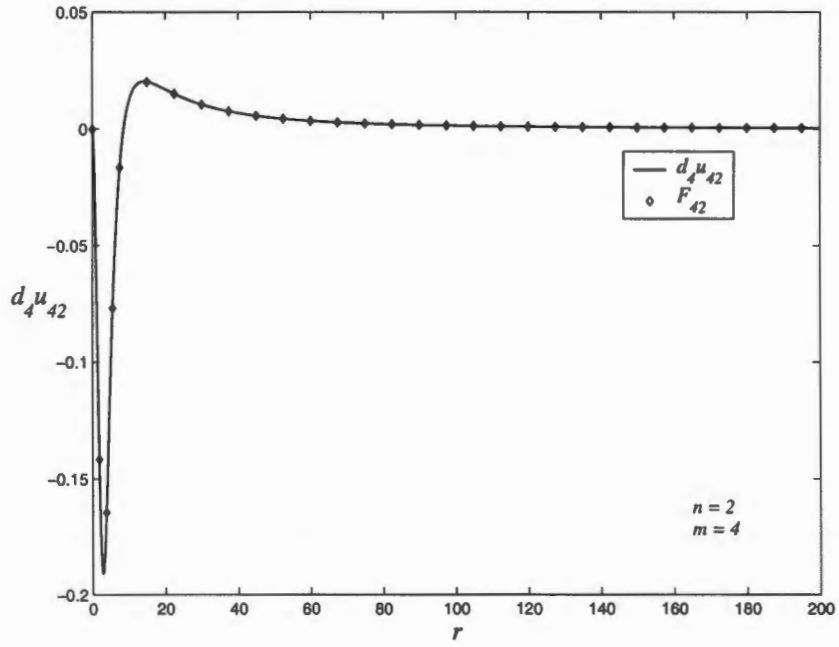


Figure 3.20: $d_4 u_{42}$ and F_{42} as functions of r

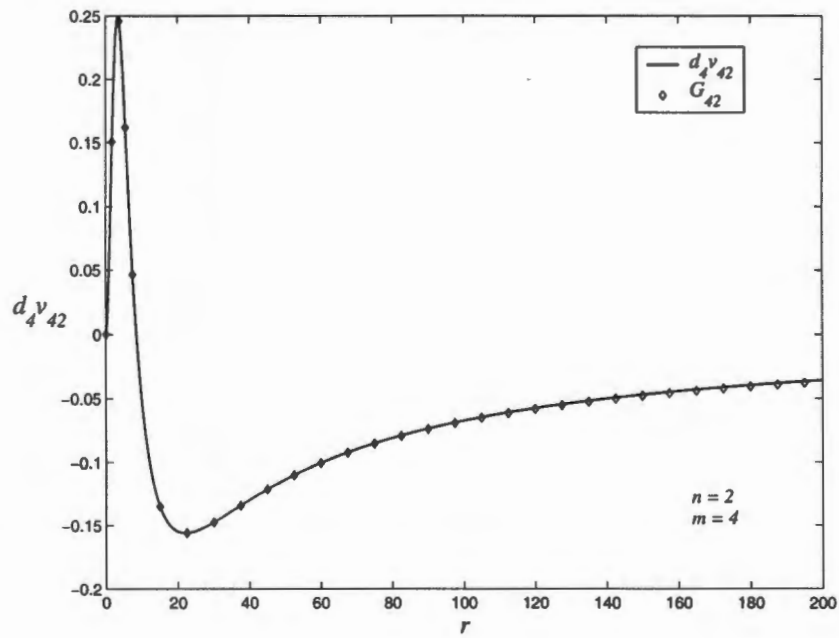


Figure 3.21: $d_4 v_{42}$ and G_{42} as functions of r

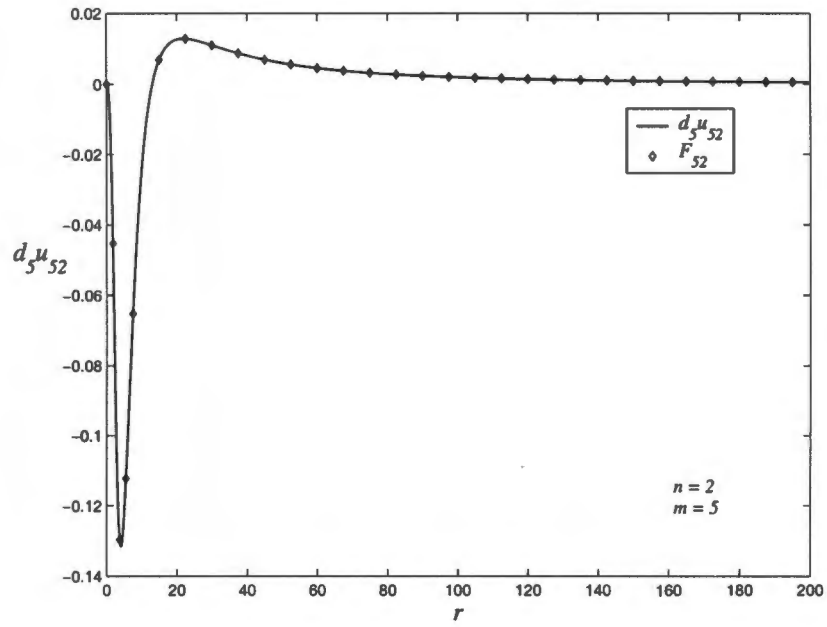


Figure 3.22: $d_5 u_{52}$ and F_{52} as functions of r

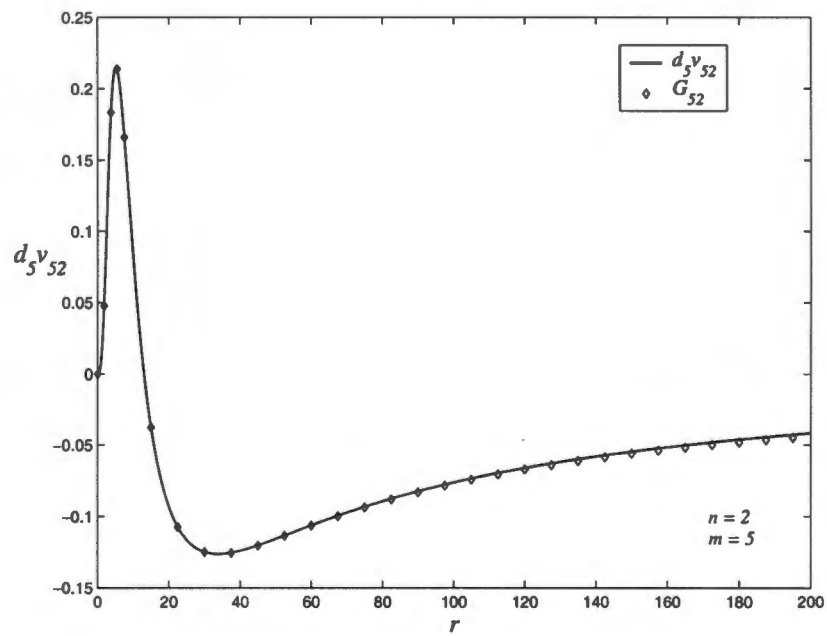


Figure 3.23: $d_5 v_{52}$ and G_{52} as functions of r

3.3.5 The excitations of the coaxial triple-vortex Ψ_3 with azimuthal quantum numbers $m \geq 2$

For Ψ_3 the nonsymmetric eigenvalue problem (3.15) is solved directly for $m = 3$, while for azimuthal quantum numbers $m = 2, 4$ and 5 the symmetric eigenvalue problem (3.61) is solved. The four smallest eigenvalues ω^2 computed for each azimuthal quantum number m are displayed in Table 3.7. And the components u_{m3} and v_{m3} corresponding to the

m	ω_0^2	ω_1^2	ω_2^2	ω_3^2
2	8.18×10^{-7}	3.06×10^{-4}	1.17×10^{-3}	2.56×10^{-3}
3	-6.49×10^{-5}	4.91×10^{-4}	2.01×10^{-3}	4.42×10^{-3}
4	4.65×10^{-6}	4.08×10^{-4}	1.44×10^{-3}	3.05×10^{-3}
5	8.49×10^{-6}	4.76×10^{-4}	1.61×10^{-3}	3.35×10^{-3}

Table 3.7: Table of smallest eigenvalues (ω^2) for the coaxial triple-vortex ($n = 3$) for $m = 2$ to 5 .

smallest eigenvalues, ω_0^2 , for $m = 2, 3, 4$ and 5 are given in Figs. 3.24-3.25, Figs. 3.26-3.27, Figs. 3.28-3.29 and Figs. 3.30-3.31, respectively.

These components, as is clearly seen from the graphs, display the asymptotics of zero modes; (3.31) and (3.51). Again, the components u_{m3} and v_{m3} of the eigenfunctions corresponding to eigenvalues $\omega^2 > \omega_0^2$ all oscillate with wave number $k \sim \omega$ and thus are not zero modes. Hence, there are only two zero modes for each azimuthal quantum number $2 \leq m \leq 5$. This is identical to the two previous vortices, Ψ_1 and Ψ_2 .

Here, we expect the zero modes correspond to the continuous parameters of the non-coaxial multivortex $\hat{\Psi}_3$ of vorticity 3 [86]. This non-coaxial multivortex is described by:

$$\hat{\Psi}_3 = \frac{Z_3(Z_0^2 - Z_{-1}Z_1) + Z_{-1}Z_2^2 + Z_1^3 - 2Z_0Z_1Z_2}{Z_0(Z_0^2 - 2Z_{-1}Z_1 - Z_{-2}Z_2) + Z_{-1}^2Z_2 + Z_1^2Z_{-2}}, \quad (3.74)$$

with Z_k as in (3.66) and the restriction $\sum_{m \geq 1} |\beta_m| \leq 1$ still valid for the β_m 's. By setting $\beta_m = 0$ for $m \geq 1$, this non-coaxial multivortex $\hat{\Psi}_3$ reduces to the coaxial triple-vortex (3.58c).

Following the same procedure as before and taking the partial derivative of (3.65) with respect to β_m and then setting all $\beta_j = 0$ gives:

$$\left. \frac{\partial \hat{\Psi}_3}{\partial \beta_m} \right|_{\beta=0} = [F_{m3}(r) \cos(m\theta + \delta_m) + iG_{m3}(r) \sin(m\theta + \delta_m)] e^{3i\theta}, \quad (3.75)$$

where

$$F_{m3} = \frac{\tilde{C}_m + \tilde{C}_{-m}}{\tilde{B}} - 2 \frac{\tilde{A}\tilde{D}}{\tilde{B}^2},$$

$$G_{m3} = \frac{\tilde{C}_m - \tilde{C}_{-m}}{\tilde{B}}, \quad (3.76)$$

and

$$\begin{aligned}
\tilde{A} &= I_3(I_0^2 - I_1^2) + I_1I_2^2 + I_1^3 - 2I_0I_1I_2, \\
\tilde{B} &= I_0(I_0^2 - 2I_1^2 - I_2^2) + 2I_1^2I_2, \\
\tilde{C}_m &= \frac{1}{2} [2I_m(I_3I_0 - I_1I_2) - I_{m+1}(I_1I_3 - 3I_1^2 + 2I_0I_2) + I_{m-1}(I_2^2 - I_1I_3) \\
&\quad + 2I_{m+2}(I_1I_2 - I_0I_1) + I_{m+3}(I_0^2 - I_1^2)], \\
\tilde{D} &= \frac{1}{2} [I_m(3I_0^2 - 2I_1^2 + I_2^2) + 2I_1(I_2 - I_0)(I_{m+1} + I_{m-1}) \\
&\quad + (I_1^2 - I_0I_2)(I_{m+2} + I_{m-2})].
\end{aligned} \tag{3.77}$$

When the graphs of $e_m u_{m3}$ and $e_m v_{m3}$, for some $e_m \in \mathbb{R}$, are compared to those of F_{m3} and G_{m3} , respectively, we find they are identical except when $m = n = 3$. As with the previous cases this results from imposing the boundary condition (3.56) for the nonsymmetric eigenvalue problem (3.15). The relative differences between the various curves at $r = R$ are given in Table 3.8

Since

$$\begin{pmatrix} u_{m3} \\ v_{m3} \end{pmatrix} \propto \begin{pmatrix} F_{m3} \\ G_{m3} \end{pmatrix} \tag{3.78}$$

the computed zero modes $\tilde{\varphi}_{m3}e^{i\theta}$ and $\hat{\varphi}_{m3}e^{i\theta}$ are the zero modes $\frac{\partial \tilde{\Psi}_3}{\partial \beta_m} |_{\beta_m=\pi}$ with $\delta_m = 0$ and $\delta_m = \frac{\pi}{2}$, respectively

We conclude from these results that $\hat{\Psi}_3$ is the largest, continuous parameter, family of solutions with $\tilde{\Psi}_3$ as a member.

m	e_m	$ 1 - \frac{F_{m3}(R)}{e_m u_{m3}(R)} \times 100\%$	$ 1 - \frac{G_{m3}(R)}{e_m v_{m3}(R)} \times 100\%$
1	210	0.121	0.121
2	388	0.320	0.320
3	1.09	35.9	35.7
4	612	0.567	0.567
5	655	0.655	0.655

Table 3.8: Table of relative differences at $r = R$ for $m = 1, 2, 3, 4$ and 5 for the coaxial triple-vortex.

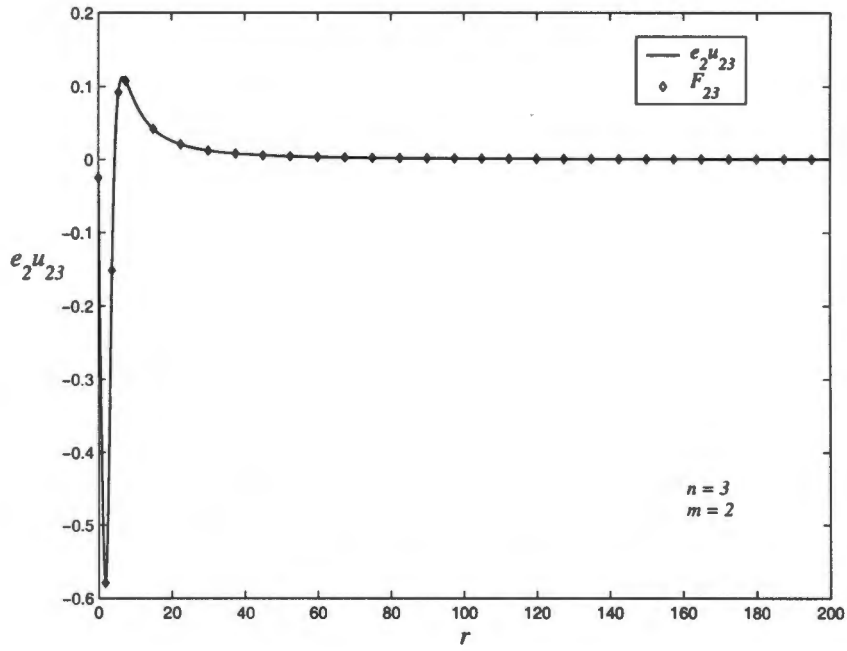


Figure 3.24: $e_2 u_{23}$ and F_{23} as functions of r

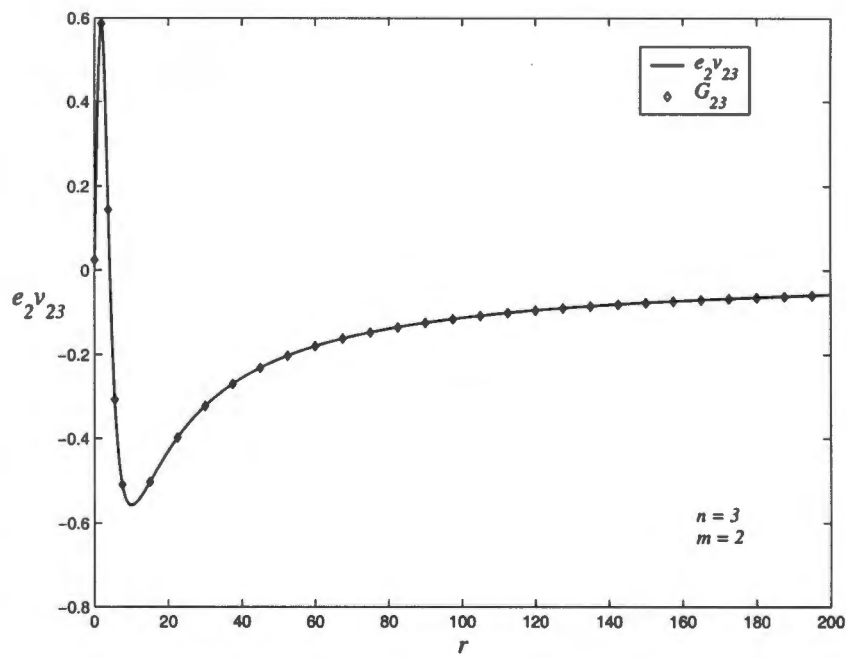


Figure 3.25: $e_2 v_{23}$ and G_{23} as functions of r

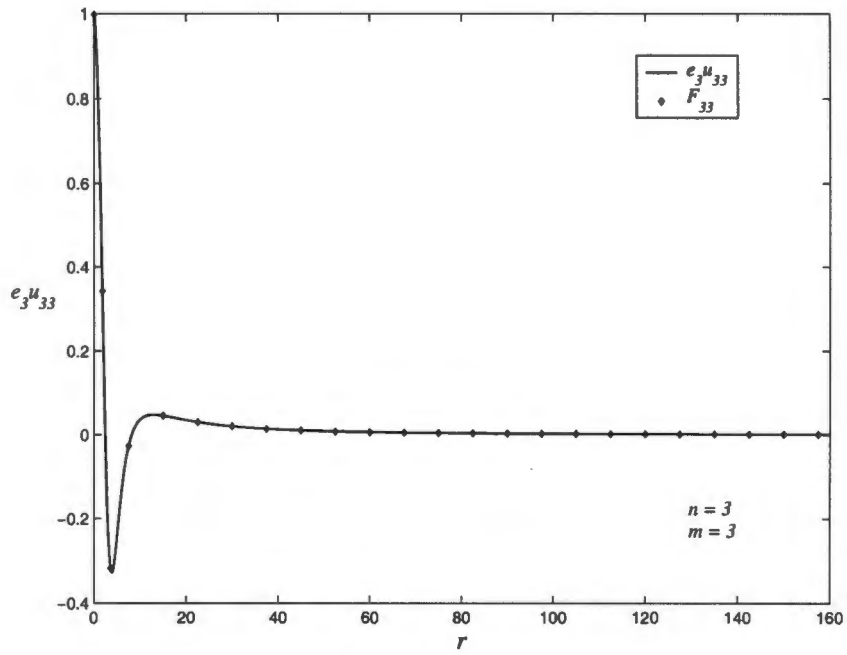


Figure 3.26: $e_3 u_{33}$ and F_{33} as functions of r

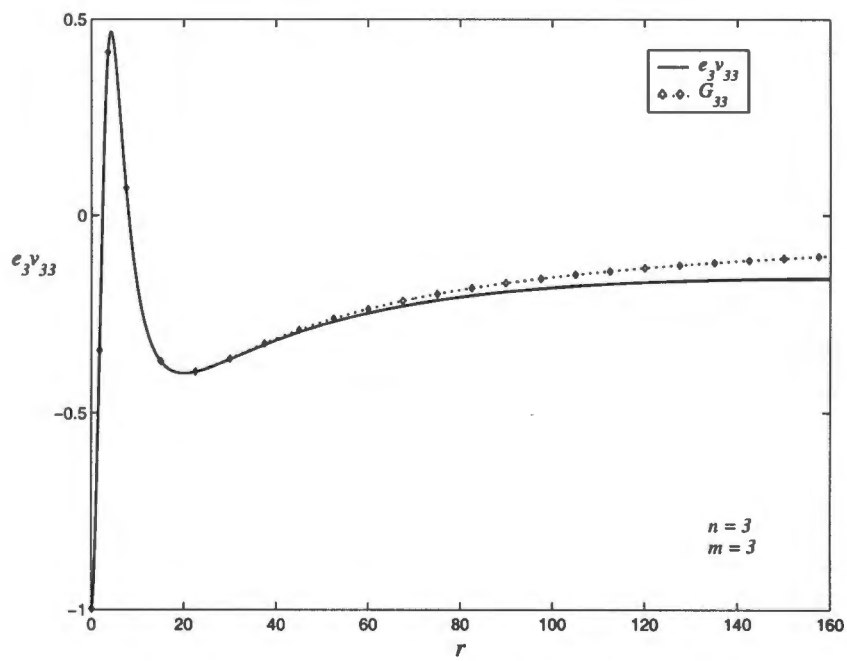


Figure 3.27: $e_3 v_{33}$ and G_{33} as functions of r

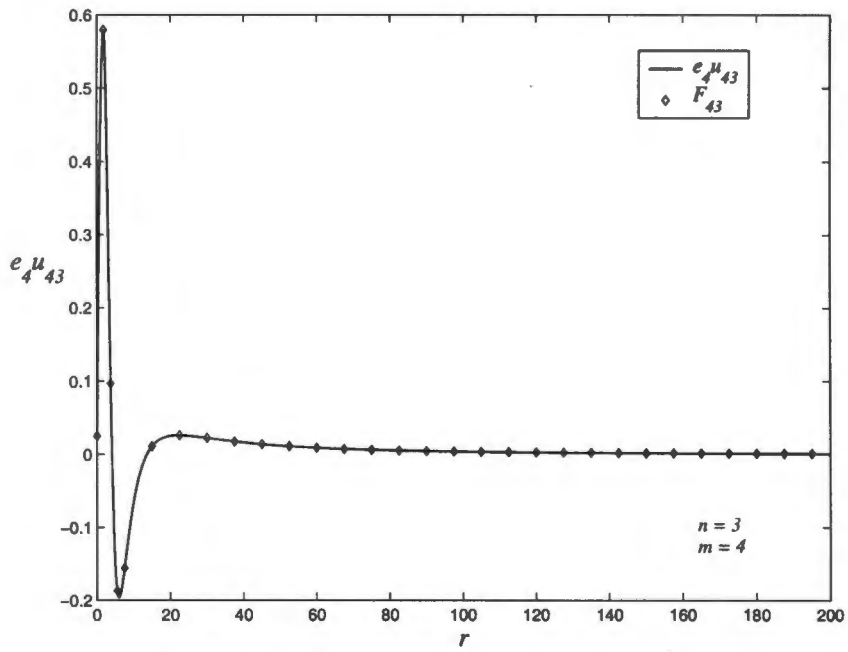


Figure 3.28: $e_4 u_{43}$ and F_{43} as functions of r

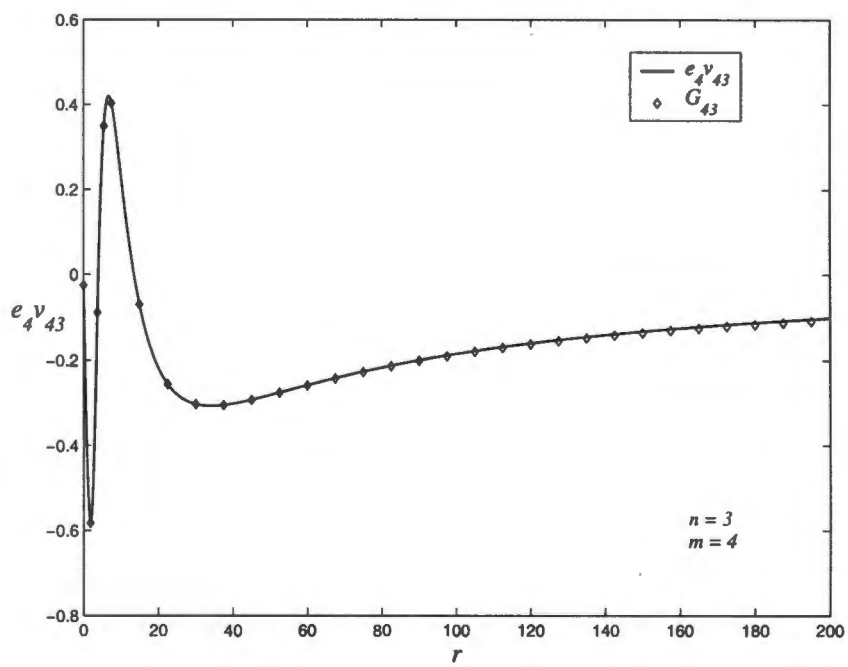


Figure 3.29: $e_4 v_{43}$ and G_{43} as functions of r

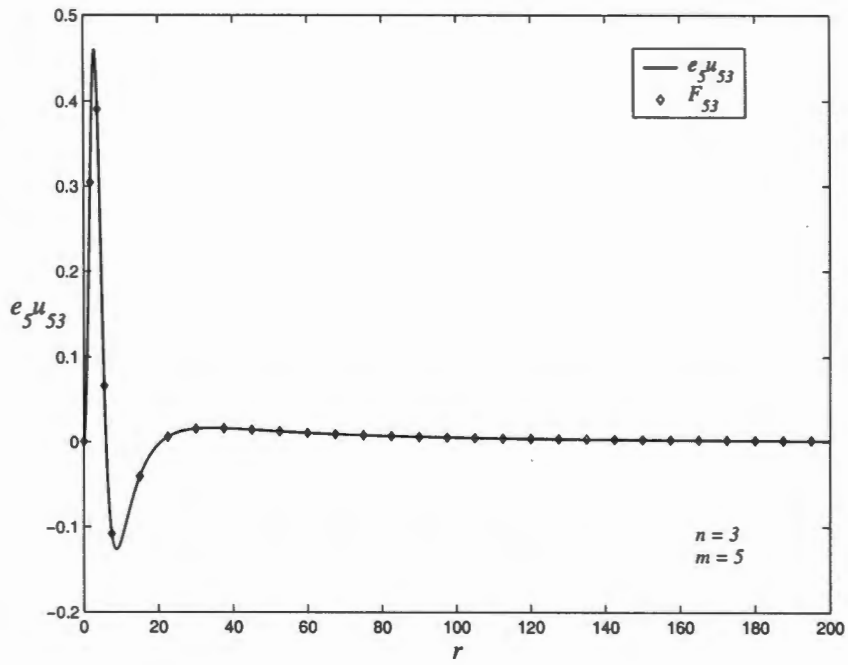


Figure 3.30: $e_5^u_{53}$ and F_{53} as functions of r

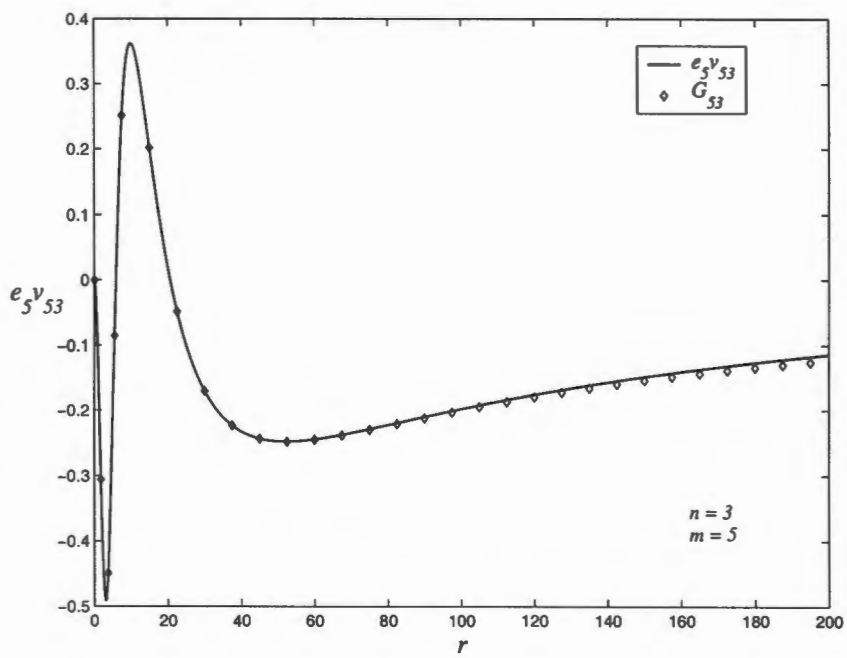


Figure 3.31: $e_5^v_{53}$ and G_{53} as functions of r

3.4 Summary

One of the most important results of this chapter is that the coaxial multivortices Ψ_1 , Ψ_2 and Ψ_3 belong to a family of solutions which depends on an infinite number of continuous parameters. This follows from the fact that the zero eigenvalue ($\omega^2 = 0$) belongs to the continuous spectrum for all m , implying that there is at least one zero mode for each azimuthal quantum number m . Since there are an infinite number of values of m ($m = 0, 1, 2, \dots$), there are an infinite number of zero modes.

We confirmed that the zero mode for $m = 0$ corresponds to a global $U(1)$ degree of freedom and the two zero modes for $m = 1$ correspond to translational degrees of freedom. More importantly, we were able to show that for $m = 2$ to 5 the zero modes correspond to the continuous parameters of the non-coaxial vortices $\tilde{\Psi}_n$ [86]. We conjecture from these results that the family of solutions $\tilde{\Psi}_n$ is the largest continuous parameter family of solutions which have the coaxial vortices Ψ_n as members.

Chapter 4

Complex Sine-Gordon-2

In the previous chapter we analysed the zero modes of the complex sine-Gordon-1 model. This is an integrable complexification of the sine-Gordon model. In this chapter we analyse the zero modes of another integrable complexification of the sine-Gordon model, the complex sine-Gordon-2:

$$\nabla^2\psi + \frac{(\nabla\psi)^2\bar{\psi}}{2 - |\psi|^2} + \frac{1}{2}\psi(1 - |\psi|^2)(2 - |\psi|^2) = 0. \quad (4.1)$$

In particular we consider the zero modes of the coaxial multivortices. These coaxial multivortex solutions, obtained by Barashenkov and Pelinovsky in [67], are of the form

$$\psi = \sqrt{Q_n(r)}e^{in\theta}, \quad (4.2)$$

where the $Q_n(r)$ are rational functions and n is the vorticity (2). In this chapter we consider the single vortex and the coaxial double and triple vortices:

$$\begin{aligned} Q_1(r) &= \frac{r^2}{r^2 + 4}, & Q_2(r) &= \frac{r^4(r^2 + 24)^2}{r^8 + 64r^6 + 1152r^4 + 9216r^2 + 36864}, \\ Q_3(r) &= r^6(r^6 + 144r^4 + 5760r^2 + 92160)^2/\mathcal{D}, \\ \mathcal{D} &= r^{18} + 324r^{16} + 41472r^{14} + 2820096r^{12} + 114130944r^{10} + 2919628800r^8 \\ &\quad + 50960793600r^6 + 611529523200r^4 + 4892236185600r^2 + 19568944742400. \end{aligned} \quad (4.3)$$

The equation of motion for the complex sine-Gordon-2 model (4.1) is obtained from the action

$$\mathcal{S} = \int \left\{ \frac{|\nabla\psi|^2}{1 - \frac{1}{2}|\psi|^2} + \frac{1}{2}(1 - |\psi|^2)^2 \right\} d^2x. \quad (4.4)$$

The equation of motion (4.1) is the 2-dimensional Euclidean version of the (1+1)-dimensional model, which can be derived as the bosonic limit of a generalised supersymmetric sine-Gordon equation [101]. The (1+1)-dimensional complex sine-Gordon-2 model was also derived in [102] and its Lax representation found, thereby showing that it is an integrable theory. This model, like the complex sine-Gordon-1 model [95, 96], arises as a reduction of the $SU(2)_N$ gauged Wess-Zumino-Witten model perturbed by a

multiplet of primary fields, in this case $\Phi^{(2)}$ [103]. Also, like the complex sine-Gordon-1, the (1+1)-dimensional complex sine-Gordon-2 reduces to the real sine-Gordon by making the substitution $\psi = \sin(\alpha/2)$ and performing some rescalings.

In order to study the zero modes we consider a (2+1)-dimensional generalisation of (4.1)

$$\psi_{tt} - \nabla^2 \psi - \frac{(\nabla \psi)^2 \bar{\psi}}{2 - |\psi|^2} - \frac{1}{2} \psi (1 - |\psi|^2)(2 - |\psi|^2) = 0. \quad (4.5)$$

Note that this is not Lorentz invariant and as such negative eigenvalues of the associated linearised operator will have no physical relevance. We now continue with the analysis of the zero modes.

4.1 Linearisation

For this model we follow the formalism set out in the previous two chapters. Since most of the details have been dealt with before, we will be fairly concise. However, those interested in seeing more detail are referred to chapters 2 and 3.

Linearising the equation of motion (4.5) about the coaxial multivortex Ψ_n , we obtain

$$\begin{aligned} \delta\psi_{tt} - \nabla^2 \delta\psi - \frac{2\nabla\Psi_n\bar{\Psi}_n}{5 - |\Psi_n|^2} \cdot \nabla(\delta\psi) - \left[\frac{2(\nabla\Psi_n)^2}{(2 - |\Psi_n|^2)^2} - \frac{1}{2}\Psi_n^2(3 - 2|\Psi_n|^2) \right] \delta\bar{\psi} \\ - \left[\frac{(\nabla\Psi_n)^2\bar{\Psi}_n}{(2 - |\Psi_n|^2)^2} + \frac{1}{2}(3|\Psi_n|^4 - 6|\Psi_n|^2 + 2) \right] \delta\psi = 0, \end{aligned} \quad (4.6)$$

for the perturbation $\delta\psi$. Then using $\Psi_n = \sqrt{Q_n}e^{in\theta}$ and letting $\delta\psi = \varphi(r, \theta)e^{in\theta} \cos \omega t$, transforms this equation to

$$-\partial_r^2 \varphi + B_n(r)\partial_r \varphi - \frac{1}{r^2}\partial_\theta^2 \varphi - iA_n(r)\partial_\theta \varphi + C_n(r)\varphi + D_n(r)\bar{\varphi} = \omega^2 \varphi, \quad (4.7)$$

where

$$\begin{aligned} A_n(r) &= \frac{4n}{r^2} \frac{1}{2 - Q_n}, \\ B_n(r) &= -\frac{1}{r} - \frac{Q'_n}{2 - Q_n}, \\ C_n(r) &= \frac{\frac{16n^2}{r^2} - (Q'_n)^2}{4(2 - Q_n)^2} - \frac{1}{2}(2 - 6Q_n + 3Q_n^2), \\ D_n(r) &= \frac{\frac{4n^2}{r^2}Q_n^2 - (Q'_n)^2}{2Q_n(2 - Q_n)^2} + \frac{1}{2}Q_n(3 - 2Q_n), \end{aligned} \quad (4.8)$$

and the prime denotes the derivative with respect to r . As previously, we will refer to (4.7) as the eigenvalue problem for the complex eigenfunction φ . Note, that it is actually (4.7) along with its complex conjugate that form an eigenvalue problem for the vector $(\varphi, \bar{\varphi})^T$.

Next we expand φ in the Fourier series in θ :

$$\varphi(r, \theta) = \phi_0(r) + \sum_{m=1}^{\infty} \left\{ \phi_m(r) e^{im\theta} + \phi_{-m}(r) e^{-im\theta} \right\}, \quad (4.9)$$

where $\phi_m = \{f_m(r) + ig_m(r)\}$ and $f_m(r)$ and $g_m(r)$ are real functions. We then substitute this expansion into (4.7), like harmonics and separate into real and imaginary parts. This procedure yields two sets of coupled differential eigenvalue problems:

$$\left[-\frac{d^2}{dr^2} + B_n(r) \frac{d}{dr} + \frac{m^2}{r^2} + C_n(r) \right] f_m + mA_n(r)f_m + D_n(r)f_{-m} = \omega^2 f_m, \quad (4.10a)$$

$$\left[-\frac{d^2}{dr^2} + B_n(r) \frac{d}{dr} + \frac{m^2}{r^2} + C_n(r) \right] f_{-m} - mA_n(r)f_{-m} + D_n(r)f_m = \omega^2 f_{-m}, \quad (4.10b)$$

and

$$\left[-\frac{d^2}{dr^2} + B_n(r) \frac{d}{dr} + \frac{m^2}{r^2} + C_n(r) \right] g_m + mA_n(r)g_m - D_n(r)g_{-m} = \omega^2 g_m, \quad (4.11a)$$

$$\left[-\frac{d^2}{dr^2} + B_n(r) \frac{d}{dr} + \frac{m^2}{r^2} + C_n(r) \right] g_{-m} - mA_n(r)g_{-m} - D_n(r)g_m = \omega^2 g_{-m}. \quad (4.11b)$$

Thus, we can solve for the eigenfunctions of (4.7) by solving the eigenvalue problem*

$$\mathcal{L}_{mn} \begin{pmatrix} u_m \\ v_m \end{pmatrix} = \omega^2 \begin{pmatrix} u_m \\ v_m \end{pmatrix}, \quad (4.12)$$

for $m \geq 0$, where the operator \mathcal{L}_{mn} is defined as

$$\mathcal{L}_{mn} \equiv \begin{pmatrix} -\frac{d^2}{dr^2} + B_n(r) \frac{d}{dr} + \frac{m^2}{r^2} + C_n(r) + D_n(r) & mA_n(r) \\ mA_n(r) & -\frac{d^2}{dr^2} + B_n(r) \frac{d}{dr} + \frac{m^2}{r^2} + C_n(r) - D_n(r) \end{pmatrix}. \quad (4.13)$$

This is evident if we compare (4.10) and (4.11) to (3.9) and (3.17) in §3.1. Therefore two linearly independent, complex eigenfunctions to (4.12) are given by

$$\tilde{\varphi} = \left(\frac{u_m + v_m}{2} e^{im\theta} + \frac{u_m - v_m}{2} e^{-im\theta} \right) = u_m \cos m\theta + iv_m \sin m\theta, \quad (4.14a)$$

$$\hat{\varphi} = i \left(\frac{u_m + v_m}{2} e^{im\theta} - \frac{u_m - v_m}{2} e^{-im\theta} \right) = -u_m \sin m\theta + iv_m \cos m\theta, \quad (4.14b)$$

for azimuthal quantum numbers $m \geq 1$ and

$$\tilde{\varphi} = \left(\frac{u_0 + v_0}{2} + \frac{u_0 - v_0}{2} \right) = u_0, \quad (4.15a)$$

$$\hat{\varphi} = i \left(\frac{u_0 + v_0}{2} - \frac{u_0 - v_0}{2} \right) = iv_0, \quad (4.15b)$$

*Note that u_m and v_m carry a second, implicit index n . Its omission simplifies the notation

for the azimuthal quantum number $m = 0$. Similarly to the previous chapters, we can expect at most two zero modes for each azimuthal quantum number.

Since we expect a zero mode for the global $U(1)$ degree of freedom and two for the translational degrees of freedom, we would like to know which azimuthal quantum numbers these zero modes correspond to. The zero mode from the global $U(1)$ degree of freedom is $\delta\psi = i\sqrt{Q_n(r)}e^{in\theta}$, therefore $\varphi = i\sqrt{Q_n(r)}$ and it corresponds to the azimuthal quantum number $m = 0$. For the translational degrees of freedom the zero modes are

$$\begin{aligned}\partial_x[\sqrt{Q_n(r)}e^{in\theta}] &= \left[\frac{Q'_n}{2\sqrt{Q_n}}\partial_x r + in\sqrt{Q_n}\partial_x\theta \right] e^{in\theta} \\ &= - \left[-\frac{Q'_n}{2\sqrt{Q_n}}\cos\theta + i\frac{n\sqrt{Q_n}}{r}\sin\theta \right] e^{in\theta},\end{aligned}\quad (4.16a)$$

for the x direction and

$$\begin{aligned}\partial_y[\sqrt{Q_n(r)}e^{in\theta}] &= \left[\frac{Q'_n}{2\sqrt{Q_n}}\partial_y r + in\sqrt{Q_n}\partial_y\theta \right] e^{in\theta} \\ &= \left[\frac{Q'_n}{2\sqrt{Q_n}}\sin\theta + i\frac{n\sqrt{Q_n}}{r}\cos\theta \right] e^{in\theta},\end{aligned}\quad (4.16b)$$

for the y direction. By comparing this with (4.14) it is clear that these two zero modes correspond to the azimuthal quantum number $m = 1$: $u_1 = -\frac{Q'_n}{2\sqrt{Q_n}}$ and $v_1 = \frac{n\sqrt{Q_n}}{r}$. This we is expected from the analysis of the Ginzburg-Landau and the complex sine-Gordon-1.

Although it is useful to know which azimuthal quantum numbers the global $U(1)$ degree of freedom and translational degrees of freedom correspond to, these are not the most important questions for us. What interests us most is whether there are any other zero modes. If there are, then it might be possible to split the multivortices.

Even though the coefficients (4.8) of the eigenvalue problem (4.12) are rational functions it would most likely prove very difficult to solve analytically. Also these rational functions become complicated very quickly as the vorticity n increases. Thus, we will solve the eigenvalue problem (4.8) numerically. While solving the system we need to impose boundary conditions. Therefore, we need to analyse the asymptotic behaviour of the eigenfunctions. Note that the previously implicit index is now made explicit: $u_m \rightarrow u_{mn}$ and $v_m \rightarrow v_{mn}$, so as to make it easier to distinguish between the solutions for the various vortices when presenting the results.

4.2 Asymptotic Behaviour of Zero Modes

4.2.1 Asymptotics for small r

For small r we assume an expansion of the form

$$\begin{aligned}u_{mn} &= r^p [(u_0r + u_1r^1 + u_2r^2 + \dots) + \ln r(u'_0r + u'_1r^1 + u'_2r^2 + \dots)] \\ v_{mn} &= r^p [(v_0r + v_1r^1 + v_2r^2 + \dots) + \ln r(v'_0r + v'_1r^1 + v'_2r^2 + \dots)],\end{aligned}\quad (4.17)$$

where p is a real constant. We then substitute this expansion along with the Taylor expansions for the coefficients (4.8) into the eigenvalue problem (4.12). The Taylor expansions for the coefficients,

$$\begin{aligned} A_n(r) &= \frac{2n}{r^2} + \frac{n}{(2^n n!)^2} r^{2n-2} + \mathcal{O}(r^{2n}), \\ B_n(r) &= -\frac{1}{r} - \frac{n}{(2^n n!)^2} r^{2n-1} + \mathcal{O}(r^{2n+1}), \\ C_n(r) &= \frac{n^2}{r^2} - 1 + \frac{n^2}{(2^n n!)^2} r^{2n-2} + \mathcal{O}(r^{2n}), \\ D_n(r) &= \mathcal{O}(r^{2n}), \end{aligned}$$

follow from the Taylor expansion[†] for Q_n ;

$$Q_n(r) = \frac{r^{2n}}{(2^n n!)^2} \left[1 - \frac{r^2}{2(n+1)} + \mathcal{O}(r^4) \right]. \quad (4.18)$$

After substituting, we then collect terms of like powers of r to obtain constraints on the coefficients in the expansion for u_{mn} and v_{mn} .

It is interesting that up to and including terms $\mathcal{O}(r^{p-1})$, the expansion of (4.12) is identical to that of the Ginzburg-Landau model (§2.2.1) and the complex sine-Gordon-1 (§3.2.1). Therefore, following the formalism in §2.2.1, we know that the eigenfunctions of (4.12) obey the following four linearly independent behaviours as $r \rightarrow 0$:

$$\begin{aligned} Z_1 &= r^{n+m} [1 + o(r)] \begin{pmatrix} 1 \\ 1 \end{pmatrix}; & Z_2 &= r^{-|n-m|} [1 + o(r)] \begin{pmatrix} 1 \\ -1 \end{pmatrix}; \\ Z_3 &= r^{-(n+m)} [1 + o(r)] \begin{pmatrix} 1 \\ 1 \end{pmatrix}; \\ Z_4 &= r^{|n-m|} [1 + o(r)] \begin{pmatrix} 1 \\ -1 \end{pmatrix}; & m &\neq n \\ Z_4 &= \ln r [1 + o(r)] \begin{pmatrix} 1 \\ -1 \end{pmatrix}, & m &= n \end{aligned} \quad (4.19)$$

where the notation $Z = (u_m, v_m)^T$ has been used. It is clear from these that Z_3 and Z_4 are not bounded while Z_1 and Z_2 are.

From the behaviours Z_1 and Z_2 , we infer the following boundary conditions. For $m \neq n \pm 1$ the first derivatives of the components $u_{mn}(r)$ and $v_{mn}(r)$ are equated to zero at the origin:

$$\frac{d}{dr} u_{mn}(0) = \frac{d}{dr} v_{mn}(0) = 0, \quad m \neq n \pm 1. \quad (4.20a)$$

[†]This general expansion was determined from the expansions of Q_1 , Q_2 and Q_3 . Therefore we can only guarantee that this expansion holds for the vorticities $n = 1, 2$ and 3 .

This is allowed as u and v are proportional to r only when $m = n \pm 1$. When $m = n \pm 1$, we equate the components themselves to zero:

$$u_{n\pm 1,n}(0) = v_{n\pm 1,n}(0) = 0, \quad m = n \pm 1. \quad (4.20b)$$

These boundary conditions reduce the chance that the numerics yield "false" solutions. Now that we know the boundary conditions at $r = 0$ we will consider the asymptotic behaviours for large r .

4.2.2 Asymptotics for large r

By considering the eigenvalue problem (4.12) for large r it is easy to see that the eigenvalues $\omega^2 > 0$ belong to the continuous spectrum. But is $\omega^2 = 0$ part of the continuous spectrum, in other words, does the zero eigenvalue exist? If the answer is yes, for all m , then we know immediately that, as for the complex sine-Gordon-1, there are an infinite number of zero modes. It is in trying to answer this question as well as determining the boundary conditions, that we consider the asymptotic behaviour of the eigenfunctions for large r .

Firstly, we assume an expansion for u_{mn} and v_{mn} of the form

$$\begin{aligned} u_{mn} &= \Re \left\{ e^{ikr} r^p \left[\left(u_0 + \frac{u_1}{r} + \frac{u_2}{r^2} + \frac{u_3}{r^3} + \dots \right) + \ln r \left(\frac{u'_1}{r} + \frac{u'_2}{r^2} + \frac{u'_3}{r^3} \dots \right) \right] \right\}, \\ v_{mn} &= \Re \left\{ e^{ikr} r^p \left[\left(v_0 + \frac{v_1}{r} + \frac{v_2}{r^2} + \frac{v_3}{r^3} + \dots \right) + \ln r \left(\frac{v'_1}{r} + \frac{v'_2}{r^2} + \frac{v'_3}{r^3} \dots \right) \right] \right\}, \end{aligned} \quad (4.21)$$

where $p, k, u_j, v_j, u'_j, v'_j \in \mathbb{C}$. We then substitute these, together with the asymptotic expansions of the coefficients (4.8);

$$\begin{aligned} A_n(r) &= \frac{4n}{r^2} - \frac{16n^3}{r^4} + \frac{64n^3(3n^2 - 1)n}{r^6} + \mathcal{O}(r^{-8}), \\ B_n(r) &= -\frac{1}{r} - \frac{8n^2}{r^3} + \frac{32n^2(5n^2 - 1)}{r^5} + \mathcal{O}(r^{-7}), \\ C_n(r) &= \frac{1}{2} + \frac{4n^2}{r^2} - \frac{56n^4}{r^4} + \mathcal{O}(r^{-6}), \\ D_n(r) &= \frac{1}{2} + \frac{4n^2}{r^2} - \frac{8n^2(7n^2 - 1)}{r^4} + \mathcal{O}(r^{-6}), \end{aligned} \quad (4.22)$$

into the eigenvalue problem (4.12). The behaviours of the coefficients are determined from the behaviour[†] of $Q_n(r)$:

$$Q_n(r) = 1 - \frac{4n^2}{r^2} + \frac{16n^2(2n^2 - 1)}{r^4} + \mathcal{O}(r^{-6}). \quad (4.23)$$

Once we have substituted the various behaviours into the eigenvalue problem we collect terms of like powers of r , obtaining constraints for the coefficients and constants

[†]Again, we only guarantee that this expansion holds for $n = 1, 2$ and 3 .

in (4.21). The constraints obtained are as follows:

From the terms $\mathcal{O}(r^p)$,

$$\begin{aligned}(k^2 - \omega^2 + 1)u_0 &= 0, \\ (k^2 - \omega^2)v_0 &= 0,\end{aligned}\tag{4.24}$$

while the terms $\mathcal{O}(r^{p-1} \ln r)$ give

$$\begin{aligned}(k^2 - \omega^2 + 1)u'_1 &= 0, \\ (k^2 - \omega^2)v'_1 &= 0.\end{aligned}\tag{4.25}$$

From these two sets of equations it follows that there are two cases; either (a) $k^2 = \omega^2 - 1$, $v_0 = v'_1 = 0$ and u_0 and u'_1 are arbitrary or (b) $k^2 = \omega^2 - 1$, $u_0 = u'_1 = 0$ and v_0 and v'_1 are arbitrary. Before we consider these cases any further we note that the constraints obtained from higher order terms are as follows. We obtain from terms $\mathcal{O}(r^{p-1})$:

$$\begin{aligned}-i(2p+1)ku_0 + (k^2 - \omega^2 + 1)u_1 &= 0, \\ -i(2p+1)kv_0 + (k^2 - \omega^2)v_1 &= 0;\end{aligned}\tag{4.26}$$

$\mathcal{O}(r^{p-2} \ln r)$:

$$\begin{aligned}i(1-2p)ku'_1 + (k^2 - \omega^2 + 1)u'_2 &= 0, \\ i(1-2p)kv'_1 + (k^2 - \omega^2)v'_2 &= 0;\end{aligned}\tag{4.27}$$

$\mathcal{O}(r^{p-2})$:

$$\begin{aligned}(m^2 + 8n^2 - p^2)u'_0 + 4mnv_0 + i(1-2p)ku_1 - 2iku'_1 + (k^2 - \omega^2 + 1)u_2 &= 0, \\ 4mnu_0 + (m^2 - p^2)v_0 + i(1-2p)kv_1 - 2ikv'_1 + (k^2 - \omega^2)v_2 &= 0;\end{aligned}\tag{4.28}$$

$\mathcal{O}(r^{p-3} \ln r)$:

$$\begin{aligned}[m^2 + 8n^2 - (p-1)^2]u'_1 + 4mnv'_1 + i(3-2p)ku'_2 + (k^2 - \omega^2 + 1)u'_3 &= 0, \\ 4mnu'_1 + [m^2 - (p-1)^2]v'_1 + i(3-2p)kv'_2 + (k^2 - \omega^2)v'_3 &= 0;\end{aligned}\tag{4.29}$$

$\mathcal{O}(r^{p-3})$:

$$\begin{aligned}-8in^2ku_0 + [m^2 + 8n^2 - (p-1)^2]u_1 + 4mnv_1 \\ + 2(1-p)u'_1 - 2iku'_2 + i(3-2p)ku_2 + (k^2 - \omega^2 + 1)u_3 &= 0, \\ -8in^2kv_0 + 4mnu_1 + [m^2 - (p-1)^2]v_1 \\ + 2(1-p)v'_1 - 2ikv'_2 + i(3-2p)kv_2 + (k^2 - \omega^2)v_3 &= 0.\end{aligned}$$

First, we consider case (a). For this case equations (4.26) and (4.27), from terms $\mathcal{O}(r^{p-1})$ and $\mathcal{O}(r^{p-2} \ln r)$ reduce to

$$k(1 + 2p)u_0 = 0, \quad v_1 = 0,$$

and

$$k(1 - 2p)u'_1 = 0, \quad v'_2 = 0,$$

respectively. Thus for case (a) $v_1 = v'_2 = 0$. Since we are interested in zero modes, we need only consider values of $\omega^2 \ll 1$, which implies that $k \neq 0$. Therefore, terms $\mathcal{O}(r^{p-1})$ and $\mathcal{O}(r^{p-2} \ln r)$ yield two subcases; either (ai) $p = \frac{1}{2}$ and $u_0 = 0$ or (aii) $p = -\frac{1}{2}$ and $u'_1 = 0$. If we consider the case (ai), the terms $\mathcal{O}(r^{p-2})$ yield $u'_1 = 0$. Thus, for case (ai) we have $v_0 = v'_1 = u_0 = u'_1 = 0$ and hence it is *not* allowed.

However considering case (aii) for the higher order terms we find that the terms $\mathcal{O}(r^{p-2})$ yield

$$u_1 = \frac{4m^2 - 1 + 32n^2}{-8ik} u_0, \quad v_2 = 4mnu_0,$$

terms $\mathcal{O}(r^{p-3} \ln r)$ give

$$u'_2 = v'_3 = 0,$$

and finally terms $\mathcal{O}(r^{p-3})$ give

$$u_2 = \frac{4m^2 - 9 + 32n^2}{-16ik} u_1 + 2n^2 u_0, \quad v_3 = 4mnu_1 + 4ikv_2.$$

This implies that

$$Y_{3,4} = \frac{e^{\pm\sqrt{1-\omega^2}r}}{\sqrt{r}} \left(1 \pm \frac{4(m^2+8n^2)-1}{8\sqrt{1-\omega^2}r} + \mathcal{O}\left(\frac{1}{r^2}\right) \right) \left(\frac{4mn}{r^2} + \mathcal{O}\left(\frac{1}{r^3}\right) \right) \quad (4.30)$$

are two possible behaviours for the eigenfunctions of (4.12) for large r . Note that Y_3 is unbounded while Y_4 is bounded.

Next, we consider case (b). Recall that here $k^2 = \omega^2$ and $u_0 = u'_1 = 0$. Under these conditions, equations (4.26) and (4.27), from terms $\mathcal{O}(r^{p-1})$ and $\mathcal{O}(r^{p-2} \ln r)$, reduce to

$$u_1 = 0, \quad k(1 + 2p)v_0 = 0,$$

and

$$u'_2 = 0, \quad k(1 - 2p)v'_1 = 0,$$

respectively. This time three subcases emerge; either (bi) $p = \frac{1}{2}$ and $v_0 = 0$ or (bii) $p = -\frac{1}{2}$ and $v'_1 = 0$ else (biii) $k = 0$. For the first of these three, case (bi), the terms $\mathcal{O}(r^{p-2})$ give $v'_1 = 0$. Hence case (bi) is not allowed; $u_0 = u'_1 = v_0 = v'_1 = 0$. However

considering higher order terms for case (bii) yields;
from terms $\mathcal{O}(r^{p-2})$:

$$u_2 = -4mnv_0, \quad v_1 = \frac{4m^2 - 1}{-8ik}v_0,$$

terms $\mathcal{O}(r^{p-3} \ln r)$:

$$u'_3 = v'_2 = 0,$$

and from terms $\mathcal{O}(r^{p-3})$:

$$u_3 = -4mnv_1 - 4iku_2, \quad v_2 = \frac{4m^2 - 9}{-16ik}v_1 + 2n^2v_0.$$

It follows from these results that the two behaviours

$$Y_{1,2} = \Re \left\{ \frac{e^{\pm i\omega r}}{\sqrt{r}} \left(1 \pm \frac{4m^2 - 1}{8\omega r} + \mathcal{O}\left(\frac{1}{r^2}\right) \right) \right\} \quad (4.31)$$

are allowed for $k = \pm\omega \neq 0$. Finally, consider the case (biii), in other words $k = \omega = 0$. For this case the terms $\mathcal{O}(r^{p-2})$ give the constraints

$$\begin{aligned} 4mnv_0 + u_2 &= 0, \\ (m^2 - p^2)v_0 &= 0. \end{aligned}$$

Thus, either $p = \pm m$ or $v_0 = 0$. If $p = \pm m$ then the terms $\mathcal{O}(r^{p-3} \ln r)$ reduce to

$$\begin{aligned} 4mnv'_1 + u'_3 &= 0, \\ (\pm 2m - 1)v'_1 &= 0, \end{aligned}$$

implying $u'_3 = v'_1 = 0$, as m is integer. Also the terms $\mathcal{O}(r^{p-3})$ give $u_3 = v_1 = 0$. However, if $v_0 = 0$ then $u_2 = 0$ and the terms $\mathcal{O}(r^{p-3} \ln r)$ reduce to

$$\begin{aligned} 4mnv'_1 + u'_3 &= 0, \\ [m^2 - (p - 1)^2]v'_1 &= 0. \end{aligned}$$

Since we already have $u_0 = u'_1 = v_0 = 0$, we must have $p = \pm m + 1$ for these conditions to be satisfied. When $p = \pm m + 1$, the terms $\mathcal{O}(r^{p-3})$ give

$$\begin{aligned} 4mnv_1 + u_3 &= 0, \\ mv'_1 &= 0, \end{aligned}$$

implying that $m = 0$ and hence $p = 1$. Thus we have the following asymptotic behaviours for $k = \omega = 0$:

$$Y_{1,2} = r^{\pm m} \begin{pmatrix} -\frac{4mn}{r^2} + \mathcal{O}\left(\frac{1}{r^4}\right) \\ 1 + \mathcal{O}\left(\frac{1}{r^2}\right) \end{pmatrix} \quad m \neq 0 \quad (4.32a)$$

$$Y_1 = \ln r [1 + \mathcal{O}\left(\frac{1}{r^2}\right)] \begin{pmatrix} 0 \\ 1 \end{pmatrix}; \quad Y_2 = [1 + \mathcal{O}\left(\frac{1}{r^2}\right)] \begin{pmatrix} 0 \\ 1 \end{pmatrix} \quad m = 0. \quad (4.32b)$$

Note that the asymptotic solution Y_1 is *unbounded* while Y_2 is bounded.

One of the reasons for analysing the asymptotic behaviour for large r was to determine the boundary condition at the right-hand boundary ($r = R$). And the following boundary conditions for eigenfunctions of (4.12) are inferred from the behaviours $Y_{1,2,3,4}$: At the right hand boundary ($r = R$) the derivatives of the components are set to zero:

$$\frac{d}{dr}u_{mn}(R) = \frac{d}{dr}v_{mn}(R) = 0, \quad (4.33)$$

for all m and n .

Another reason for analysing the asymptotic behaviour was to try to ascertain whether the zero eigenvalue ($\omega^2 = 0$) exists. For answer this, notice that the asymptotics for small and large radii are very similar to those of the Ginzburg-Landau model. In other words, there are two solutions which are bounded at the origin ($Z_{1,2}$) and two which are not ($Z_{3,4}$). Also there are two solutions which are bounded ($Y_{2,4}$) and two which are not ($Y_{1,3}$), as $r \rightarrow \infty$. Therefore, as was the case for the Ginzburg-Landau theory, we can not determine, simply, from the asymptotics whether the eigenvalue $\omega^2 = 0$ exists.

A useful byproduct of the asymptotic analysis is a means of distinguishing between zero modes and eigenfunctions corresponding to small positive eigenvalues. Recall that the numerics do not obtain the zero eigenvalue exactly but a value within a small neighbourhood of zero. Notice that zero modes will display the behaviour Y_2 in (4.32) while those corresponding to small positive eigenvalues will display the behaviour Y_2 in (4.31).

Now that the appropriate boundary conditions have been selected, we can continue with the numerical computations.

4.3 Numerical Calculations

Since the eigenvalue problem (4.12) contains first derivatives the matrix eigenvalue problem, obtained by discretising[†] the system, will be non-symmetric. This unfortunately means that we must use the less optimised routines to solve the system. However, in certain circumstances we can make use of a transformation to convert our system to a symmetric matrix eigenvalue problem. This is done by implementing a transformation which eliminates the first derivatives. Thus, the transformation needed is an integrating factor;

$$\eta_{mn} = u_{mn}e^{-\frac{1}{2}\int B_n(r)dr}, \quad \zeta_{mn} = v_{mn}e^{-\frac{1}{2}\int B_n(r)dr}, \quad (4.34)$$

which has the simple form;

$$e^{-\frac{1}{2}\int B_n(r)dr} = \frac{\sqrt{r}}{\sqrt{2-Q(r)}}. \quad (4.35)$$

With this transformation the eigenvalue problem (4.12) transforms to

$$\begin{pmatrix} \mathcal{P}_n + D_n(r) & mA_n(r) \\ mA_n(r) & \mathcal{P}_n - D_n(r) \end{pmatrix} \begin{pmatrix} \eta_{mn} \\ \zeta_{mn} \end{pmatrix} = \omega^2 \begin{pmatrix} \eta_{mn} \\ \zeta_{mn} \end{pmatrix}, \quad (4.36)$$

[†]We discretise the system using a second order finite difference scheme. Appendix A

where

$$\mathcal{P}'_n \equiv -\frac{d^2}{dr^2} + \left[\frac{1}{4}B_n^2(r) - \frac{1}{2}\frac{dB_n(r)}{dr} + \frac{m^2}{r^2} + C_n(r) \right]. \quad (4.37)$$

Since this eigenvalue problem has no first derivatives of η or ζ the corresponding matrix eigenvalue problem will be symmetric, enabling us to implement faster numerical routines while solving the system. The original vector $(u_{mn}, v_{mn})^T$ is then obtained via the inverse transformation. As mentioned earlier the transformation can only be used for certain azimuthal quantum numbers m and vortices n . If $m = n$ or $m = 0$, then the transformation does not work, as we now explain.

First, let $m = n$. Note that the integrating factor behaves as $\frac{\sqrt{r}}{\sqrt{2}}$ as $r \rightarrow 0$. Now, since the components u_{nn} and v_{nn} may approach a constant as $r \rightarrow 0$ (4.19), the corresponding η_{mn} and ζ_{mn} may go to zero as $c_1\sqrt{r}$, for some constant c_1 . This behaviour creates large errors in the numerical calculations as the derivatives blow up at the origin. Hence, the transformation cannot be used when $m = n$.

The other case where the transformation does not work is, $m = 0$. As $r \rightarrow \infty$, the integrating factor (4.35) grows as \sqrt{r} . And since the component v_{0n} ($m = 0$) goes to constant as $r \rightarrow \infty$, the corresponding ζ_{0n} will grow as \sqrt{r} . The problem arises from the fact that we have to implement homogeneous boundary conditions in the numerics and the boundary $\zeta_{0n} \sim \sqrt{r}$ condition can't be written as a homogeneous boundary condition.

When it is possible to exploit this transformation we implement the following boundary conditions in the numerics: At the origin we set η_{mn} and ζ_{mn} to zero:

$$\eta_{mn}(0) = \zeta_{mn}(0) = 0, \quad (4.38)$$

while at the right hand boundary, their first derivatives are set to zero:

$$\frac{d}{dr}\eta_{mn}(R) = \frac{d}{dr}\zeta_{mn}(R) = 0. \quad (4.39)$$

These boundary conditions follow from the behaviours of the components u_{mn} , v_{mn} (4.19), (4.30), (4.31), (4.32) and the asymptotic behaviour of the integrating factor.

While solving for the eigenvalues numerically we follow the following strategy: If $m \neq n$ and $m \neq 0$, we solve the symmetric matrix eigenvalue problem obtained from (4.36) using a step size $\Delta r = 0.05$ over a domain length $R = 200$ and use the inverse transformation to get the corresponding u_{mn} and v_{mn} (i.e. a grid of 4000 points is used). If, however, $m = n$ or $m = 0$ then we solve the non-symmetric matrix eigenvalue problem obtained from (4.12), directly for u_{mn} and v_{mn} , with a step size $\Delta r = 0.1$ over a domain length $R = 160$ (i.e. we use a grid with 1600 points).

We will now present the results using the same layout as used for the complex sine-Gordon-1 model. First we discuss the azimuthal quantum number $m = 0$ and then the azimuthal quantum number $m = 1$ for the three vorticities ($n = 1, 2, 3$). Thereafter we consider each vortex separately for azimuthal quantum numbers $2 \leq m \leq 5$.

4.3.1 Azimuthal quantum number $m = 0$

As mentioned earlier we are unable to take advantage of the transformation (4.34) when $m = 0$ and have to solve the non-symmetric matrix eigenvalue problem obtained from (4.12). The four smallest eigenvalues computed for each vortex are given in Table 4.1. When the components u_{0n} , corresponding to these eigenvalues are examined, we find that they are identically zero. However, when we examine the components v_{0n} , corresponding to the smallest of these eigenvalues (ω_0^2), we find $v_{0n} \propto \sqrt{Q_n}$ for each n . Thus we have at least one zero mode, $\hat{\varphi}_n = iv_{0n}$, for each vortex. A graph of the component v_{0n} associated with ω_0^2 is given in Fig. 4.1, for each n .

n	ω_0^2	ω_1^2	ω_2^2	ω_3^2
1	5.44×10^{-9}	5.79×10^{-4}	1.95×10^{-3}	4.10×10^{-3}
2	4.55×10^{-8}	5.88×10^{-4}	1.98×10^{-3}	4.18×10^{-3}
3	1.08×10^{-7}	5.99×10^{-4}	2.02×10^{-3}	4.26×10^{-3}

Table 4.1: Table of the four smallest eigenvalues (ω^2) for azimuthal quantum number $m = 0$.

Examining the components v_{0n} corresponding to eigenvalues ω_1^2 , ω_2^2 and ω_3^2 , we observe that they display the asymptotic behaviours associated not with zero modes (4.32), but eigenfunctions associated with small positive eigenvalues (4.31). Therefore, there is only one zero mode with azimuthal quantum number $m = 0$ for each vortex. This zero mode corresponds to the global $U(1)$ symmetry of the vortices, as is expected.

Next we consider the results for azimuthal quantum number $m = 1$ for the three vortices.

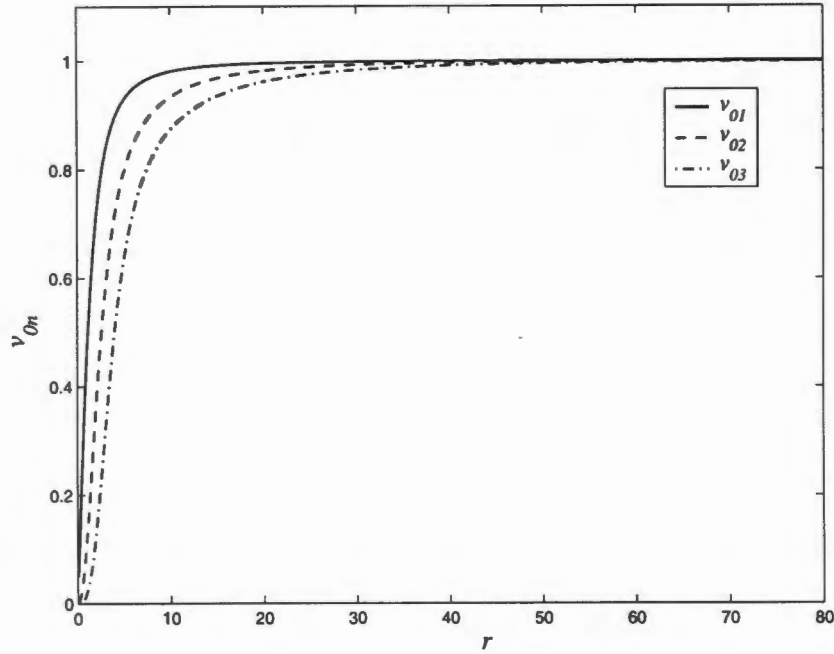


Figure 4.1: v_{01} , v_{02} and v_{03} as functions of r

4.3.2 Azimuthal quantum number $m = 1$

For the single vortex we have to solve the non-symmetric eigenvalue problem (4.12) as $m = n = 1$ in this case. However, for the coaxial double- and triple-vortices we are able to make use of the transformation (4.34) and may take advantage of the symmetric eigenvalue problem (4.36). The four smallest eigenvalues for the three vortices are given in Table 4.2.

n	ω_0^2	ω_1^2	ω_2^2	ω_3^2
1	-4.52×10^{-5}	2.10×10^{-4}	1.35×10^{-3}	3.27×10^{-3}
2	-7.90×10^{-6}	1.84×10^{-4}	9.28×10^{-4}	2.19×10^{-3}
3	-5.22×10^{-6}	1.97×10^{-4}	9.63×10^{-4}	2.25×10^{-3}

Table 4.2: Table of the four smallest eigenvalues (ω^2) for azimuthal quantum number $m = 1$.

The graphs of the components u_{1n} and v_{1n} corresponding to the smallest eigenvalues (ω_0^2) are given in Figs. 4.2-4.3, Figs. 4.4-4.5 and Figs. 4.6-4.7 for vorticities $n = 1, 2$ and 3, respectively. These components clearly display the asymptotic behaviours (4.32) associated with the zero eigenvalue ($\omega^2 = 0$). Thus we have two zero modes; $\tilde{\varphi}_{1n} = u_{1n} \cos \theta + iv_{1n} \sin \theta$ and $\hat{\varphi}_{1n} = -u_{1n} \cos \theta + iv_{1n} \sin \theta$ (4.14), with azimuthal quantum

number $m = 1$ for each vortex. Recall that there may be at most two zero modes for each m and n . This is confirmed when we consider the components corresponding to eigenvalues $\omega^2 > \omega_0^2$, as these components display the behaviours (4.31) associated with small, positive eigenvalues.

As is the case with the previous two models these zero modes correspond to the two translational degrees of freedom. This is supported by the comparison of the graphs of $\frac{Q'_n}{2\sqrt{Q_n}}$ and $\frac{nQ_n}{r}$ to normalised graphs of u_{1n} and v_{1n} , respectively (Figs 4.2-4.7). Recall that if these are the same then the zero modes correspond to the translational degrees of freedom (4.16). Note that for each vortex, u_{1n} and v_{1n} are normalised using the same normalisation constant.

Now that we have found the zero modes we were expecting we would like to know whether any other zero modes exist. We continue with the results for the single vortex ($n = 1$) for azimuthal quantum numbers $2 \leq m \leq 5$.

4.3.3 Excitations of the single vortex with azimuthal quantum numbers $2 \leq m \leq 5$

For all the azimuthal quantum numbers considered here we are able to implement the transformation (4.34) and solve the symmetric eigenvalue problem (4.36). The four smallest eigenvalues for each azimuthal quantum number are given in Table 4.3

m	ω_0^2	ω_1^2	ω_2^2	ω_3^2
2	2.74×10^{-4}	1.15×10^{-3}	2.50×10^{-3}	4.35×10^{-3}
3	4.89×10^{-4}	1.63×10^{-3}	3.24×10^{-3}	5.34×10^{-3}
4	7.61×10^{-4}	2.18×10^{-3}	4.04×10^{-3}	6.39×10^{-3}
5	1.09×10^{-3}	2.80×10^{-3}	4.92×10^{-3}	7.51×10^{-3}

Table 4.3: Table of smallest eigenvalues (ω^2) for the single vortex ($n = 1$) for azimuthal quantum numbers $m = 2$ to 5.

When the components u_{m1} and v_{m1} are examined for these eigenvalues they are found to display the asymptotic behaviours associated with small positive eigenvalues: v_{m1} oscillates with amplitude $\sim \sqrt{r}$ and $u_{m1} \rightarrow -4mv_{m1}/r^2$, as $r \rightarrow \infty$ (4.31). Therefore they are not zero modes. Hence, there are no zero modes for azimuthal quantum numbers $2 \leq m \leq 5$ for the single vortex. We conjecture that there are in fact no zero modes for the single vortex with azimuthal quantum number greater than 1.

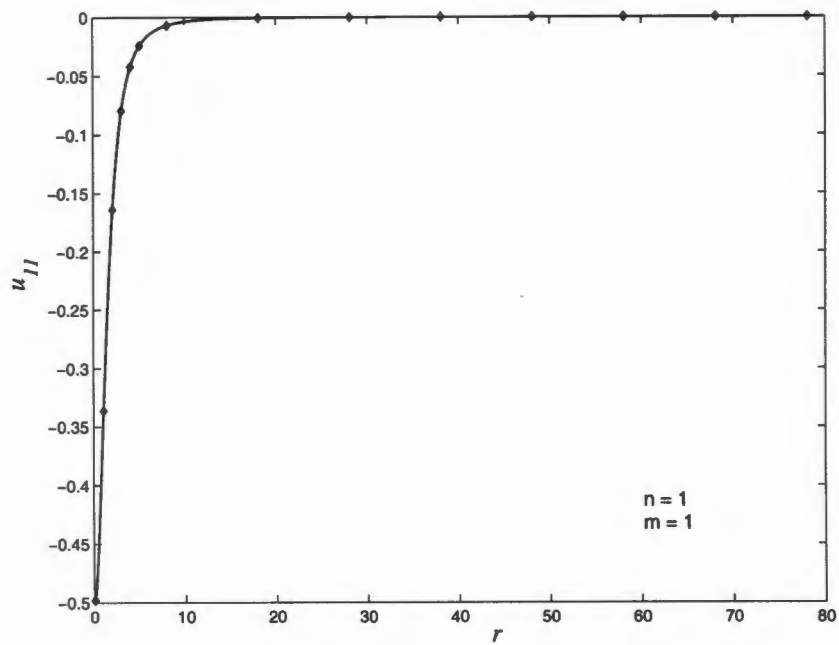


Figure 4.2: u_{11} (solid line) and $-\frac{Q'_1}{2\sqrt{Q_1}}$ (\diamond) as functions of r (Numerical calculation with $R = 160$)

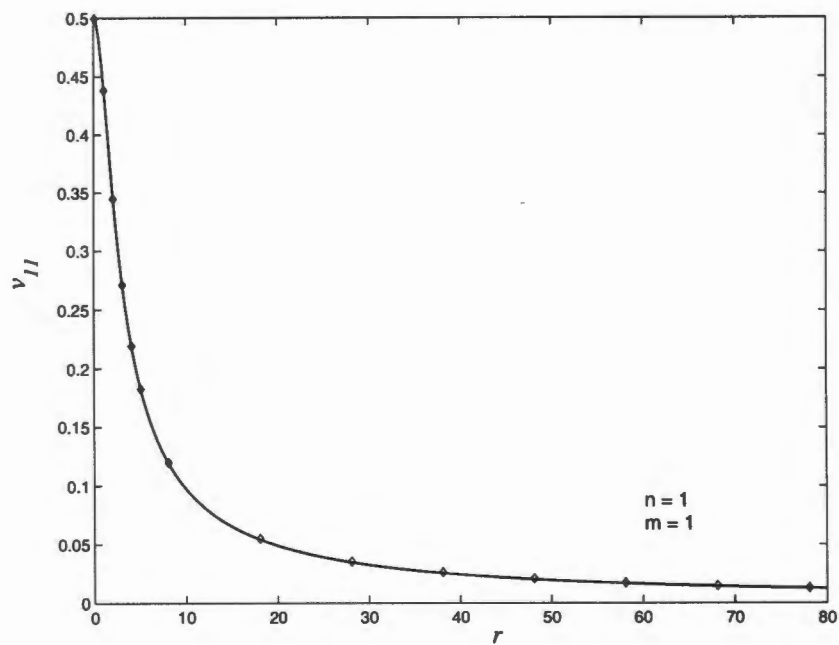


Figure 4.3: v_{11} (solid line) and $\frac{\sqrt{Q_1}}{r}$ (\diamond) as functions of r (Numerical calculation with $R = 160$)

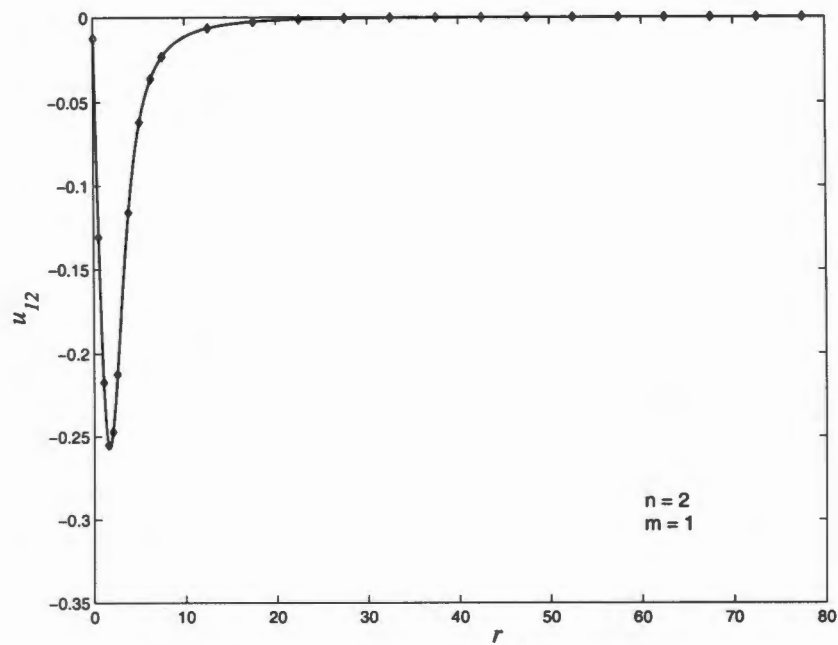


Figure 4.4: u_{12} (solid line) and $-\frac{Q'_2}{2\sqrt{Q_2}}$ (\diamond) as functions of r (Numerical calculation with $R = 200$)

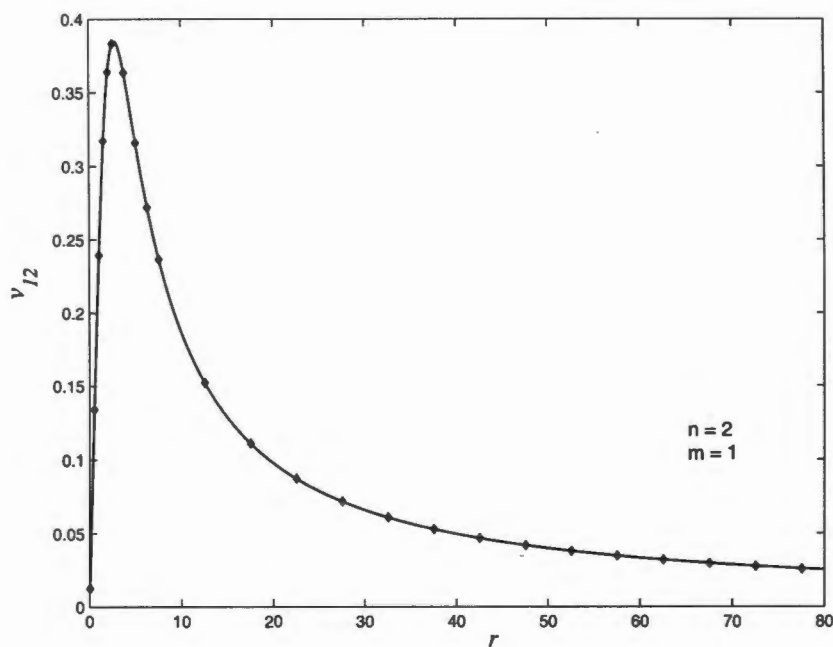


Figure 4.5: v_{12} (solid line) and $\frac{2\sqrt{Q_2}}{r}$ (\diamond) as functions of r (Numerical calculation with $R = 200$)

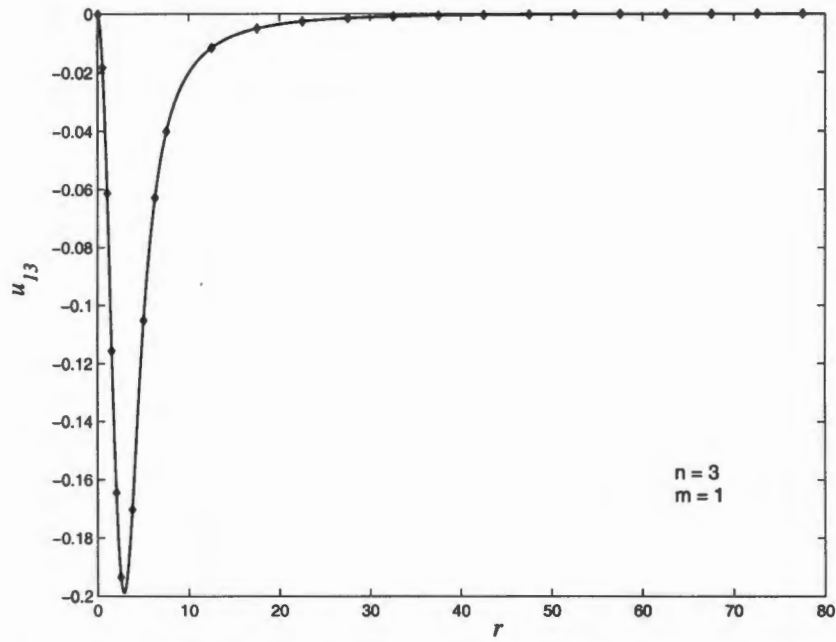


Figure 4.6: u_{13} (solid line) and $-\frac{Q'_3}{2\sqrt{Q_3}}$ as (\diamond) functions of r (Numerical calculation with $R = 200$)

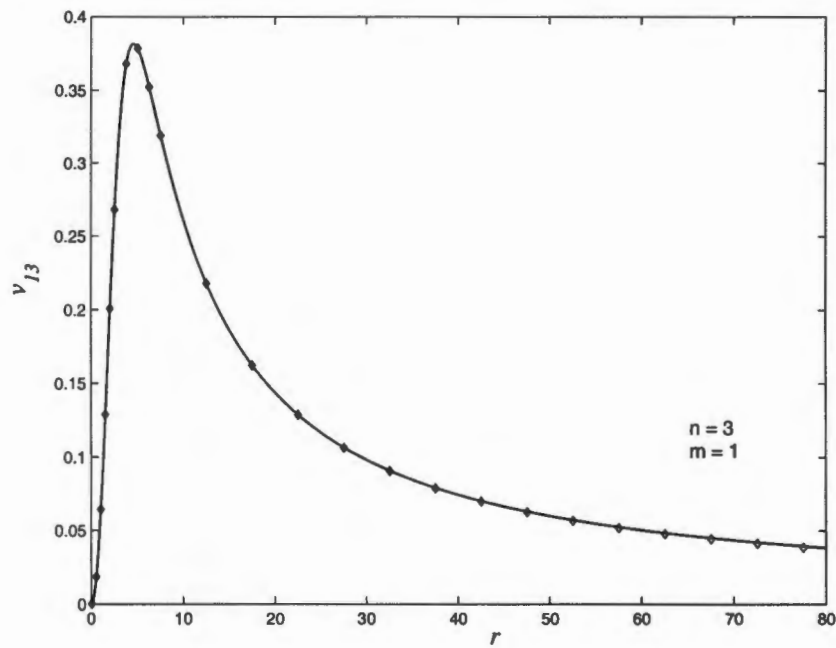


Figure 4.7: v_{13} (solid line) and $\frac{3\sqrt{Q_3}}{r}$ as (\diamond) functions of r (Numerical calculation with $R = 200$)

4.3.4 Excitations of the coaxial double-vortex with azimuthal quantum numbers $2 \leq m \leq 5$

For the coaxial double vortex we solve the non-symmetric eigenvalue problem (4.12) for $m = n = 2$ and the symmetric one for the other azimuthal quantum numbers. Again, the four smallest eigenvalues can be found in Table 4.4 for each azimuthal quantum number.

m	ω_0^2	ω_1^2	ω_2^2	ω_3^2
2	3.62×10^{-4}	1.74×10^{-3}	3.82×10^{-3}	6.63×10^{-3}
3	-6.19×10^{-5}	4.88×10^{-4}	1.63×10^{-3}	3.23×10^{-3}
4	7.60×10^{-4}	2.18×10^{-3}	4.03×10^{-3}	6.36×10^{-3}
5	1.09×10^{-3}	2.79×10^{-3}	4.90×10^{-3}	7.49×10^{-3}

Table 4.4: Table of smallest eigenvalues (ω^2) for the coaxial double-vortex ($n = 2$) for azimuthal quantum numbers $m = 2$ to 5.

When the components u_{m2} and v_{m2} for azimuthal quantum numbers $m = 2, 4$ and 5 are examined for the eigenvalues $\omega_{0,1,2,3}^2$, we observe that they display the asymptotics associated with small positive eigenvalues (4.31): v_{m2} oscillates with amplitude $\sim \sqrt{r}$ and $u_{m2} \rightarrow -8mv_{m2}/r^2$, as $r \rightarrow \infty$. Thus, there are no zero modes for these azimuthal quantum numbers for the coaxial double-vortex.

However, the components u_{32} and v_{32} ($m = 3$) corresponding to the eigenvalue ω_0^2 exhibit asymptotics which are associated with zero modes (see Figs. 4.9-4.10). Therefore, we have two zero modes $\tilde{\varphi}_{32}$ and $\hat{\varphi}_{32}$ with azimuthal quantum number $m = 3$. These are the only zero modes as the components corresponding to $\omega^2 > \omega_0^2$ obey the asymptotics associated with positive eigenvalues. Hence, the coaxial double-vortex has at least *two* zero modes other than the three expected zero modes. We speculate that these zero modes correspond to a solution with three vortices placed symmetrically about the origin and an anti-vortex at the origin, see Fig. 4.8

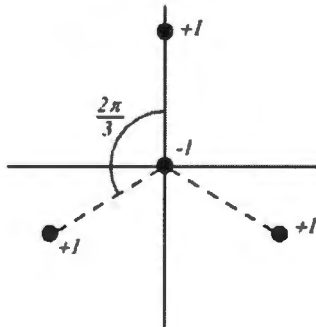


Figure 4.8: Suggested form of the multivortex configuration leading to the zero mode with azimuthal quantum number $m = 3$ for the two vortex ($n = 2$)

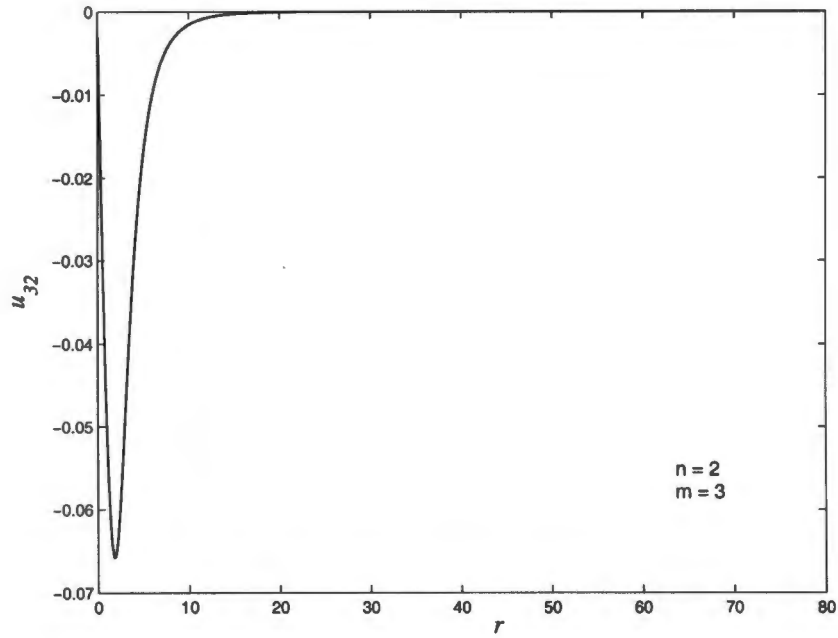


Figure 4.9: u_{32} as a function of r (Numerical calculation with $R = 200$)

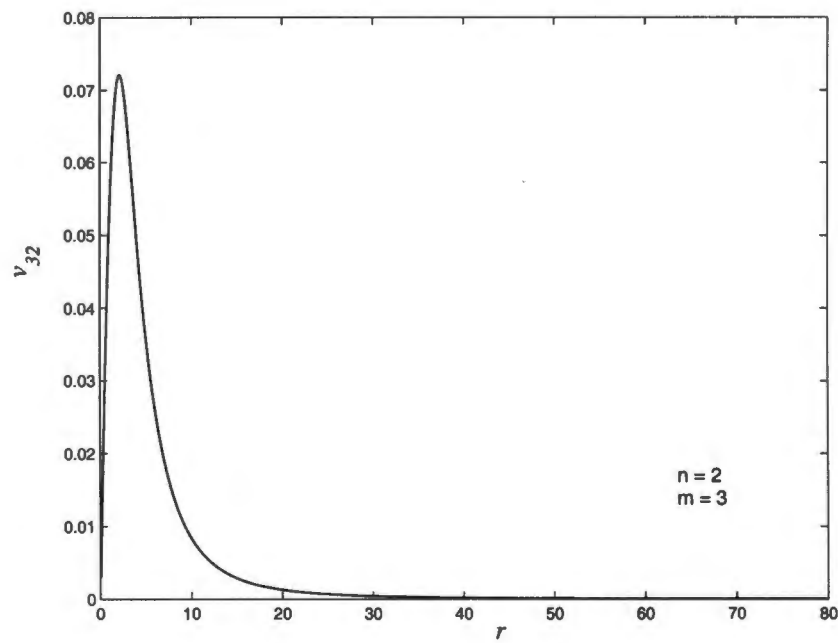


Figure 4.10: v_{32} as a function of r (Numerical calculation with $R = 200$)



Figure 4.11: Suggested forms for the multivortex configurations leading to the zero modes, for the three vortex ($n = 3$). (a) is the case for azimuthal quantum number $m = 3$ and (b) is for azimuthal quantum number $m = 5$.

4.3.5 Excitations of the coaxial triple-vortex with azimuthal quantum numbers $2 \leq m \leq 5$

The results of the coaxial triple-vortex are very similar to those of the coaxial double-vortex. As before, we solve the non-symmetric eigenvalue problem (4.12) when $m = n = 3$ and the symmetric eigenvalue problem for the other azimuthal quantum numbers. And as we have done before, the four smallest eigenvalues are given in Table 4.5.

This time there are no zero modes for $m = 2$ and 4. There are, as was with the double-vortex, two zero modes for $m = 3$. The corresponding components u_{33} and v_{33} can be seen in Figs. 4.12-4.13. But, unlike the double-vortex though, there are also two zero modes with azimuthal quantum number $m = 5$. The components u_{53} and v_{53} are shown in Figs. 4.14-4.15

Hence, the coaxial triple-vortex has at least four zero modes other than the three expected zero modes. We speculate from these results that these zero modes correspond to the configurations in Fig. 4.11(a) and Fig. 4.11(b) for $m = 3$ and 5, respectively.

m	ω_0^2	ω_1^2	ω_2^2	ω_3^2
2	2.72×10^{-4}	1.13×10^{-3}	2.45×10^{-3}	4.23×10^{-3}
3	-1.24×10^{-4}	6.83×10^{-4}	2.47×10^{-3}	4.93×10^{-3}
4	7.58×10^{-4}	2.17×10^{-3}	4.01×10^{-3}	6.32×10^{-3}
5	-1.38×10^{-5}	1.08×10^{-3}	2.78×10^{-3}	4.88×10^{-3}

Table 4.5: Table of smallest eigenvalues (ω^2) for the coaxial triple-vortex ($n = 3$) for azimuthal quantum numbers $m = 2$ to 5.

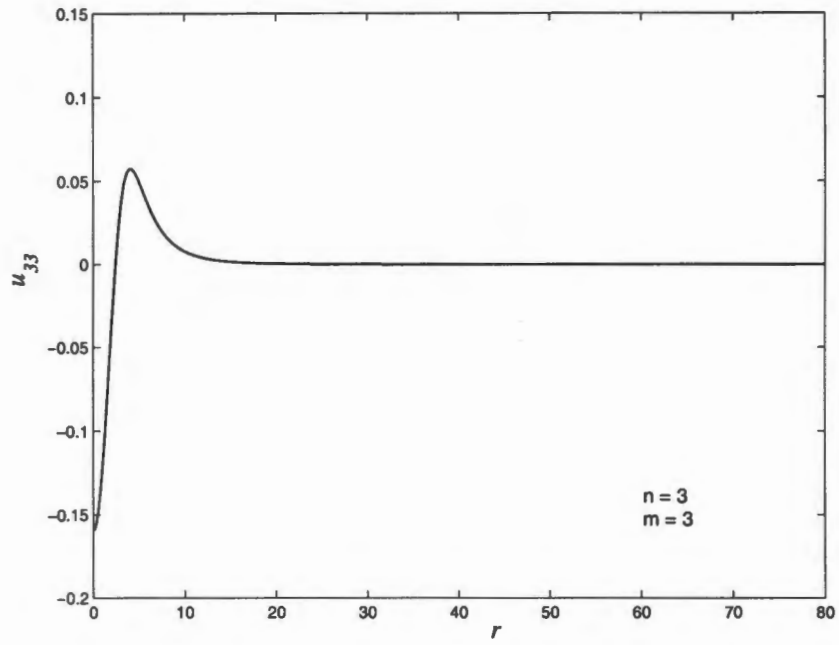


Figure 4.12: u_{33} as a function of r (Numerical calculation with $R = 160$)

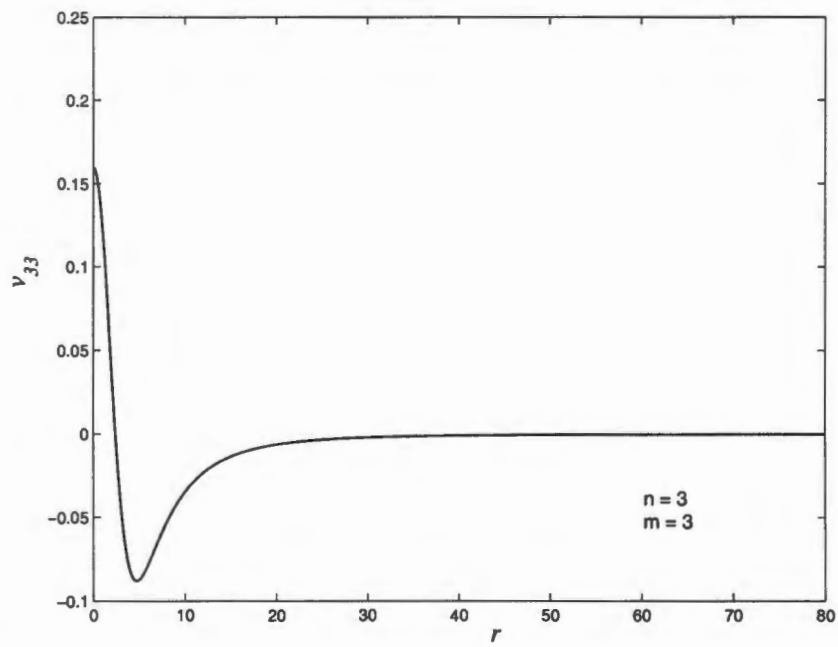


Figure 4.13: v_{33} as a function of r (Numerical calculation with $R = 160$)

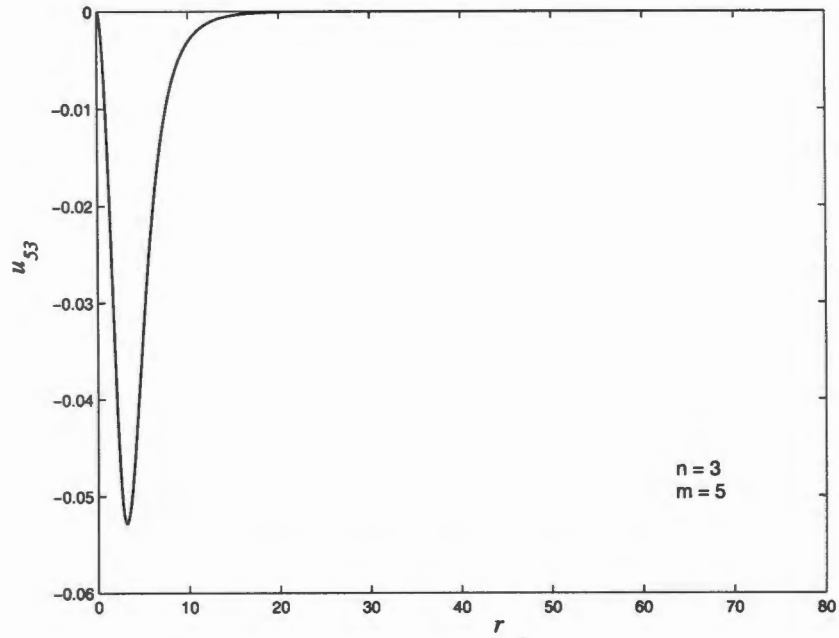


Figure 4.14: u_{53} as a function of r (Numerical calculation with $R = 200$)

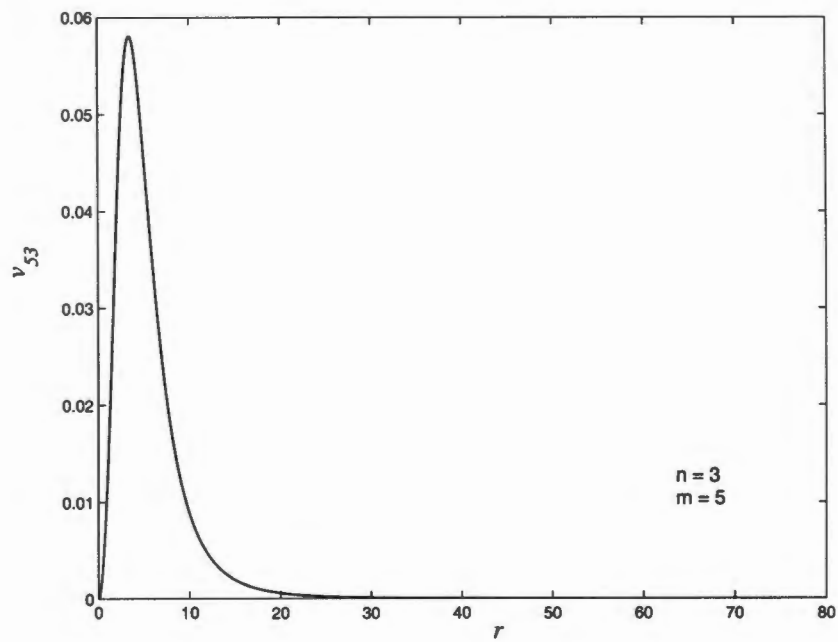


Figure 4.15: v_{53} as a function of r (Numerical calculation with $R = 200$)

4.4 Summary

We were unable to show simply from the asymptotics that the zero eigenvalue ($\omega^2 = 0$), of the linearised operator of the complex sine-Gordon-2, exists. This is also occurred with the Ginzburg-Landau model. Therefore, we had to solve the system numerically in order to determine the number of zero modes.

Our results show that there are two extra zero modes for the double-vortex and four, for the triple-vortex. By extra, we mean zero modes other than the two from two translational degrees of freedom and the one from the global $U(1)$ symmetry. Therefore the coaxial double- and triple-vortices belong to a larger family of solutions. We speculate that the zero modes found arise from the non-coaxial multivortex configurations given in Figs. 4.8 and 4.11.

Conclusion

In Chapter 1, we explored zero modes by considering various “toy” models, for example the sine-Gordon, the Klein-Gordon model and the nonlinear σ -model. We noted that determining the number of zero modes of a soliton yields the number of continuous parameters describing the largest family of solutions, with the soliton as a member. This chapter gave insight into just how powerful this simple method is. We were also able, in general, to determine which degrees of freedom the zero modes correspond to.

There were two unresolved points in Chapter 1. Firstly, there exists the possibility that a third zero mode to the lump of the massless cubic-quintic equation (§1.2.3) exists. It would be interesting to examine this further, for if this zero mode does exist then there is a larger family of solutions to this theory. Secondly, the Belavin-Polyakov soliton of the $O(3)$ nonlinear σ -model (§1.4.2) with topological charge $\nu = 2$ has two zero modes which do not correspond to any of the “expected” degrees of freedom. Thus, this BP soliton belongs to a larger class of solutions, than currently known. It may be that these two degrees of freedom correspond to the splitting of the two solitons in the x and y directions. This might provide an interesting project for further study.

With the ideas formulated in Chapter 1, we then proceeded to analyse the zero modes of the coaxial multivortices of the Ginzburg-Landau (GL), Euclidean complex sine-Gordon-1 (CSG1) and Euclidean complex sine-Gordon-2 (CSG2) models, in (2+0)-dimensions, in Chapters 2, 3 and 4, respectively. The first thing we note is that the zero eigenvalue $\omega^2 = 0$ belongs to the continuous spectrum in the case of the CSG1, for all azimuthal quantum numbers m . This was determined by analysing the eigenfunctions', of the linearised operator, asymptotics. Unfortunately, we were not able to determine simply from the asymptotic analysis whether the zero eigenvalues for the GL and the CSG2, exist or not. In summary, for the GL and the CSG2 we are not guaranteed to have a zero mode for all azimuthal quantum numbers m while for the CSG1 we are. This implies that coaxial multivortices of the CSG1 belong to a family of solutions which depend on an infinite number of continuous parameters : $0 \leq m \leq \infty$.

Since, for the GL, we were unable to determine whether the zero eigenvalue exists, simply from the asymptotic analysis, we had to solve the eigenvalue problems directly to obtain the number of zero modes. This was done numerically as no analytical form for the GL vortices is known. The results show that there is only one zero mode for $m = 0$ (global $U(1)$ symmetry or equivalently rotations in the plane) and two zero modes for $m = 1$ (two translational degrees of freedom), for the single vortex and the coaxial double- and triple-vortices. The results also show that there are no zero modes for azimuthal quantum numbers $m = 2, 3, 4$ and 5 , for the three vortices ($n = 1, 2$ and 3). When we combine these results with the known result [85] that there are no zero modes for $m \geq 2n$, it then follows that there are no zero modes with $m \geq 2$ for the single nor coaxial double- and triple-vortices. We conjecture that this holds for all coaxial vortices of the GL. Therefore there are no continuous degrees of freedom other than the global

$U(1)$ symmetry and translations in the plane. *Hence, it is not possible to continuously deform the coaxial vortices of the Ginzburg-Landau model into a configuration of non-coaxial vortices with finite separation.*

Once we had realised, from the analysis of the asymptotics, that the single and coaxial double- and triple-vortices of the CSG1 have infinitely many zero modes, we proceeded to show their origin. We compared the coaxial multivortices' zero modes to those of the recently discovered non-coaxial multivortices [86]. Note that this is possible as zero modes are dependent on the largest family of solutions and not specific members of the family. Our results show that, for azimuthal quantum numbers $m = 2$ to 5, the numerically obtained zero modes of the coaxial multivortices are the same as those of the non-coaxial vortices', with the same vorticity. We conclude that this holds for all azimuthal quantum numbers, hence, the non-coaxial vortices in [86] is the largest class of solutions to which the coaxial multivortices belong. *We note that the coaxial multivortices of the Euclidean complex sine-Gordon-1 model can be continuously deformed into configurations of non-coaxial multivortices.*

Chapter 4 produced three main results, firstly, we were able to show that the single vortex of the CSG2 has only the three expected zero modes; one from the global $U(1)$ symmetry and two from translations in the plane.

Secondly, the coaxial double-vortex has two zero modes other than the three expected ones and we speculate that they arise from the ability of the double vortex to continuously deform into a configuration of non-coaxial vortices, Fig. 4.8.

Thirdly we showed that the triple vortex has four extra zero modes and speculate that they arise from the ability of the triple vortex to deform continuously into the configuration of non-coaxial vortices shown in Fig. 4.11. *Thus, the coaxial vortices of the complex sine-Gordon-2 model belong to a larger class of solutions. We speculate that this larger class corresponds to symmetrically orientated, non-coaxial multivortices.*

We finish off with one final remark: The analysis of the asymptotics of zero modes of solitons may provide a simple yet powerful approach to studying the dimension of the solution space of field theories. It was this analysis that indicated, immediately, that there was an infinite parameter class of solutions to the Euclidean complex sine-Gordon-1 model. It is not even necessary to know the exact form of the solitons, just their allowed asymptotic behaviours.

The purpose of writing is to inflate weak ideas, obscure pure reasoning, and inhibit clarity. With a little practice, writing can be an intimidating and impenetrable fog!

– Calvin (Calvin and Hobbes)

Appendix A

Finite Difference Scheme for the Eigenvalue Problem

We made use of second order finite difference schemes [104] to convert the differential eigenvalue problem into a matrix eigenvalue problem. We reproduce the scheme here, purely for completeness. Generally the central difference equation for the first derivative

$$y'_n \sim \frac{y_{n+1} - y_{n-1}}{2\Delta r},$$

and the second derivative

$$y''_n \sim \frac{y_{n+1} - 2y_n + y_{n-1}}{\Delta r^2},$$

was used, where y_i is the i 'th element and Δr is the step size. When at the left and right boundaries, however, we made use of the forward

$$y'_n \sim \frac{-3y_n + 4y_{n+1} - Y_{n+2}}{2\Delta r},$$
$$y''_n \sim \frac{2y_n - 5y_{n+1} + 4y_{n+2} - y_{n+3}}{\Delta r^2},$$

and backward difference schemes

$$y'_n \sim \frac{3y_n - 4y_{n-1} + y_{n-2}}{2\Delta r},$$
$$y''_n \sim \frac{2y_n - 5y_{n-1} + 4y_{n-2} - y_{n-3}}{\Delta r^2},$$

respectively. Since these are second order finite difference schemes the truncation order is $\sim (\Delta r)^2$.

Then rearranging the vector $(u, v)^T$ as $(u_0, v_0, u_1, v_1, \dots, u_{n-1}, v_{n-1}, u_n, v_n)^T$, where u_i is the i 'th element of u and similarly for v , the matrix eigenvalue problem becomes a 5-band matrix eigenvalue problem.

Bibliography

- [1] A.C. Scott, F.Y.F. Chiu and D.W. Mclaughlin, *Proc. I.E.E.E.*, **61** (1973) 1443
- [2] R. Rajaraman, *Solitons and Instantons*, (North-Holland, Amsterdam, 1989)
- [3] K.G. Wilson, *Phys. Rep.*, **23** (1976) 331
- [4] K.G. Wilson, in *New Phenomena in Subnuclear Physics*, (ed. A. Zichichi, Plenum Press, 1977)
- [5] R. Jackiw, *Rev. Mod. Phys.*, **49** (1977) 681
- [6] L.D. Faddeev and A.A. Slavnov, *Phys. Rep.*, **42** (1978) 1
- [7] G.H. Derrick, *J. Math. Phys.*, **5** (1964) 1252
- [8] R. Hobart, *Proc. Phys. Soc.*, **82** (1963) 201
- [9] I. Chuang, R. Durrer, N. Turok and B. Yurke, *Science*, **251** (1991) 1336
- [10] R.K. Dodd, J.C. Eilbeck, J.D. Gibbon and H.C. Morris, *Solitons and Nonlinear Wave Equations*, (Academic Press, London, 1982)
- [11] A.A. Belavin and A.M. Polyakov, *JETP Lett*, **49**, (1975) 245
- [12] A.M. Din and W.J. Zakrzewski, *Nucl. Phys.*, **B174**, (1980) 397
- [13] W. Vinen, *Proc. Roy. Soc. A*, **260** (1961) 218
- [14] V.L. Ginzburg and L.P. Pitaevskii, *Sov. Phys. JETP*, **7** (1958) 858
- [15] L. Onsager, *Nuovo Cimento Suppl.*, **6** (1949) 249
- [16] R. Feynman, in *Progress in Low Temperature Physics I*, (North Holland, Amsterdam, 1955)
- [17] L. Bardeen, L.N. Cooper and J.R. Schrieffer, *Phys. Rev.*, **108** (1957) 1175
- [18] N. Bontemps, Y. Bruynseraede, G. Deutscher and A. Kapitulnik, *The Vortex state*, (Kluwer Academic Publishers, Netherlands, 1994)
- [19] D.R. Tilley and J. Tilley, *Superfluidity and Superconductivity*, (Van Nostrand Reinhold Company, London, 1974)

- [20] H.B. Nielsen and P. Olesen, *Nucl. Phys.*, **B61** (1973) 45
- [21] Y. Nambu, *Proc. Int. Conf. on symmetries and quark models*, (Wayne State University, 1969)
- [22] L. Susskind, *Nuovo Cimento*, **69A** (1970) 457
- [23] A. Vilenkin and E.P.S. Shellard, *Cosmic Stringd and Topological Defects*, (Cambridge University Press, Cambridge, 1994)
- [24] R.Durrer, in *The Formation and Evolution of Cosmic Strings*, (ed G. Gibbons, S. Hawking and T. Vachaspati, Cambridge University Press, 1990, 195)
- [25] R.M. Kiehn, *The falaco soliton - cosmic strings in a swimming pool*, (1997)
<http://www.uh.edu/rkiehn>
- [26] S.S.Chern and J. Simons, *Ann. Math.*, **99** (1974) 48
- [27] J. Hong, Y. Kim and P.Y. Pac, *Phys. Rev. Lett.*, **64** (1990) 2230
- [28] R. Jackiw and E.J. Weinberg, *Phys. Rev. Lett.*, **64** (1990) 2234
- [29] I.V. Barashenkov and A.O. Harin, *Phys. Rev. Lett.*, **72** (1994) 1575
- [30] I.V. Barashenkov and A.O. Harin, *Phys. Rev. D*, **52** (1995) 2471
- [31] S. Hyun, J. Shin and J.H. Yee, *Phys. Rev. D*, **55** (1997) 3900
- [32] H. Lee, J.Y. Lee and J.H. Yee, preprint hep-th/9802062 v2
- [33] J.H. Yee, Preprint hep-th/9803236
- [34] B.S. Kim, H. Lee and J.H. Yee, preprint hep-th/9903138 v2
- [35] R. Jackiw and S.-Y. Pi, *Phys. Rev. D*, **42** (1990) 3500
- [36] R.L Anderson and N.H. Ibragimov, *Lie-Bäcklund Transformations in Applications*, (SIAM Studies in Applied Mathematics, Philadelphia, 1979)
- [37] H.T. Davis, *Introduction to Nonlinear Differential and Integral Equations*, (Dover, New York, 1962)
- [38] P.D. Lax, *Comm. Pure Appl. Math.*, **21** (1968) 467
- [39] R. Hirota, *Phys. Rev. Lett.*, **27** (1971) 1192
- [40] V.E. Zakharov and A.B. Shabat, *Funct. Anal. Appl.*, **8** (1974) 226
- [41] C.S Gardner, J.M. Greene, K.M. Kruskal and R.M. Miura, *Phys. Rev. Lett.*, **19** (1967) 1095
- [42] V.E. Zakharov and A.B. Shabat, *Sov. Phys. JETP*, **34** (1972) 62

- [43] M.J. Ablowitz, D.J. Kaup, A.C. Newell and H. Segur, *Phys. Rev. Lett.*, **31** (1973) 125
- [44] M. Wadati, H. Sanuki and K. Konno, *Prog. Theor. Phys.*, **53** (1975) 419
- [45] C. Rebbi and G Soliani, *Solitons and Particles*, (World Scientific Publishing Co, Singapore, 1984)
- [46] N.S. Manton, *Ann.Phys.*, **256** (1997) 114
- [47] N.S. Manton, *Solitons and Their Moduli Spaces*, (In: Solitons, Properties, Dynamics, Interactions and Applications, Ed: R. MacKenzie, M.B. Paranjape and W.J. Zakrzewski, Springer, New York, 1999)
- [48] R. Jackiw, *Physics Today*, **49** (1996) 1
- [49] R. Jackiw and C. Rebbi, *Phys. Lett.*, **67B** (1977) 189
- [50] A. Belavin, A.M. Polyakov, A.S. Shvarts and Yu.S. Tyupkin, *Phys. Lett.*, **59B** (1975) 85
- [51] R. Jackiw, C. Nohl and C. Rebbi, *Phys. Rev. D*, **15** (1977) 1642
- [52] A.S. Schwarz, *Phys. Lett.* , **67B** (1977) 172
- [53] M.F. Atiyah and I.M. Singer, *Ann. Math.*, **87** (1968) 484
- [54] E. Corrigan, D.B. Fairlie, P. Goddard and R.G. Yates, *Phys. Lett.*, **72B** (1978) 345
- [55] E. Corrigan, D.B. Fairlie, P. Goddard and R.G. Yates, *Commun. Math. Phys.*, **58** (1978) 223
- [56] M.F. Atiyah, V.G. Drinfeld, N.J. Hitchin and Yu.I. Manin, *Phys. Lett.*, **65A** (1978) 185
- [57] R. Jackiw, *Rev. Mod. Phys.*, **49** (1977) 681
- [58] E.B. Bogomol'nyi, *Sov. J. Nucl. Phys*, **24** (1976) 449
- [59] E.J. Weinberg, *Phys. Rev. D*, **19** (1979) 3008
- [60] L. Jacobs and C. Rebbi, *Phys. Rev. B*, **19** (1979) 4486
- [61] J. Burzlaff and D.H. Tchrakian, *J. Math. Phys.*, **37** (1996) 650
- [62] J. Hong, Y. Kim and P.Y. Pac, *Phys. Rev. Lett.*, **64** (1990) 2230
- [63] R. Jackiw and E.J. Weinberg, *Phys. Rev. Lett.*, **64** (1990) 2234
- [64] S.K. Kim, W. Namgung, K.S. Soh and J.H. Yee, *Phys. Rev. D*, **46** (1992) 3544
- [65] S.K. Kim, K.S. Soh and J.H. Yee, *Phys. Rev. D*, **42** (1990) 4139
- [66] A.M. Kosevich, V.P. Voronov and I.V. Manzhos, *Sov. Phys. JETP*, **34** (1958) 858

- [67] I.V. Barashenkov and D.E. Pelinovsky, *Phys Lett B*, **439** (1998) 117
- [68] B.I. Gromak, *Diff. Eqns.*, **12** (1976) 519
- [69] A.S. Fokas, U. Mugan and M.J. Ablowitz, *Physica D*, **34** (1988) 247
- [70] C.P. Bean and R.W. deBolis, *Bull. Amer. Phys. Soc.*, **4** (1959) 53
- [71] P. Lebowitz and M.J. Stephen, *Phys. Rev.*, **163**, (1967) 376
- [72] A.C. Scott, *Bull. Amer. Phys. Soc.*, **12** (1967) 308
- [73] T.H.R Skyrme, *Proc. Roy. Soc.*, **A247** (1958) 260
- [74] T.H.R Skyrme, *Proc. Roy. Soc.*, **A262** (1961) 237
- [75] L.P. Eisenhart, *Differential geometry of curves and surfaces*, (Dover, New York, 1960)
- [76] G. Rosen, *J. Math. Phys.* , **6** (1965) 1269
- [77] G. Rosen, *Phys. Rev* , **183** (1969) 1186
- [78] W. Greiner, *Quantum Mechanics An Introduction*, (Springer-Verlag, Berlin Heidelberg, 1994)
- [79] B.A. Ivanov, V.M. Murav'ev and D.D. Sheka, *JETP*, **89** (1999) 583
- [80] K. Pohlmeier, *Commun. Math. Phys.*, **58** (1976) 207
- [81] Yu.N. Ovchinnikov and I.M. Sigal, "Non-radially symmetric solutions to the Ginzburg-Landau", Preprint, June 6, 2000:
<http://www.math.toronto.edu/~sigal/publications/72.pdf>
- [82] L.P. Pitaevskii, *JETP* , **13** (1961) 451
- [83] E.P. Gross, *J. Math. Phys.*, **4** (1963) 195
- [84] P.S. Hagan, *SIAM J. Appl. Math.*, **42** (1982) 762
- [85] Yu.N. Ovchinnikov and I.M. Sigal, in "Partial Differential equations and their Applications" *CRM Proceedings and Lecture Notes*, **12** (1997) 199
- [86] I.V. Barashenkov, V.S. Schesnovich and R.M. Adams, preprint nlin.SI/0202018, to appear in *Nonlinearity* (2002)
- [87] K. Pohlmeier, *Comm. Math. Phys.*, **46** (1976) 207
- [88] F. Lund and T. Regge, *Phys. Rev.*, **D14** (1976) 1524
- [89] A. Neveu and N. Papanicolaou, *Comm. Math. Phys.*, **58** (1978) 31
- [90] Y. Fukumoto and M. Miyajima, *J. Phys. A*, **29** (1996) 8025

- [91] H. Stuedel, *Phys. Lett. A*, **156** (1991) 491
- [92] J. Tafel, *J. Math. Phys.*, **34** (1993) 1892
- [93] N. Dorey and T.J. Hollowood, *Nucl. Phys.*, **B440** (1995) 215
- [94] Q-H. Park and H.J. Shin, *Phys. Lett.*, **B359** (1995) 125
- [95] I. Bakas, *Int. J. Mod. Phys.*, **A9** (1994) 3443
- [96] Q-H. Park, *Phys. Lett.*, **B328** (1994) 329
- [97] F. Lund, *Phys. Rev. Lett.*, **38** (1977) 1175
- [98] F. Lund, *Ann. Phys.* **115** (1978) 251
- [99] B.S. Getmanov, *JETP Lett.*, **25** (1977) 119
- [100] I.V. Barashenkov and B.S. Getmanov, *Comm. Math. Phys.*, **112** (1987) 423
- [101] S. Sciuto, *Phys. Lett.*, **B90** (1980) 75
- [102] B.S. Getmanov, *Theor. Math. Phys.*, **48** (1982) 572
- [103] V.A. Brazhnikov, *Nucl. Phys.*, **B501** (1997) 685
- [104] M.G. Salvadori and M.L. Baron, *Numerical Methods in Engineering*, (Prentice-Hall inc., New York, 1952)